FOSSIL ENERGY

312
4-26-78

FE-2206-14

DRW-18

CATALYTIC CONVERSION OF COAL ENERGY TO HYDROGEN

Project Final Report

By
John A. Starkovich
James D. Pinkerton
Ethelyn Motley

October 1977
Date Published

Work Performed Under Contract No. EX-76-C-01-2206

Chemistry and Chemical Engineering Laboratory
TRW Defense and Space Systems Group
Redondo Beach, California

U. S. DEPARTMENT OF ENERGY

NOTICE

FE-2206-14
Distribution Category UC-90c

CATALYTIC CONVERSION OF COAL ENERGY TO HYDROGEN

John A. Starkovich
James D. Pinkerton
Ethelyn Motley

Date Published - October 1977

PREPARED FOR THE UNITED STATES
ENERGY RESEARCH AND DEVELOPMENT ADMINISTRATION

Under Contract No. E(49-18)2206

TABLE OF CONTENTS

ACKNOWLEDGEMENT

The experimental and engineering work performed on this program and described in this report has been supported by several people. It is appropriate that their contributions be acknowledged. Messrs. Lorenzo Beason, Donald Kilday and Michael Nishina were responsible for performing the experimental work while Ms. J. Anastasi and Ms. B. Cruz supported the engineering studies. Dr. Jack Blumenthal has provided valuable project guidance and review. The valuable contributions that these individuals have made to the program are greatly appreciated.

TABLE OF CONTENTS (Continued)

LIST OF FIGURES

LIST OF FIGURES (Continued)

LIST OF FIGURES (Continued)

LIST OF TABLES

LIST OF TABLES (Continued)

1. SUMMARY

This project was concerned with the catalytic gasification of coal char and specifically with the use of alkali salt based catalyst systems for promoting the char-lime-steam, char-steam, and char-oxygen-steam gasification reactions. The major objective of the project was to provide a preliminary assessment of the potential of catalytic char gasification for the production of high purity hydrogen by means of the char-lime-steam reaction. A secondary objective was to develop information on the performance of alkali catalysts for methane production from the more conventional gasification reactions such as the char-steam and char-oxygen-steam reactions. Catalyst performance properties determined under the program's laboratory-scale experimental studies were used in an engineering effort to develop a preliminary process design for the catalytic hydrogen process. The economics of the process were evaluated and compared with other fossil fuel conversion processes.

During the course of this study, the activity and recyclability performance of selected alkali catalyst systems were evaluated using both fixed and fluid-bed reactors. Using a fixed-bed reactor system the effects of application technique, concentration, acceptor and char types, and carbon dioxide acceptor regeneration treatment on these performance properties were determined. The effectiveness of fluorspar and phosphate salt addition on catalyst recyclability was studied and the fate of recycled alkali catalysts and mechanisms by which they lose their activity were also investigated. Acceptor and alkali catalyst performance properties were confirmed using two fluid-bed reactors, one for studying catalyst performance at atmospheric reaction pressures, and a second, larger system for studies at pressures between 1 and 6 atmospheres. Char sulfur retentions were also measured for some of the fluid-bed tests.

It was established in both fixed and fluid-bed reactor tests that all char gasification reactions could be made to rapidly occur at 650°C with steam using alkali catalysts such as sodium and potassium carbonate. This reaction temperature is approximately 150 to 200 degrees lower than the temperature at which rapid reaction can be effected for uncatalyzed char

gasification reactions. Further, it was demonstrated that these high catalyst activities are achieved through simple admixing of the dry solid catalyst with char or char-acceptor mixtures. Hydrogen is the principal fuel product produced from alkali catalyzed char-steam and char-acceptor-steam reactions under the experimental conditions employed. It was shown in reactions carried out in fluidized bed reactors, that a 95% pure hydrogen product is obtainable from catalyzed char-acceptor-steam reactions at 650°C and for 3 to 6 atmosphere reaction pressures. In addition to the good carbon dioxide absorption properties of lime shown in these experiments, tests atmospheric pressure showed good (50 to 70%) sulfur retention during char gasification.

In recycle experiments where reaction residues from steam gasification reactions were remixed with fresh char, alkali catalyst systems could be used to catalytically gasify between 12 to 35 times their own weight of char before losing their activity. Recyclability performance was shown to depend on catalyst and char type, 950-1000°C acceptor regeneration treatment, and the presence of lime and stabilizing additives such as fluorspar and phosphate salts. Volatilization and conversion of alkali catalysts to less active forms were shown to be possible mechanisms in the loss of catalyst activity with recycle.

Preliminary engineering analysis indicates that a conceptual process based on alkali catalyzed char-acceptor-steam gasification reactions for high purity hydrogen production could be competitive on a product cost per energy unit basis with other advanced coal conversion processes producing different fuel products.

2. INTRODUCTION AND BACKGROUND

Fundamentally, the production and extraction of synthetic fuels and other important chemicals from coal involves increasing the hydrogen to carbon ratio in the coal. The original source of the hydrogen to accomplish this must be water and the methodology of extracting the hydrogen from water is the key to much of the synthetic fuels technology currently being developed. The cost of producing either coal-derived liquids or high BTU gas is highly dependent on the cost of producing the required hydrogen so that processing schemes which more economically utilize the energy of lower grade fuels such as coal itself or residual coal char to separate hydrogen from water can have a major impact on the costs of producing synthetic fuels.

Preliminary research conducted over the last few years at TRW has indicated that significant improvements in the production of hydrogen and probably methane may be achieved through the use of alkali-based catalyst systems for coal gasification reactions. Catalytic coal gasification offers the possible advantages of significantly improving the technical and economic viability of producing useful synthetic fuels from coal. Present noncatalytic coal gasification processes suffer the disadvantages of having to react coal generally around 850°C in order to obtain acceptable conversion rates and yields and are not very specific in either their conversion to hydrogen or methane. Usually several other relatively expensive unit operations such as separate water-gas shift reactors, methanators, oxygen plants and special high efficiency acid gas scrubbers are required in the overall conversion scheme to obtain the desired gaseous fuel product. Through the development and use of stabilized and highly effective catalyst systems for hydrogen and methane generation, some of the expensive processing stages which contribute significantly to high investment and operating costs for coal conversion processes can possibly be reduced or eliminated. For example, the lowering of gasification reaction temperatures by a few hundred degrees through the use of catalysts offers the possibility of very significantly increasing methane yields in the gasifier resulting in a smaller downstream requirement for

shift conversion and methanation reactors and a reduction in the amount of expensive oxygen required.

This report describes work performed and the results obtained under an ERDA sponsored program in catalytic gasification, conducted at TRW over the period 1 June 1976 to 30 September 1977. The objectives and scope of work for the project are discussed in Section 3 of the report while all of the details, results, and conclusions obtained from the experimental and engineering analysis effort performed under the project are presented in subsequent sections of this report.

3. PROJECT OBJECTIVES AND SCOPE OF WORK

The objective of the current program has been to develop a preliminary assessment of the potential of catalytic gasification, more particularly, the use of alkali salt based catalyst systems for promoting coal char gasification reactions involving steam and a carbon oxide acceptor for producing a high purity hydrogen product. A second objective of the program has been to evaluate the effectiveness which alkali catalyst systems have in promoting the more general char-steam and char-oxygen-steam reactions leading to methane production. A key part of the effort has been aimed at identifying and developing catalysts which show high activities in these reactions and are capable of maintaining their high activities for extended periods of performance.

The program has consisted of an experimental laboratory-scale investigation of catalyst performance properties and an engineering evaluation and analysis effort. In the experimental investigation catalyst performance properties were studied using both fixed-bed and fluid-bed reactors. Catalyst performance for use in two conversion processes were investigated. The first processing concept and the one principally investigated was a catalyzed CO_2 Acceptor process for the production of high purity hydrogen. The second concept investigated was a non-acceptor catalytic gasification process, referred to as a resident catalyst conversion process, which is aimed at methane production. In the acceptor process studies alkali catalyst system performances in promoting the char-lime-steam reaction were studied. In this processing concept lime is used to absorb carbon dioxide during catalytic char gasification and to retain char sulfur as a solid entity. In the resident catalyst conversion process studies, no acceptor material is present during gasification to absorb carbon dioxide. A sulfur absorber such as limestone or uncalcined dolomite is present however for retaining sulfur. The experimental effort was used to develop catalyst performance information which could be used in the engineering effort to develop a conceptual design and a preliminary economic analysis of the catalytic conversion processes. Under the current project, the engineering effort was concerned with developing the design and economic analysis of the catalytic acceptor gasification process.

4. EXPERIMENTAL

Study of the performance properties of catalyst systems for promoting coal char gasification reactions was performed using a batch fixed-bed reactor and two fluid-bed reactor systems. The batch fixed-bed reactor was used for screening reaction parameter effects and catalyst system properties, while experimentation with the fluid-bed reactors was used to more quantitatively assess catalyzed gasification reaction properties under fluid-bed reaction conditions. One fluid-bed reactor was designed and built for studying catalyzed reaction properties at or near atmospheric pressure, while the second fluid-bed reactor unit was used for studies at elevated reaction pressures of 3 to 10 atmospheres (50-150 psi). Descriptions of these three reactor systems, together with the experimental procedures and materials used, are presented in the remainder of this section.

4.1 FIXED-BED REACTOR SYSTEM

Experimentally the procedure for screening catalyst performance (activity and recyclability) and determining the effects of various reaction parameters on these characteristics centered around reacting stationary char, acceptor and catalyst mixtures with flowing steam. Reaction product gas volume and composition were measured as a function of time in order to determine char gasification extent and rate. Observed differences in product evolution rate could thus be interpreted as changes in catalyst performance characteristics with the parameter being studied.

The fixed-bed reactor (FBR) used in this investigation was similar in general design to that used by other workers in earlier studies of the effects of catalytic additives on the carbon-steam reaction. Incorporation of a novel method of automatically measuring and recording evolved product volume made the studies easier to complete and freer of observational errors. The FBR system used in this work is shown diagrammatically in Figure 4-1. Two such reactors were assembled and used in the experimentation. A photograph of the reactor systems is shown in Figure 4-2. The reactor systems are for the most part constructed for borosilicate glass except for the

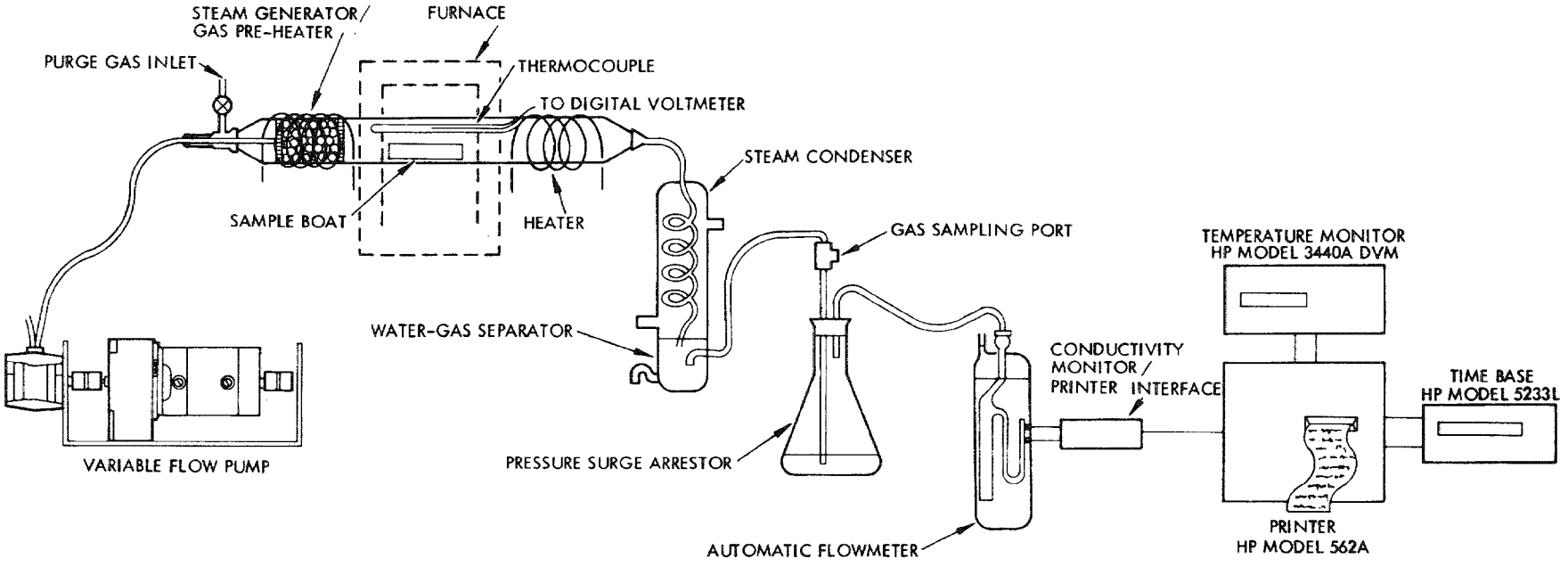

Figure 4-1. Fixed-Bed Reactor (FBR) System Used for Catalyst Performance Screening

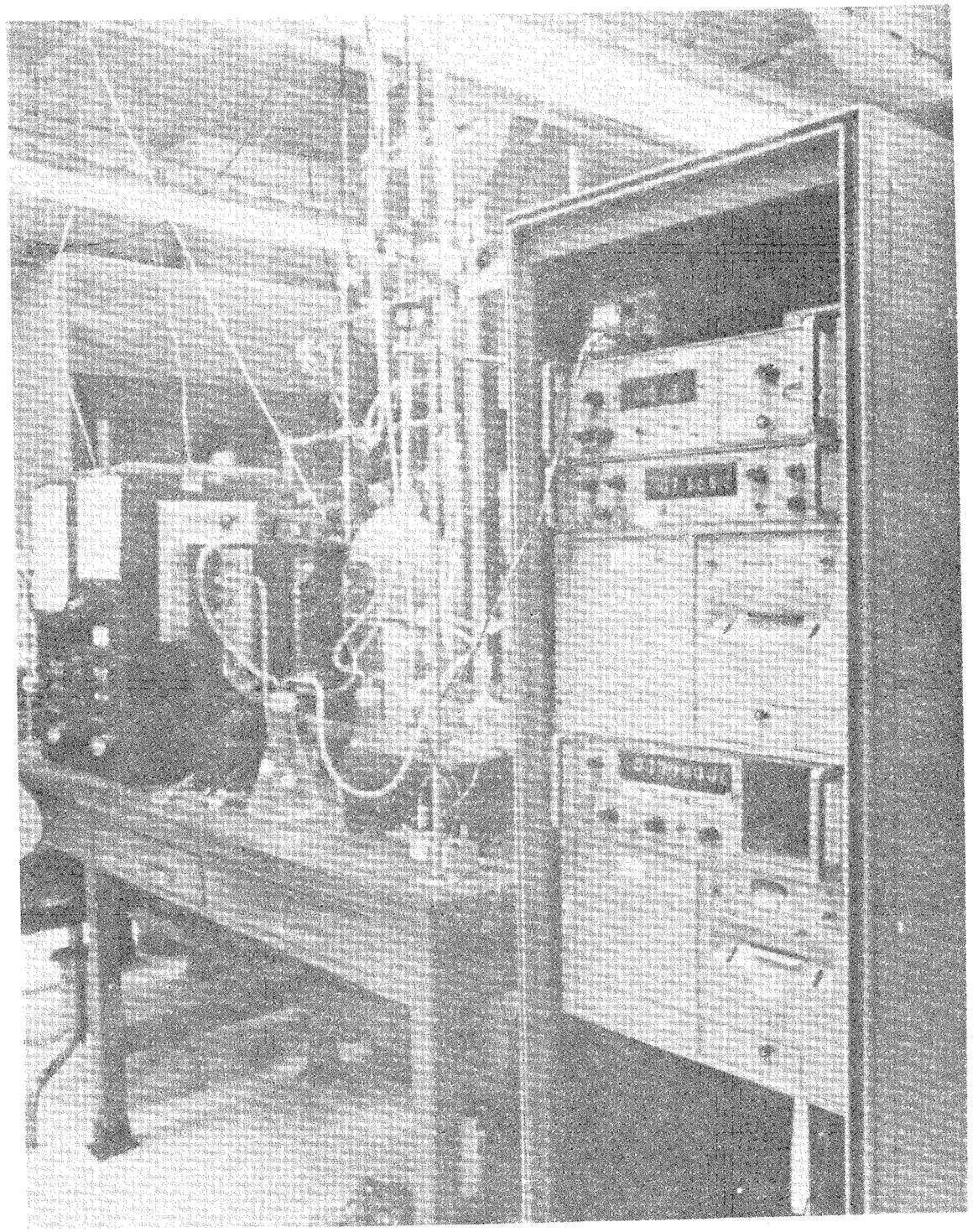

Figure 4-2. Photograph of Fixed-Bed Reactor System

preheaters, reactor tubes, and sample boats used for containing test mixtures during reaction. Since reaction temperatures greater than 600°C were of interest, the steam preheater and reactor tubes were constructed of quartz. Test mixture sample boats were machined from 304 stainless steel bar stock. Boat geometry and size permitted low resistance to steam flow through the 3 cm diameter reactor tube. Boat size was such that 1-gram samples of finely powered test mixtures evenly distributed covered the bottom of the boat to a depth of approximately 0.3 cm. Steam generation was accomplished by either of two means depending upon the flow rate desired. For steam flow rates less than 0.09 mole min^{-1}, a variable feed water pump was used to feed water into the steam generator/gas preheater unit. For high flow rates, a heated two-liter capacity boiling flask was used. By controlling the power input to the boiler flask heater, steady and reproducible steam flow rates between 0.09 and 0.33 mole min^{-1} could be obtained. After passing over a test mixture, unreacted steam and product gases are cooled to room temperature in a water cooled glass condenser. Noncondensable gases are separated from the condensed steam and allowed to flow through a surge-arrestor flask into a novel gas volume flow meter where the volume of product gas evolved from char gasification is automatically measured and recorded as a function of time. Details of construction and operation of the automatic flow meter have been presented elsewhere (11). Samples of the product gas are periodically taken by means of a gastight syringe just downstream from the condenser. Analysis of product gas samples was accomplished with a Carle Instrument Model III gas chromatograph equipped with 1.2 and 2.4 meter silica gel and 13X molecular sieve columns. Neon is used as a carrier gas for the chromatograph which permitted the separation and analysis of hydrogen, carbon monoxide, carbon dioxide, methane, nitrogen and oxygen with only a single sample injection.

4.2 ATMOSPHERIC PRESSURE FLUID-BED REACTOR

A schematic diagram of the fluid-bed reactor system used in studying catalyzed char gasification at atmospheric pressures is shown in Figure 4-3. In the reactor system either steam, purge gas, or air is metered into the bottom of the 3.16 cm (1.25 inch) diameter vertical reactor tube. The feed gas and steam are preheated to the reaction temperature by means of an

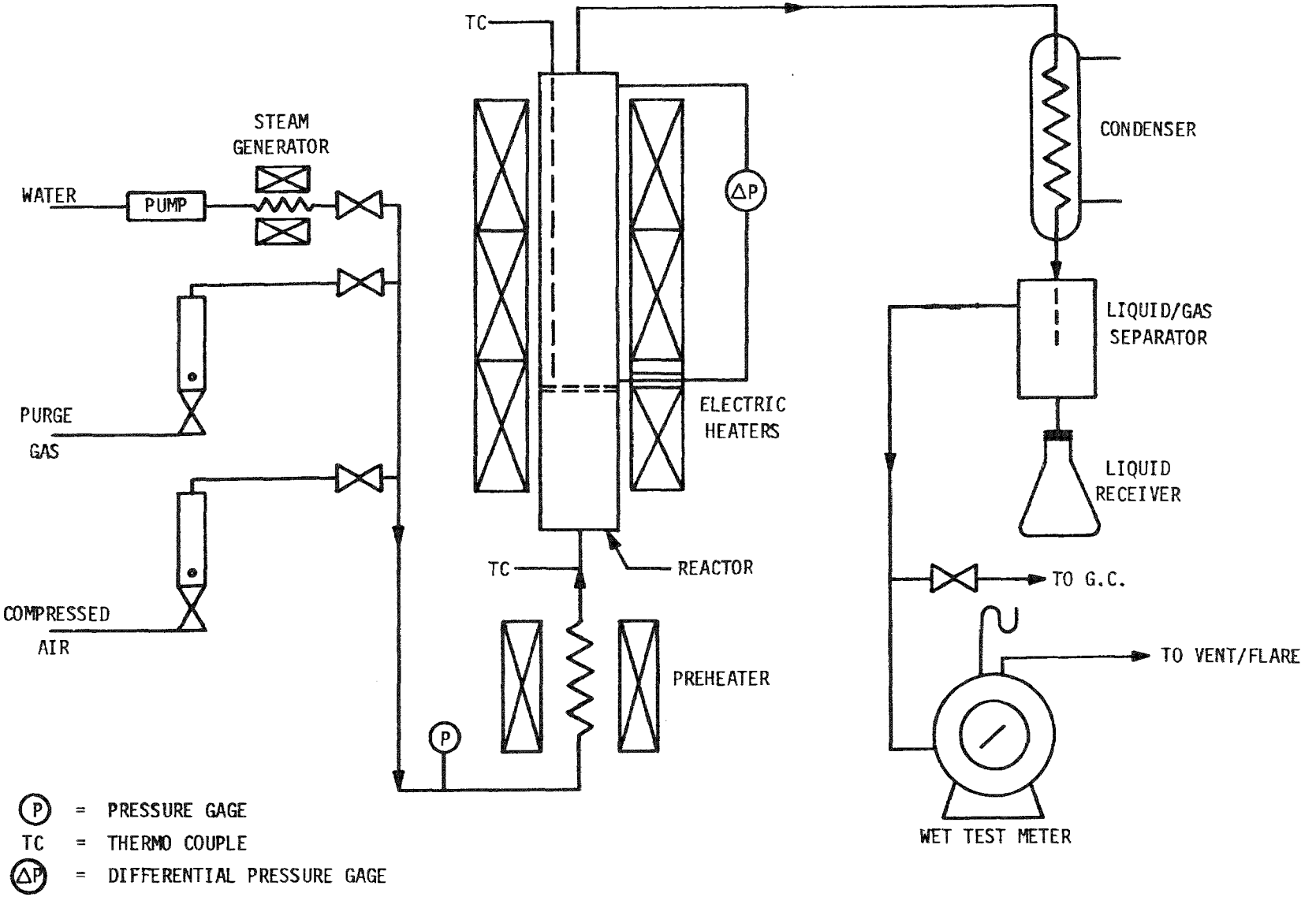

Figure 4-3. Schematic of Laboratory Scale Fluidized-Bed Reactor

electric heater. The steam fed to the preheater is generated by pumping water into a vertically mounted electrically heated, steel tube. Smooth vaporization of water and delivery of a steady steam flow is achieved by means of 0.96 cm (3/8 inch) diameter steel wick material placed within the generator tube. The generated and preheated reactant or purge gases are fed to the lower portion of the 0.8 meter, 321 SS reactor tube. The dimensions of the reactor were selected to give a contact time of 1 to 6 seconds for fluidization velocities of 6 to 12 cm/sec (0.2 to 0.4 ft/sec).

Exit gas leaves the top of the reactor and passes through a heated line to a slurry ice-cooled condenser. Liquid products are collected in a knockout pot and are drained through a manually controlled valve into the liquid receiver. The pressure drop across the fluidized-bed is measured with a water manometer. Pressure taps are provided in the top of the reactor and just above the gas distributor for measuring the pressure drop. The lines are continuously inclined from the reactor to the manometer to prevent condensate accumulation.

The volume of exit gases are measured with a wet-test meter and vented to a hood. Gas samples are periodically withdrawn by gastight syringes and injected into a gas chromatograph for analysis. The reaction product gas is analyzed for hydrogen, carbon monoxide, carbon dioxide, and methane. A more detailed description of the atmospheric pressure fluid-bed reactor system has been presented earlier (11). A photograph of the assembled system is shown in Figure 4-4.

4.3 ELEVATED PRESSURE FLUID-BED REACTOR SYSTEM

In order to study catalyst performance properties and char gasification-acceptor reactor characteristics at elevated reaction pressures, a second fluid-bed reactor system was constructed. This reactor system was designed and built for studying catalyzed char gasification reactions up to 10 atmospheric pressure and reaction temperatures in the range of 600° to 800°C. A schematic diagram of the elevated pressure fluid-bed reactor (EPFBR) system constructed is shown in Figure 4-5 with a photograph of the apparatus presented in Figure 4-6.

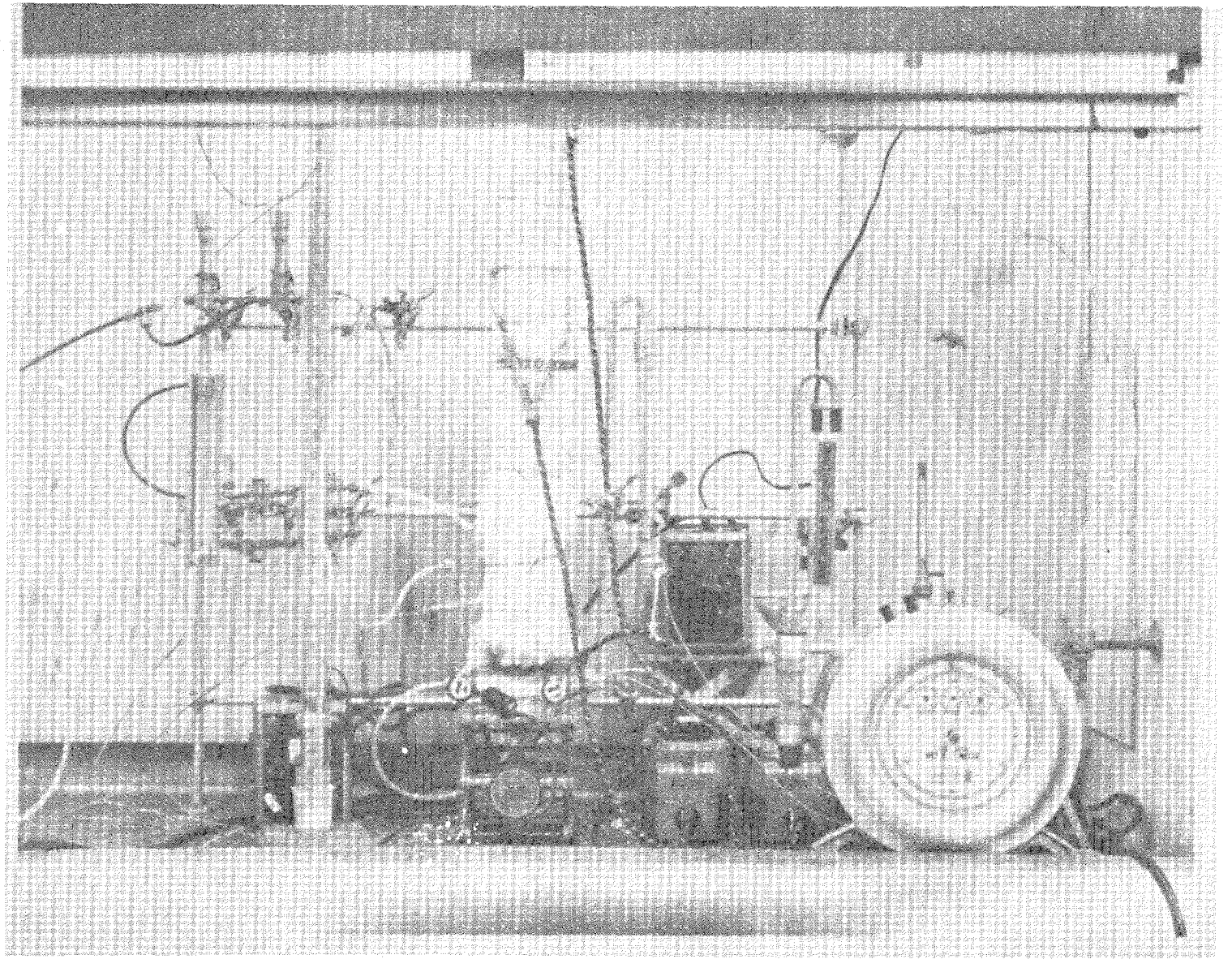

Figure 4-4. Photograph of Atmospheric Pressure Fluid Bed Reactor System

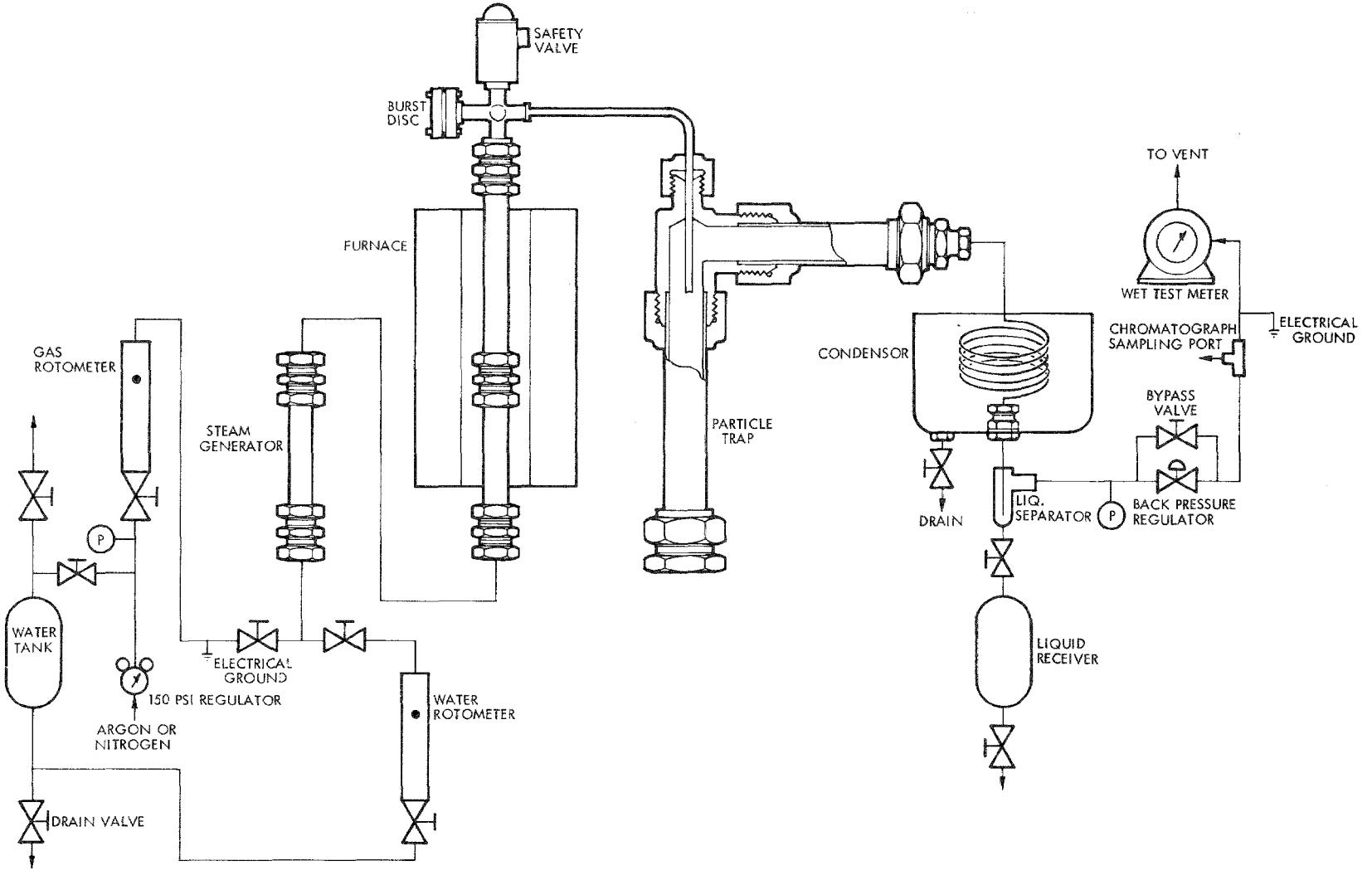

Figure 4-5. Schematic of Elevated Pressure Fluid Bed Reactor System

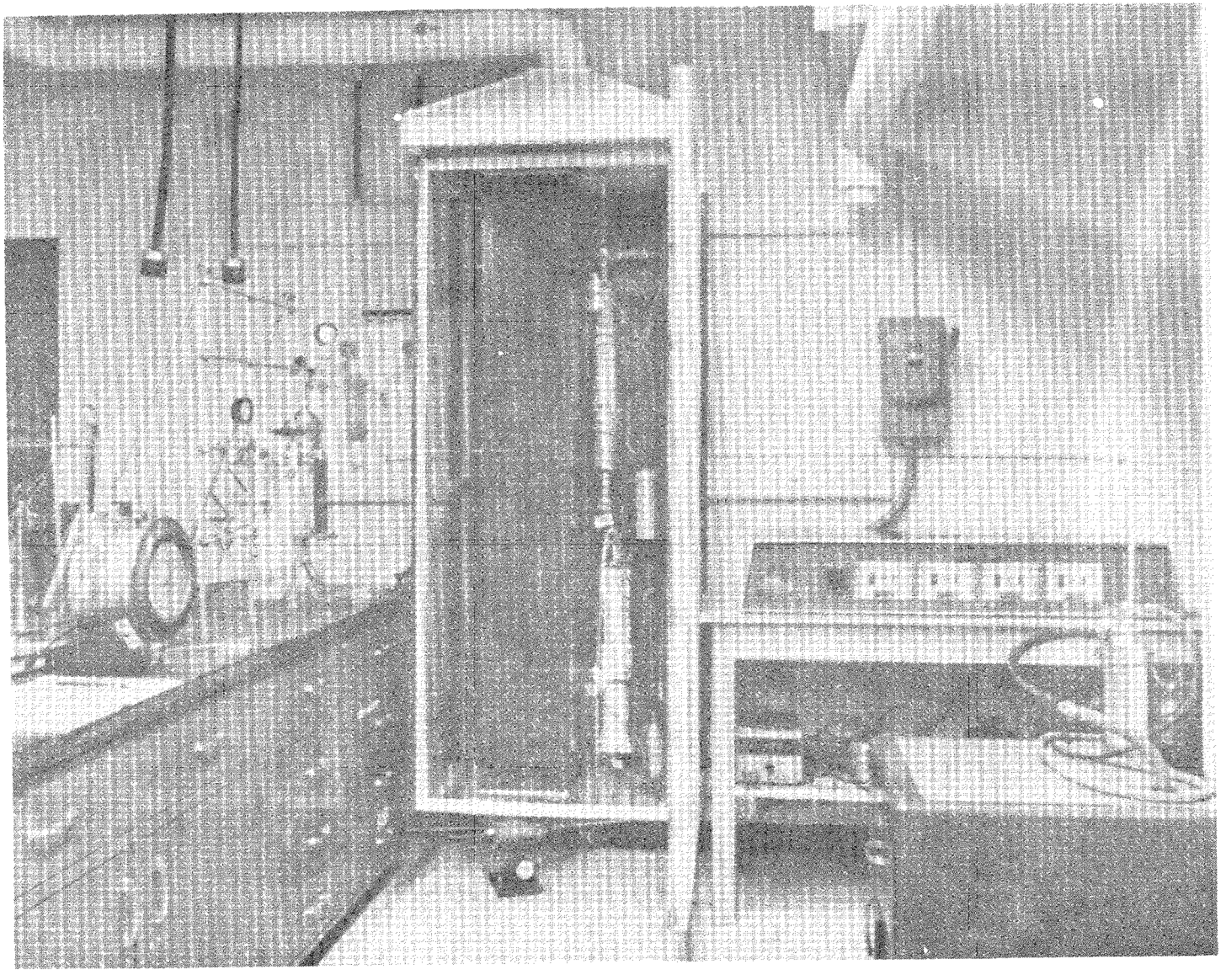

Figure 4-6. Photograph of Elevated Pressure Fluid Bed Reactor System

The diagram of the EPFBR system is similar to that of the atmospheric pressure fluidized-bed reactor system with some modifications and changes in reactor dimensions. As with the atmospheric pressure reactor, steam is generated by flowing water into a vertical, electrically heated tube filled with stainless steel wick material. The wick material is a good heat conductor and provides high surface area for smooth vaporization of water and delivery of a steady steam feed to the reactor. Water is delivered to the steam generator from an argon pressurized water tank. Flow is manually adjusted by means of a needle valve and water rotometer to the desired input rate. Argon or nitrogen purge gas is admitted to the reactor through a 150 psi regulator and rotometer. Steam and purge gas are preheated to near reaction temperature by means of an electrical heater and fed to the bottom chamber or lower section of the reactor tube, where the reactant gases are heated to reaction temperature and their flow evenly distributed prior to its passage through the gas distributor and fluidized-bed reactor zone. The reactor tube is 2.54 cm (1 inch) O.D. (2.37 cm I.D.) and 7.4 m (8 feet) long. Reactor tube material is Hastalloy 800. All other reactor system components in which hot reactant or product gases contact are made of 304 or 316 stainless steel.

Reactor exit gases and entrained solids leave the top of the reactor and are passed through heat-traced tubing to a heated particle trap and on to a condenser. Liquid products are collected in a knockout pot and are drained through a manually operated valve into a liquid receiver. A back-pressure regulator connected to the reactor controls the reactor pressure and reduces the pressure of the exit gases. The volume of exit gases are measured with a wet-test meter. A gas sample can be withdrawn and periodically analyzed with a gas chromatograph. Primary gas analysis is for H_2, CO, and CO_2. Minor components of O_2, N_2, and CH_4, are also present, and analysis for their presence is made. The gas from the wet-test meter is finally vented.

4.4 MATERIALS

4.4.1 Chars

Four char substances representing different carbon sources and methods

of char preparation were used in the present gasification studies. Two materials were supplied by ERDA and were selected to be representative of the types of char that are expected to be produced as by-product materials from future coal based synthetic fuel processes while the remaining two carbon sources included a commercially available char coal and a subbituminous coal from which a char material was experimentally prepared. The ERDA supplied materials included a sample of the residual carbon material remaining after pyrolysis or thermal devolatization of coal in the FMC corporations' COED process pilot plant, and a sample of the char or ungasified carbon material produced in the ERDA (formerly the Bureau of Mines) Synthane process development unit. The source and nature of the starting coal from which the particular "COED char" product sample was derived is unknown. The "Synthane char" represented a sample of the ungasified coal carbon material remaining after elevated pressure steam reaction of western subbituminous coal from the Colstrip seam of the Rosebud mine located in Montana. The commercial charcoal used in these studies was Norit charcoal which is prepared from peat and used in a wide variety of applications. Norit char was supplied by the Matheson Coleman and Bell Chemical Company of Norwood, Ohio. The fourth char used in the experimentation was a material prepared in the laboratory from a separate sample of the same subbituminous coal that was treated in the Synthane process. This char was prepared by heating Colstrip coal to 900°C over a 4-hour period in a helium purged, deep well furnace tube.

Ultimate, proximate, and sulfur form analysis data for the four chars are presented in Table A-1 in the Appendix. Elemental compositions of the ash fraction for each char as determined by emission spectroscopy are presented in Table A-2 in the Appendix.

4.4.2 Acceptor and Catalyst Materials

These materials were studied for their effects on catalyzed char gasification and performance as carbon dioxide and/or sulfur absorbers. These materials were chemically pure calcium oxide and magnesium oxide, and a sample of Hollister dolomite. For experimental studies in which the fixed-

bed reactor system was used, test mixtures containing CaO and MgO were prepared using the bottle reagents directly without prior drying, screening or other processing. For the gasification test carried out using either of the two fluid-bed reactor systems and calcium oxide or Hollister dolomite as acceptor materials, the reagents were sifted by means of standard Tyler mesh screens and a laboratory vibrator platform to give -60 +100 mesh powders. Before use the Hollister dolomite was calcined in air in 100 gram batches at 900°C for 12 hours to generate the acceptor material. Compositional information on the natural acceptor is presented in Table A-3 in the Appendix.

All other materials tested as catalysts or catalyst stabilizer materials met American Chemical Society specifications for reagent grade chemicals and were used without additional purification or processing. The only exception was for materials used in fluid-bed reactor tests where it was necessary to screen the materials in order to obtain the proper mesh particle sizes needed to achieve good fluidization characteristics in the reactor. In this case catalyst materials were sifted before use, as was acceptor and char, to yield -60 +100 mesh material.

4.5 Experimental Procedures

4.5.1 Fixed-Bed Reactor Tests

Reaction test cycles performed with the fixed-bed reactor consisted of reacting solid reactant mixtures with steam or steam-oxygen gas mixtures and measuring product gas composition and evolution rate as a function of reaction time. All char gasification reactions were carried out at approximately atmospheric pressure and generally in the 600° and 750°C reaction temperature range. In experiments where it was desired to determine catalyst system performance with recycle, reaction residues were treated to either a high or low temperature air exposure and mixed with fresh char and rereacted with steam. This reaction cycle was repeated several times using many different catalyst systems to determine catalyst lifetimes or recyclability. Exposure of steam reacted residues at high temperatures, 850°C to 1000°C, served to burn off unreacted char and to decompose (regenerate acceptor) any calcium carbonate that was formed between carbon dioxide and acceptor

during the char-steam reaction. Low temperature, 500°-600°C, air exposure of recycled reaction residue served only to burn off ungasified char. Reaction periods of generally 1 to 2 hours were used for both the char-steam and acceptor regeneration/char burnoff reactions. Typically between 0.4 and 1 gram samples of char or char-acceptor-catalyst mixtures were used in performing fixed-bed reactor tests.

Test samples were prepared by admixing the desired weight proportioned dry solid reactant powders in small polyethylene vials and blending the mixtures by means of a shaker. Glass beads were added to aid mixing. Generally large, 5 to 10 g, batch lots of test mixtures were prepared. In those cases in which the effects of solution dispersion or impregnation of catalyst on char were to be studied, solid reactant mixtures prepared as described above, were slurried with excess water, allowed to stand for 1 to 2 hours and then dried overnight in a vacuum oven at 120°C. Sample impregnation or slurring was performed in the stainless steel sample boat with the amount of mixture that was to be reacted with steam.

Presented above are brief descriptions of the experimental procedures used in performing fixed-bed gasification tests. These descriptions provide an adequate basis for understanding what was done experimentally and interpreting the results obtained and presented below in Section 5.0. More detailed descriptions of the experimental procedures for the fixed-bed experimentation have been reported previously (11,19) and may be consulted if further interest exists.

4.5.2 Fluid-Bed Reactor Experiments

Fluidized-bed char gasification reactions were performed using the laboratory scale fluid-bed reactors described in Sections 4.2 and 4.3. Gasification reactions carried out with these reactors were performed in the 650° to 700°C temperature range and at 1 to 10 atmospheric reactor pressures. Operating procedures used for both the atmospheric pressure and elevated pressure fluid-bed reactions were similar and are briefly described below.

Typical experiments using the fluid-bed reactors were conducted in the following manner. In experiments where it was desired to operate with a CO_2-acceptor, fresh dolomite or previously reacted reaction mixtures containing spent acceptor, accumulated char ash and catalyst were first calcined overnite at 900°C. This served to decompose calcium carbonate to generate calcium oxide and in the case of previously reacted test mixtures, to burn off any char remaining in the mixture. The various components were weighed and screened to -60 to +100 mesh. Usually between 20 to 50 grams of solid reactants were charged to the cold reactor tube. The tube was reinstalled in the reactor system and the system purged with argon and checked for leaks. With the atmospheric pressure fluid-bed reactor, the reactor was heated to 300°C and the feed gas switched to steam at this temperature. Reactor temperature was rapidly raised to the final operating temperature in the 650° to 700°C range. Only a small fraction, a few percent, of the char that was charged to the reactor was gasified during the transient heatup period. Start-up of the elevated pressure fluid-bed reactor was slightly different from that of the atmospheric pressure reactor. In bringing the elevated pressure fluid-bed reactor up to operating temperature, argon purge gas was used to fluidize and pressurize the reactant mixture until reaction temperature had been reached. The argon flow was then shut off and steam introduced into the reactor at reactor pressure. Transition from argon flow to 100% steam feed and stabilization of reactant fluidization required between 2 to 3 minutes. As with the atmospheric pressure fluid-bed reactor, less than a few percent of char was gasified during reactor start-up. Product gas volume and composition were recorded as a function of time from the point that the reactor reached the set reaction temperature or from the switch to pure steam feed. Char gasification reactions were carried out for 1 to 2 hours or until little or no product gas was being evolved. At the completion of a reaction, electric power to the reactor furnaces was cut, steam feed halted and a low argon flow to purge the reactor started. Residual solids were poured from the reactor tube when it had cooled and examined for signs of ash fusion. Residual solids were saved for recycle experiments and sulfur retention measurements.

5. FIXED BED REACTOR EXPERIMENTATION

A large experimental effort was devoted to studying catalyzed char gasification reactions in the fixed-bed reactor (FBR). The objectives of this experimental effort and allied studies were to assess catalyst performance in conversion reactions and to identify reaction and process conditions which affect catalyst performance. Char conversion reactions that were of interest included the char-acceptor-steam, char-steam and char-oxygen-steam reaction. Catalyst performance characteristics in these reactions which were thought to be of key importance in determining the technical and economics feasibility of a catalytic gasification process and that were studied in the fixed-bed experimentation were catalyst activity and recyclability or life. Presented below in this section are a summary and discussion of the results obtained from the FBR studies.

5.1 PERFORMANCE OF ALKALI CATALYSTS IN CHAR-ACCEPTOR-STEAM GASIFICATION REACTIONS

The activities of several alkali and alkali-fluorspar catalyst combinations were screened to identify the most effective systems for promoting char-acceptor-steam gasification reactions. It was of interest to determine also whether, under the conditions used for carrying out the fixed-bed gasification reactions, catalyst and char selection influenced product composition and whether catalyst activities were significantly affected by the method of application or dispersion. The aim of the experiments with the fixed-bed reactor (FBR) system was not so much to establish what the absolute quantitative differences in catalyst activities and reaction parameter effects were, but to assess simply whether significant or gross differences in catalyst performance characteristics existed. Results obtained with the FBR were used to select char-acceptor-catalyst systems for study under fluidized bed reaction conditions.

A summary of the results obtained for the FBR catalyst screening experiments is presented in Tables A-4 and A-5 in the Appendix. For the most part screening experiments were performed at 650°C steam reaction temperature. 650°C was selected as the reaction temperature for the studies

since it was a value identified as a conversion process design goal. Summarized and presented in Tables 5-1 and 5-2 are the specific reaction conditions employed and product gas evolution rates observed for the baseline (char-acceptor-steam) and catalyzed char-acceptor-steam reactions. Differences in product evaluation rates over baseline or noncatalyzed reactions can thus serve as a figure of merit or basis for comparing catalyst activities.

5.1.1 Product Gas Composition

The major products that were found to be produced from the atmospheric pressure catalyzed char-acceptor-steam reaction are hydrogen, carbon dioxide and carbon monoxide. Some methane is produced though only in minor amounts, typically accounting for less than 2% of the total gas product. No higher hydrocarbon products are produced in detectable amounts. The composition of the product gas evolved during FBR gasification is typically: 60%-80% hydrogen, 15%-25% carbon dioxide, 1%-2% carbon monoxide and 1%-2% methane. For the chars and catalyst systems used, product composition did not appear to depend on their selection. The only factor that was observed to have a significant effect on product distribution in the FBR was steam flow rate. Low steam flow rate (higher steam utilization) reduces the hydrogen and carbon dioxide contents while increasing the concentration of CO in the product stream. This is easily explained on the basis of a change in the extent of H_2O-CO shift reaction. A plot of product gas volume and gas composition versus reaction time for a low steam flow rate is shown in Figure 5-1. As illustrated in this Figure, reactions involving char and acceptor gas compositions do not vary significantly during reaction except perhaps initially where acceptor reaction with evolved CO_2 is rapid. Product composition was also observed not to vary significantly with recycle.

5.1.2 Catalyst Activities

As can be seen from the screening results presented in Table A-4 in the Appendix, the dry admixed, borate, carbonate and fluoride salts of sodium and potassium significantly catalyze the char-acceptor-steam reaction. Also apparent from a cursory examination of the results, are the observations that the salts vary markedly in their catalytic activities, and that char

Table 5-1. Baseline Char-Steam Reactivities

Char Type	Acceptor/Stabilizer	Test Mixture Composition[a]			Reaction Conditions		Product Evolution Rate[b]
		Char	Acceptor	Stabilizer	Steam Flow Rate Moles Min^{-1}	Temperature °C	
FMC COED	-	100	-	-	0.33	650 750	0.06 0.22
FMC COED	CaO	20	80	-	0.33	650 750	0.18 1.13
FMC COED	CaO	95	5	-	0.33	650 750	0.07 0.46
FMC COED	CaF_2	95	-	5	0.33	650 750	0.14 1.10
NORIT "A"	-	100	-	-	0.33	650 750	0.00 0.39
NORIT "A"	CaO	20	80	-	0.33	650	0.00
Synthane	-	100	-	-	0.0067 0.0067 0.33 0.33	650 750 650 750	0.69 1.88 0.22 1.22
	Hollister Dolomite[c]	20	80	-	0.33	650	0.27
Colstrip	-	100	-	-	0.33	650	0.12

[a]Components expressed in weight percent

[b]Moles product gas evolved per hour per mole initial carbon

[c]Material calcined at 900°C for 12 hours before use

Table 5-2. Summary of Catalyst Screening Results for Char-Acceptor-Steam Reaction Studies

Catalyst System	Char-Acceptor	Test Mixture Composition				Reaction Conditions		Product Evolution Rate[a]
		Catalyst	Stabilizer	Char	Acceptor	Steam Flow Moles Min^{-1}	Temperature °C	
K_2CO_3	FMC COED-CaO	5	-	19	76	0.33	650	2.87, 3.16, 2.91
						0.09	650	3.16
		5	-	90	5	0.33	650	0.48
						0.33	750	3.37
	FMC COED-MgO	5	-	19	76	0.33	650	3.18
		5	-	90	5	0.33	650	0.76
						0.33	750	3.18
	NORIT "A"-CaO	5	-	19	76	0.33	650	1.58, 1.71
						0.067	650	2.02
	NORIT "A"-Hollister Dolomite	5	-	19	76	0.0067	650	1.14
	Synthane-Hollister Dolomite	5	-	16	79	0.0067	650	1.41
	Colstrip-Hollister Dolomite	5	-	12	83	0.0067	650	1.47, 1.84
K_2CO_3-CaF_2	FMC COED-CaO	5	5	18	72	0.33	650	2.77
	NORIT "A"-CaO	5	5	18	72	0.33	650	1.73
						0.067	650	1.24, 1.23
	NORIT "A"-Hollister Dolomite	5	5	12	78	0.0067	650	1.10
	Synthane-Hollister Dolomite	5	5	15	75	0.0067	650	1.21
	Colstrip-Hollister Dolomite	5	5	12	78	0.0067	650	1.55, 1.55
Na_2CO_3	FMC COED-CaO	5	-	19	76	0.33	650	2.75, 2.86, 2.96
						0.09	650	2.75
Na_2CO_3-CaF_2	FMC COED-CaO	5	5	18	72	0.33	650	2.67
$Na_2B_4O_7$	FMC COED-CaO	5	-	19	76	0.33	650	2 63
$Na_2B_4O_7$-CaF_2	FMC COED-CaO	5	5	18	72	0.33	650	2.44
NaF	FMC COED-CaO	5	-	19	76	0.33	650	2.54

[a]Moles product gas evolved per mole initial carbon for one hour steam reaction period. (1st Cycle Steam Reaction)

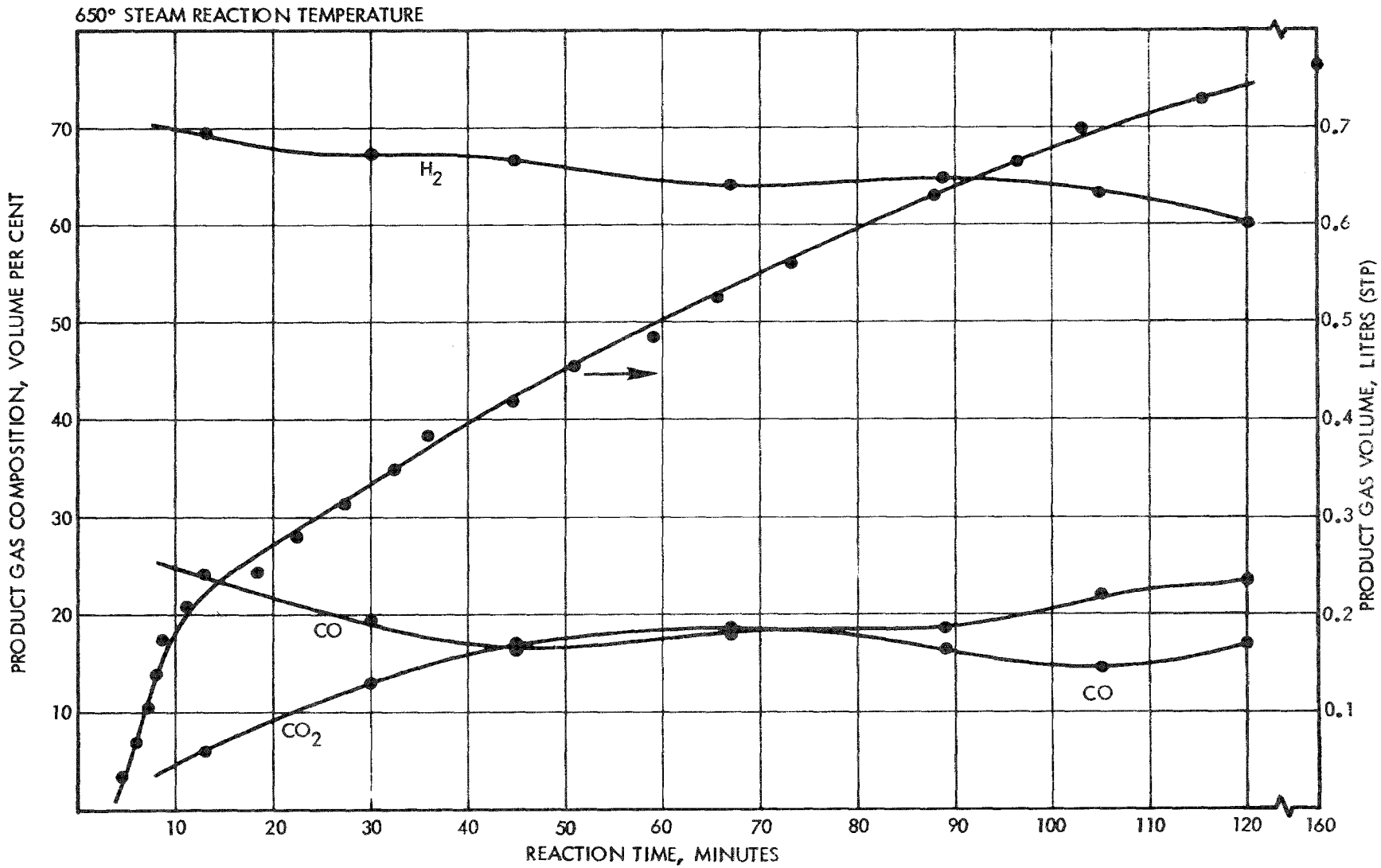

Figure 5-1. Product Composition - Reaction Time Curves for Catalyzed Colstrip Char-Acceptor-Steam Reactions (3rd Reaction Cycle)

type and catalyst concentration or more probably catalyst : char ratio play a role in determining catalyst activity. The magnitude of the catalytic effect and the variation in effectiveness with catalyst type can be seen from the reaction curves shown in Figure 5-2. For these curves, reaction progress for the 650°C steam reaction for the system consisting of COED char, CaO, and alkali catalyst is plotted as a function of time. The dashed line drawn across the top of the figure is the theoretical number of moles of H_2 and CO_2 product gas that can be evolved per mole of carbon gasified if these are the only gaseous products formed. Without alkali catalysts present, char gasification is very slow indicating that CaO is not an effective catalyst for the char-steam reaction at this temperature. Reaction half-lives for the reaction (time required to gasify one-half of the starting char) are approximately: 7-1/2, 9, 14, 19 and 20 minutes for K_2CO_3, Na_2CO_3, NaF, $Na_2B_4O_7$-CaF_2 and $Na_2B_4O_7$ respectively. The difference in catalyst effectiveness between K_2CO_3 and Na_2CO_3 for this concentration level of catalyst is small while the activity of the carbonate salts are considerably higher than the other three alkali catalysts.

The observation that sodium and potassium carbonate are more effective in promoting the char-acceptor-steam reaction than other alkali salts, at least on a weight material employed basis, agrees with the observations of other workers studying the effectiveness of alkali catalysts for the char-steam reaction.[20,21] The significant difference in magnitude in catalyst activities observed for sodium and potassium carbonate and the other alkali salts, suggest that only the former salts should be considered for use in an alkali catalyzed char conversion process. Sodium and potassium carbonate are also among the most abundant and cheapest alakli salts available so that there is an economic advantage in selecting sodium or potassium carbonate as catalyst materials. In addition,as will be shown in Section 5.3 below, sodium and potassium carbonate are also long lived catalysts, able to catalytically gasify larger amounts of char in recycle experiments. The combination of these properties make sodium and potassium carbonate the most promising catalyst candidates for deriving hydrogen from catalyzed char-acceptor-steam gasification reactions.

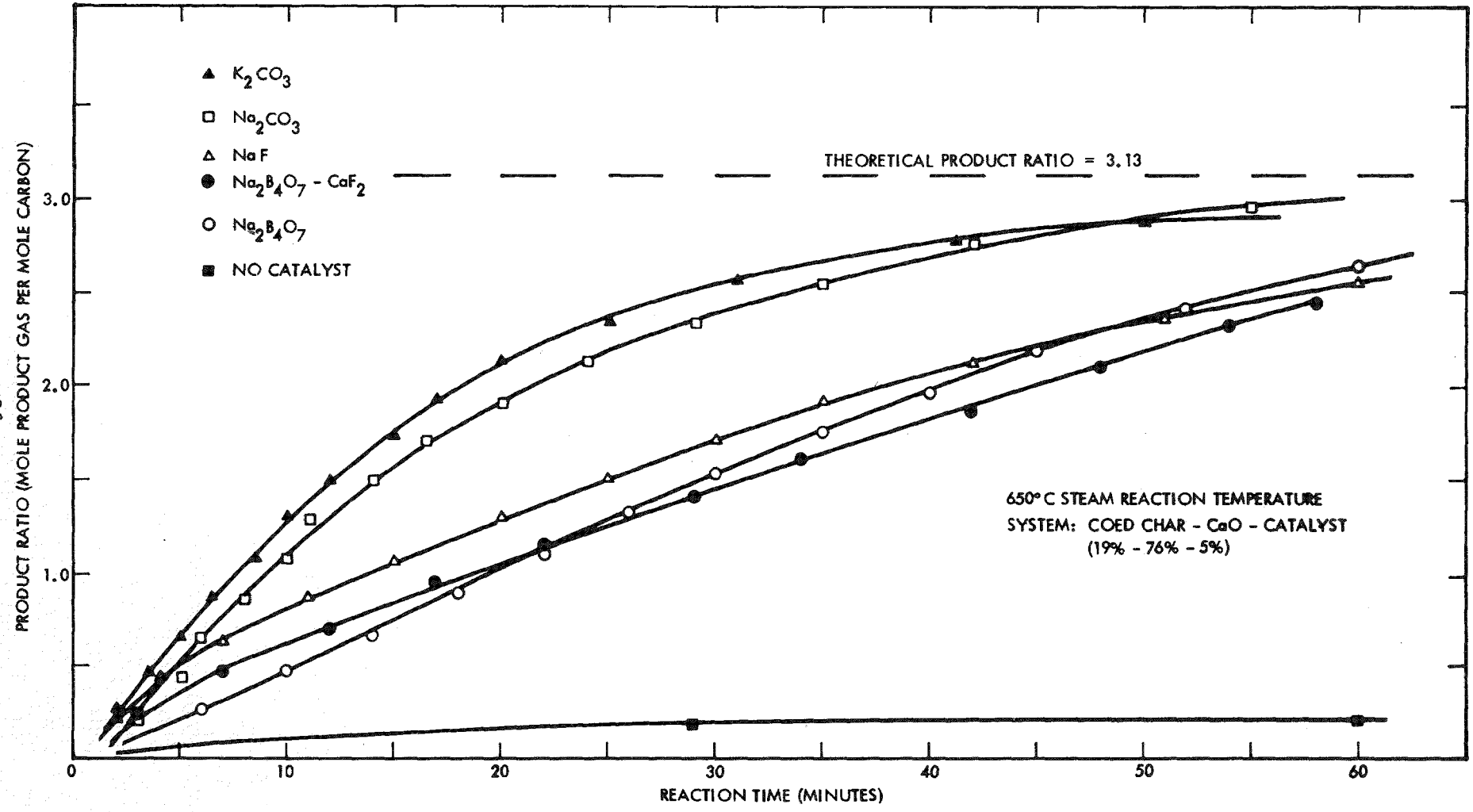

Figure 5-2. Effect of Catalyst Type on Char Gasification Rate

5.1.3 Effect of Application Technique

The comparative effects of solution dispersion and dry application of catalyst on catalyst activity in the char-acceptor-steam reaction can be seen from the reaction extent-time curves shown in Figure 5-3. Plotted in the figure are the moles of product gas evolved per mole of initial carbon as a function of reaction time for the 650°C steam reactions involving dry mixed and impregnated sodium and potassium carbonate catalysts. The curves shown are for the second reaction cycles. The product gas composition for the reactions were very similar and relatively constant during reaction and with recycle. Product gas was typically composed of 75% H_2, 1% CH_4, 4% CO, and 20% CO_2.

As can be seen from the curves in Figure 5-3, solution dispersion or impregnation had no significant effect on the rate of the K_2CO_3 catalyzed reactions relative to the dry mixed catalyst. In the case of Na_2CO_3 catalyzed reaction, application of the catalyst by impregnation improved catalyst activity to near that observed for K_2CO_3. Little is to be gained by aqueous dispersal of K_2CO_3 catalyst. These conclusions may not apply at lower or higher catalyst concentrations.

The observation that high catalyst activity can be achieved without resorting to impregnating the char with catalyst suggested that good alkali catalysts are mobile during steam reaction. To test this hypothesis and to determine whether a supported catalyst could catalyze the char-steam reaction, a fixed-bed reactor test was performed in which catalyst was deposited on support beads and the beads embedded remotely from one another in a bed of char. The beads were noncatalytic and made of silicon carbide. They were spheroidal in shape, nominally 3.7 mm x 1.8 mm in dimension and coated with 1.2 mg of K_2CO_3. The char bed with embedded catalyst beads were reacted for one hour at 750°C with a 0.33 mole min^{-1} steam flow. As can be seen from the photograph shown in Figure 5-4, considerable char in the vicinity of each bed has been reacted as is evidenced by the large cavities or void volumes created by the gasification reaction. The large extent of reaction that has occurred in the vicinity of the beads can be taken to signify that a significant concentration of catalyst existed in the region during steaming and that the catalyst was effective in promoting the carbon-steam reaction.

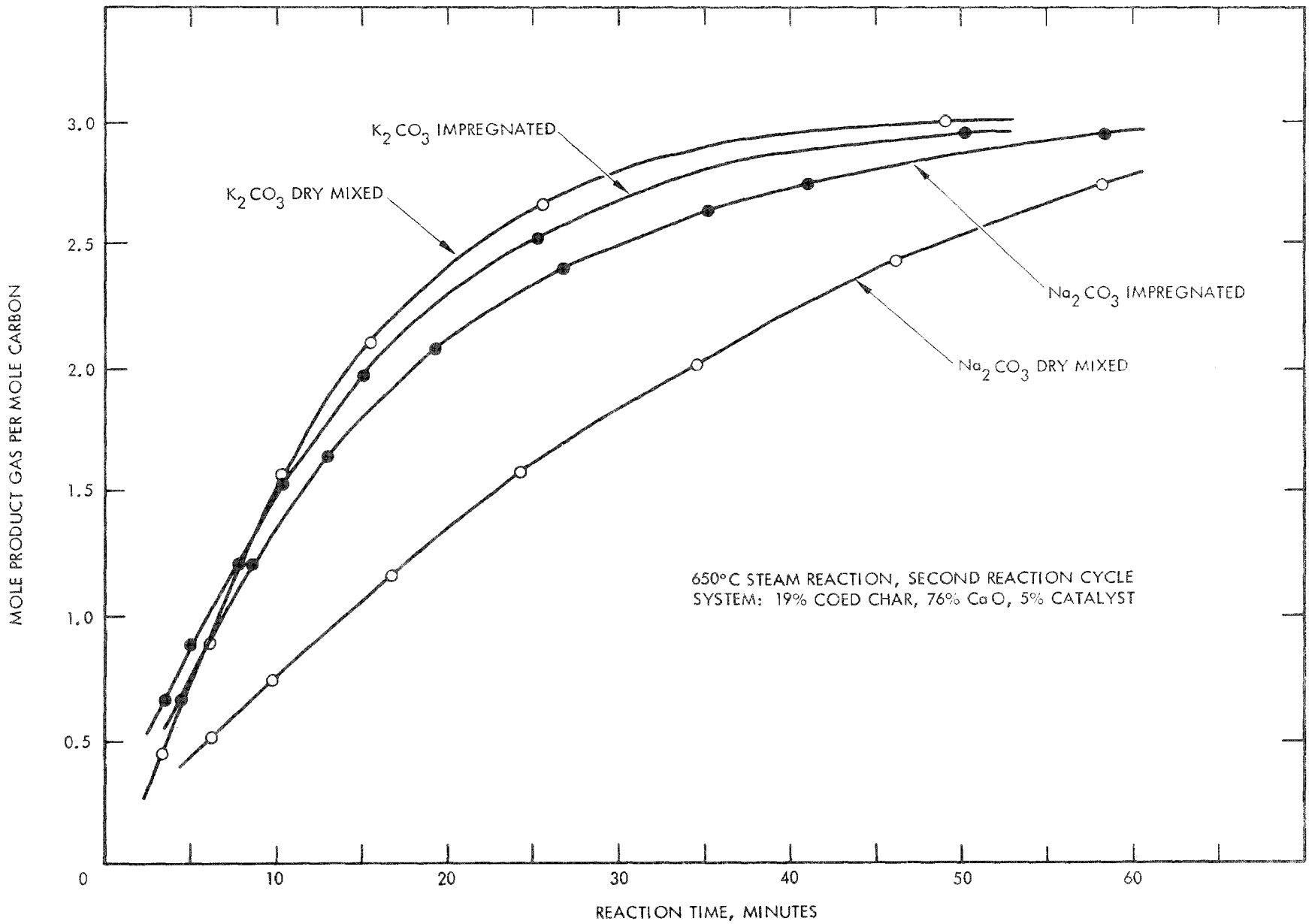

Figure 5-3. Effect of Catalyst Application Technique on Product Evolution Rate

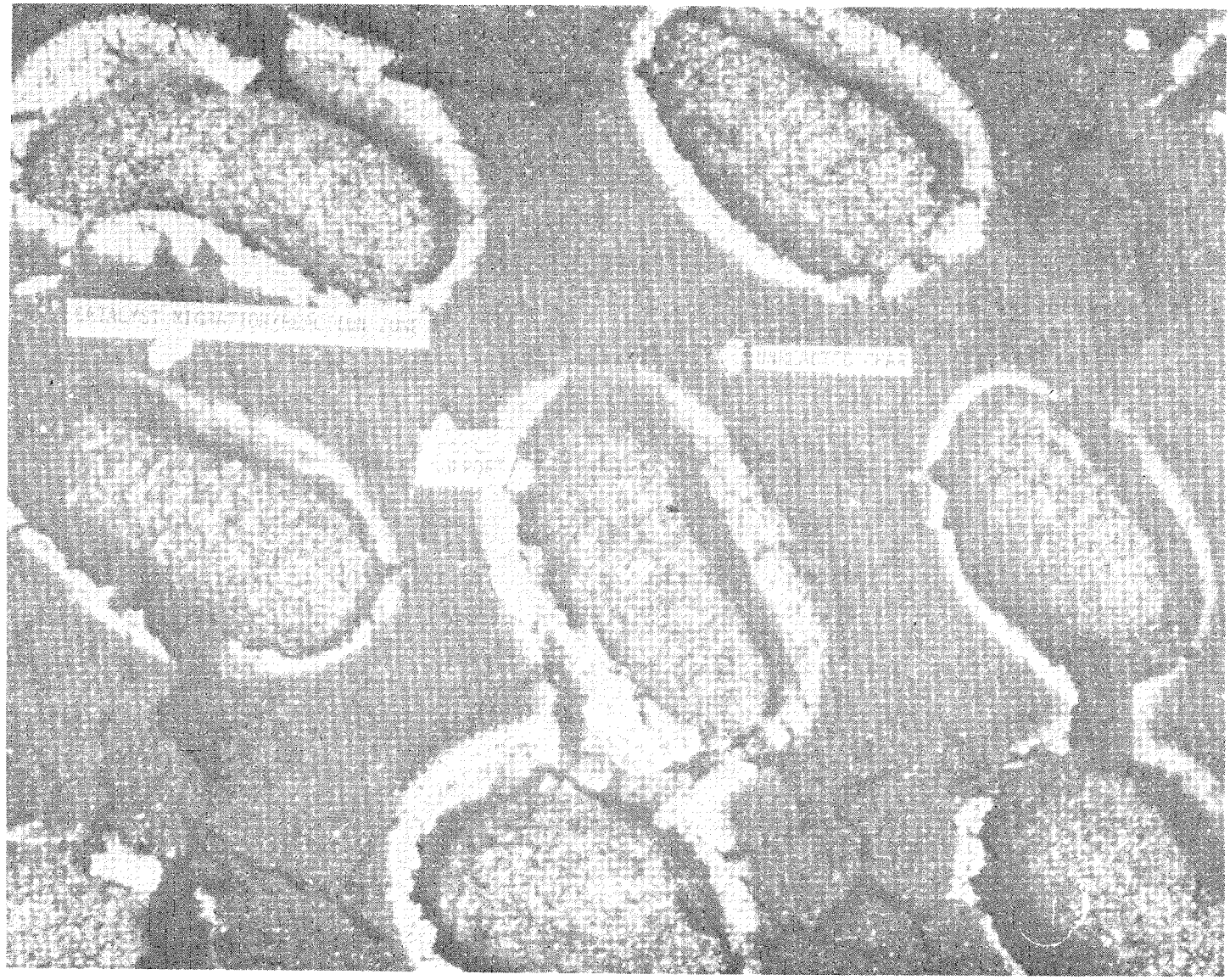

Figure 5-4. Photomicrograph of Partially Reacted Char Bed with SiC Supported K_2CO_3 Catalyst.

In similar experiments performed with SiC beads not impregnated with catalyst, little or no reaction was observed to occur. Electron microprobe analyses of the white regions or zones surrounding each reaction cavity and bead in the photograph show high concentrations of potassium and indicate that effective alkali gasification catalysts, such as potassium carbonate are mobile during reaction.

The processes which are responsible for catalyst transport or mobility have not been confirmed at this time. Two obvious transport mechanisms suggest themselves immediately and either or both could be speculated to be occurring. The first explanation is that transport of catalyst or a catalyst precursor is occurring through mobile liquid phase transfer. The second explanation is that catalyst transfer is occurring by vapor transport of a volatile catalyst compound. One possible mechanism that would fit both transport theories, is the thermal-steam decomposition of alkali carbonate and formation of alkali hydroxide. At the gasification reaction temperature employed, any hydroxide that formed could exist as a liquid or as a vapor. Sodium and potassium hydroxides melt in their pure forms in the 320°C to 360°C range. Decomposition of the carbonate salts and formation of gaseous monomeric or dimeric hydroxides species is also possible as seen in the equilibrium decomposition curves shown in Figure 5-5. Here vapor pressures for the monomer and dimeric hydroxide species involved in the reaction are plotted. Equilibria constants used in computing specie vapor pressures were calculated from JANAF thermochemical data available for the elevated reaction temperatures considered. As the curves indicate, moderate partial pressures of gaseous alkali hydroxides can exist at char gasification temperatures of 650°C to 750°C. There is some evidence from reaction residue recycle experiments, presented below in Section 5.3.4, which tends to support the volatilization theory as the mechanism of catalyst transport. On recycling residues through many gasification reaction cycles, elemental analysis of the residues show a partial loss of alkali. Further understanding of the mechanism of catalyst transport will require additional investigation.

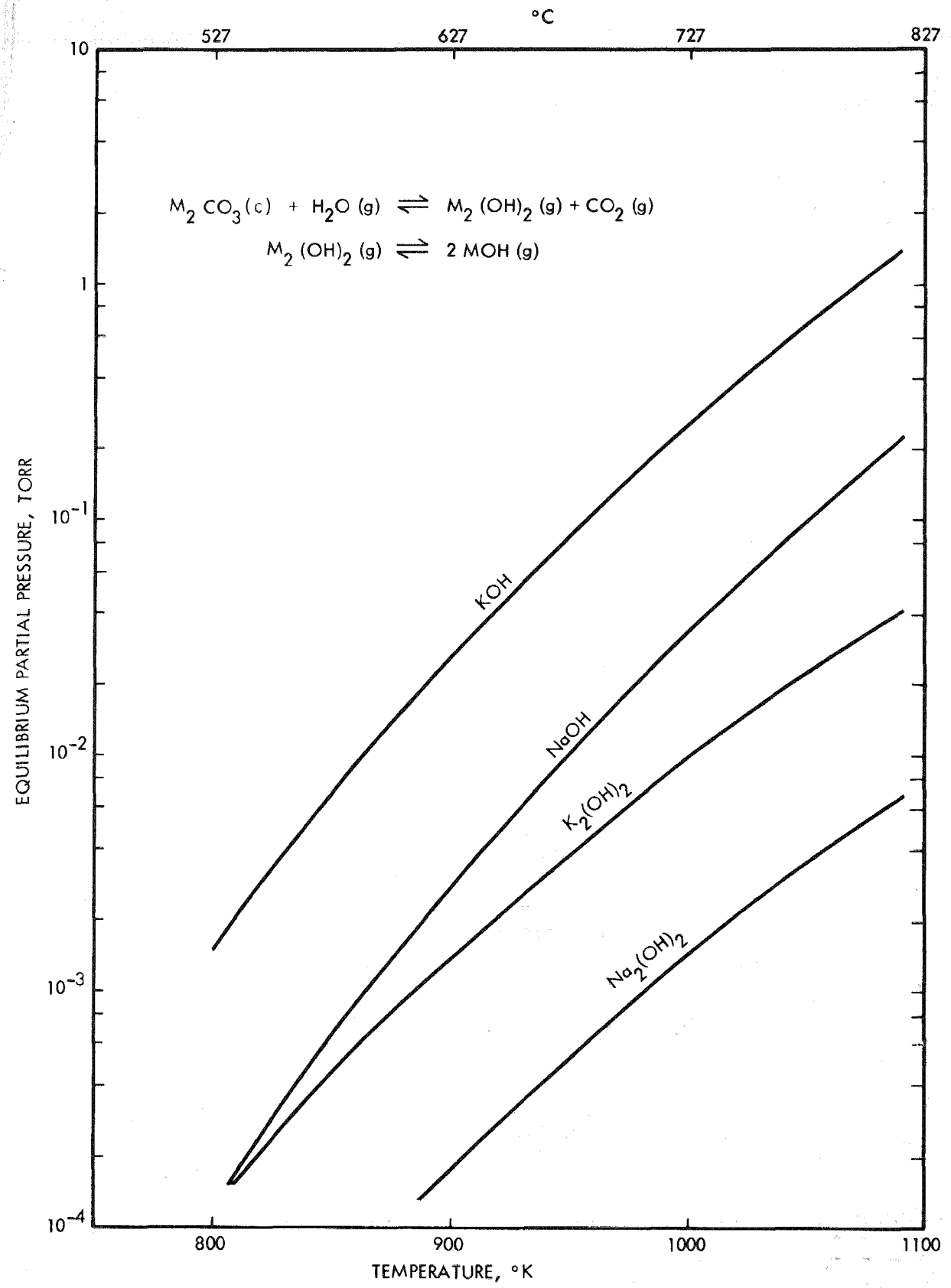

Figure 5-5. Equilibrium Vapor Pressure Curves for Alkali Carbonate-Steam Decomposition Reactions

5.2 PERFORMANCE OF ALKALI CATALYST FOR CHAR-STEAM AND CHAR-OXYGEN-STEAM REACTIONS

5.2.1 Catalyst Screening Results for the Char-Steam Reaction

Summarized and presented in Table A-6 in the Appendix are the results from FBR catalyst screening experiments for the char-steam reaction. The screening experiments were performed to evaluate catalyst performance for catalytic, nonacceptor gasification reactions. While the tests were performed without a carbon dioxide acceptor, several of the screening experiments were performed with varying concentrations of sulfur absorbers such as calcium carbonate or magnesium oxide to assess the effect which these additives had on catalyst activities.

From the results presented in Table A-6 the most effective catalysts observed for the char-steam reaction were sodium fluoride, sodium carbonate and potassium carbonate. Present at the 5 wt. % levels, these admixed catalysts are able to promote the 650°C and 750°C char gasification rates (product gas evolution rates) between 3 to 15 times over the noncatalyzed reaction rates. Other alkali catalysts such as sodium tetraborate (Borax), sodium fluoaluminate (Cryolite), and potassium sulfate were much less effective catalysts, increasing reaction rate only between 2 to 4 times over the uncatalyzed reaction. Five percent calcium fluoride and calcium oxide were similarly not as effective catalysts as NaF, Na_2CO_3 and K_2CO_3. Combinations of NaF, Na_2CO_3, and K_2CO_3 with 5% amounts of CaO, MgO, CaF_2, and $CaCO_3$ did not lower catalyst activity. Indeed, there appears at first glance, to be some synergistic effect on catalyst activity. Combinations of 5% alkali catalyst with higher, 15% to 75%, inorganic additives increases product evolution rate even more. The synergistic effect is an apparent one, and is likely a result of the increase in the concentration of alkali catalyst relative to char in the initial reaction test mixture. The same degree of improvement in product gas evolution rate could be achieved by increasing the catalyst: char ratio in binary char-catalyst mixtures.

5.2.2 Effect of Catalyst Concentration

The substantial effect noted in the screening experiments which catalyst concentration had on conversion rate was further studied. It was of

interest to know that maximum activities could be attained by varying catalyst concentration and what minimum concentrations of admixed catalysts could be used to achieve these high activities. For these experiments varying amounts of Na_2CO_3 and K_2CO_3 were dry blended with FMC COED char and then exposed to steam in the fixed-bed reactor. The reaction conditions involved a 650°C steam reaction temperature and a 0.33 mole min^{-1} steam flow rate. Catalyst concentrations studied ranged from 10-25 wt. %. Product gas evolution and composition were measured during the course of the reaction period. Reaction half-lives were determined from the product volume and composition data by noting the time required for one-half of the initial carbon charged to the reactor to be gasified.

Product gas composition observed for both the Na_2CO_3 and K_2CO_3 catalyzed char-steam reactions were similar and relatively constant over the entire reaction period. Product gas produced from the fixed-bed gasification reactions consisted of approximately 70% hydrogen, 25%-30% carbon dioxide and 1%-3% carbon monoxide. Only trace amounts of methane were observed in the product gases. Carbon mass balances for the reactions ranged from 102%-108%. These observations regarding product distribution and constancy with reaction extent agree with the results obtained from earlier experiments.

The effect of catalyst concentration on char conversion rate for the char-steam reaction can be seen from curves shown in Figure 5-6. Plotted in this figure are the reaction half-lives observed for the sodium and potassium carbonate catalyzed reactions as a function of catalyst concentration. As indicated in the figure, increasing concentration substantially increases conversion rate (decreases reaction half-life). Increases in catalyst concentrations from 10% to 25% lowers reaction half-lives by approximately an order of magnitude. The highest rate of change of reaction rate with catalyst concentration occur for the lower concentration levels of catalyst. At higher catalyst concentrations around 20% to 25%, a leveling effect in the improvement of reaction rate with catalyst concentration is observed. These results agree with observations made for other catalyzed gas-solid reactions in which a plateau in catalyst activity is reached with increasing catalyst concentration. The results here for the char-steam

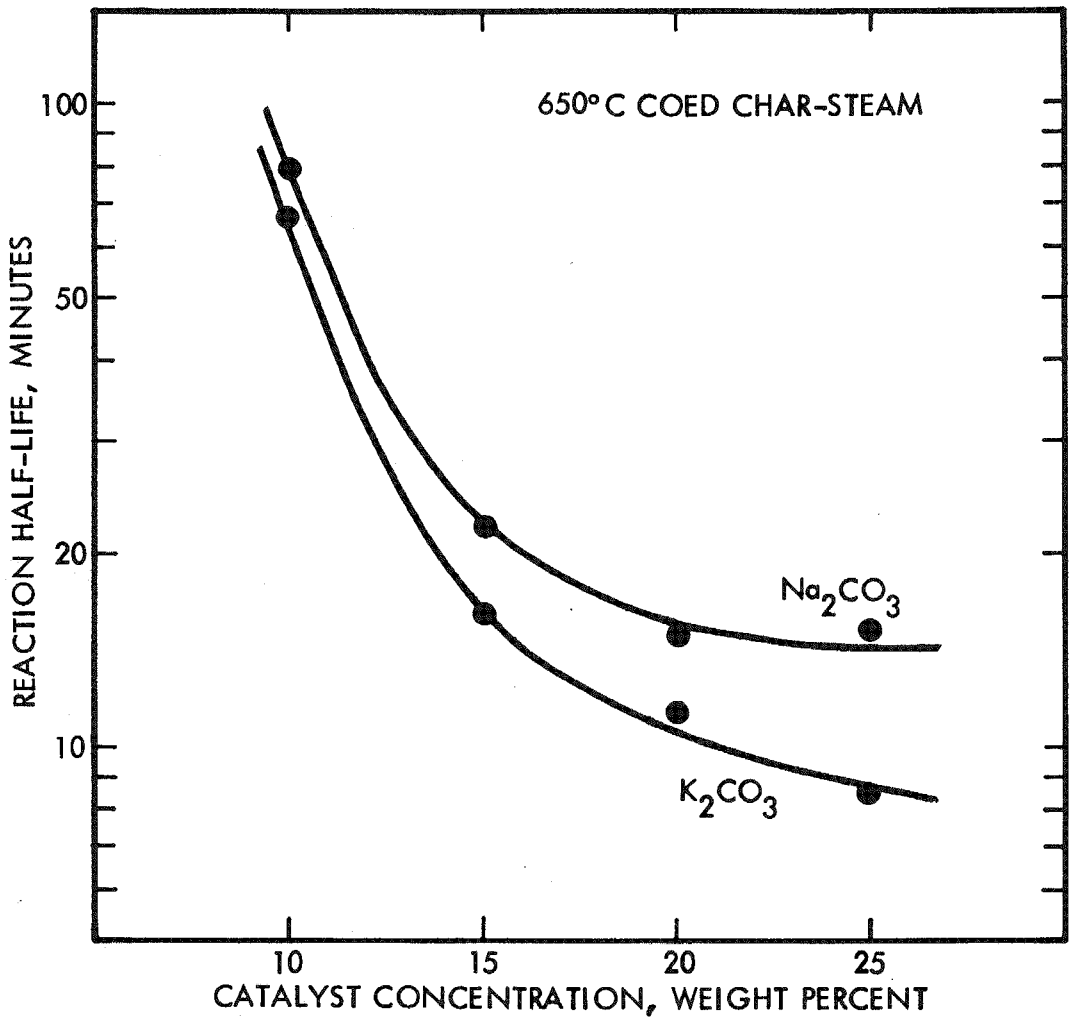

Figure 5-6. Effect of Catalyst Concentration on COED Char-Steam Reaction Half-Life.

reaction show that for admixed catalysts, little improvement in rate is gained through utilization of higher catalyst concentration than approximately 20% to 25%. Whether this conclusion is valid for catalyzed char-steam reactions carried out under fluidized-bed reaction conditions is not known. Results obtained in a fluid-bed reactor would be interesting for comparison and important, since the results would be useful in obtaining an optimized catalyst performance : cost ratio for a conceptual catalytic conversion process.

In addition to affecting char conversion rates, catalysts concentration also affected the apparent rate dependence on carbon. Plotted in Figure 5-7 is the fraction of char gasified versus a normalized reaction time for the K_2CO_3 catalyzed char-steam reaction for different concentrations on catalyst. For the 10 and 15 wt. % catalyst concentrations (K/C atomic ratios of 0.026 and 0.041), the char fraction gasified points fall on a common curve as they should in such a normalized plot if the same reaction processes are controlling rate. For the 20 wt. % catalyst case, the points fall on a distinctly different curve. For catalyst concentrations below 20%, the fraction char gasified could be linearly correlated with reaction time in the manner shown in Figure 5-8 where the apparent carbon reaction order, n, is 1/3. For catalyst concentrations 20% and greater (K/C atomic ratios 0.058) a carbon reaction order of 2/3 was needed to correlate reaction extent and time. The least square slope and intercept of the line for the 1/3 reaction order data are 0.368 and 0.01 respectively,agreeing well with theoretical values of 0.37 and zero. Similar plots made for catalyst concentrations of 20% and higher are linear and have least square slope and intercept values that agree with the theoretically predicted values for a 2/3 order dependence on carbon. The change in reaction order from 1/3 to 2/3 is consistent with a shrinking spherical carbon particle model in which reaction rate control shifts from gas diffusion through a porous ash layer, to a chemical reaction controlling process.

5.2.3 Catalyst Activities for Char-Oxygen Steam Reaction

For gasification processes in which the heat of the endothermic char-steam is not to be partially supplied by an exothermic acceptor-carbon

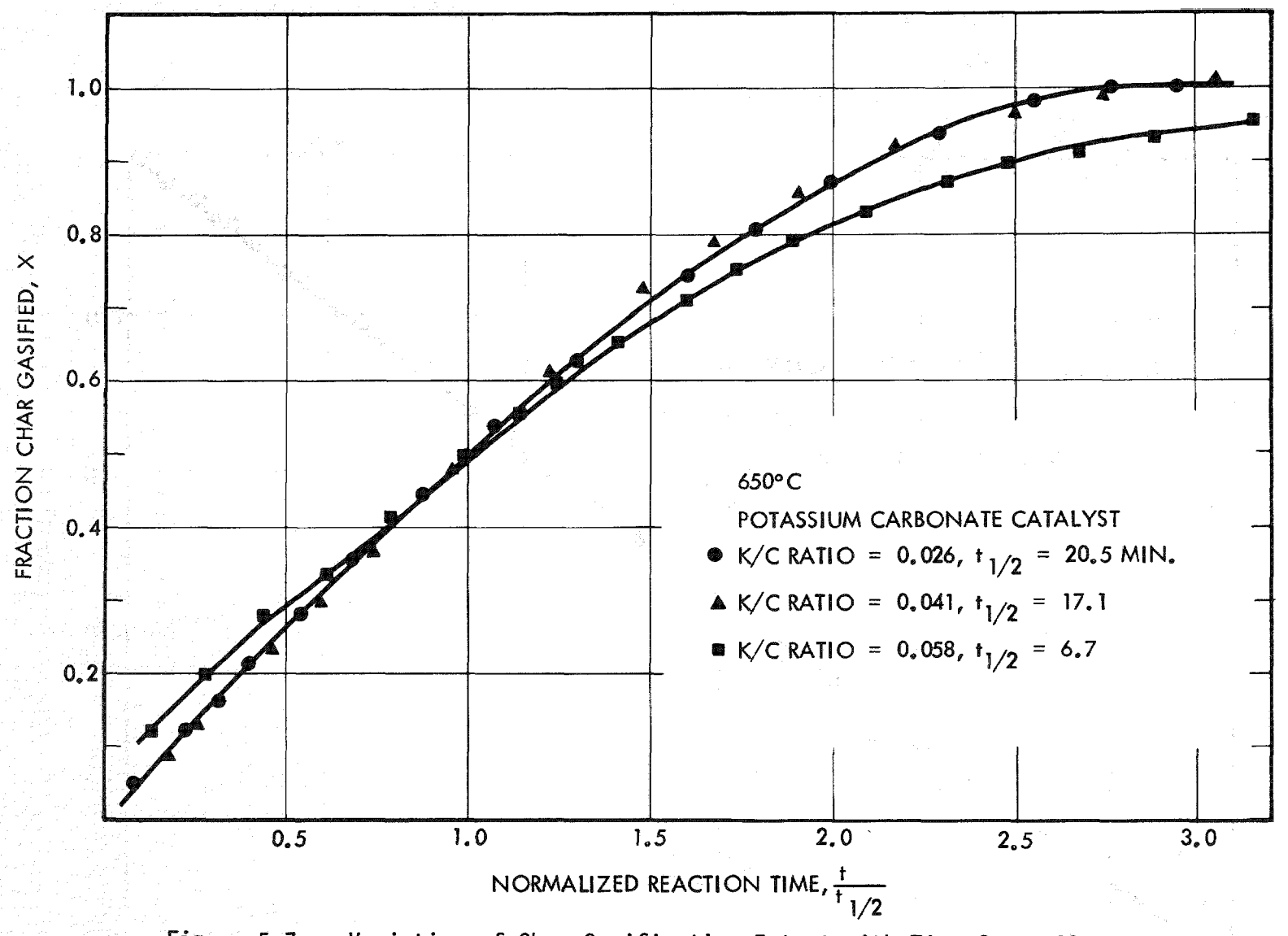

Figure 5-7. Variation of Char Gasification Extent with Time for K_2CO_3 — COED Char-Steam Reaction

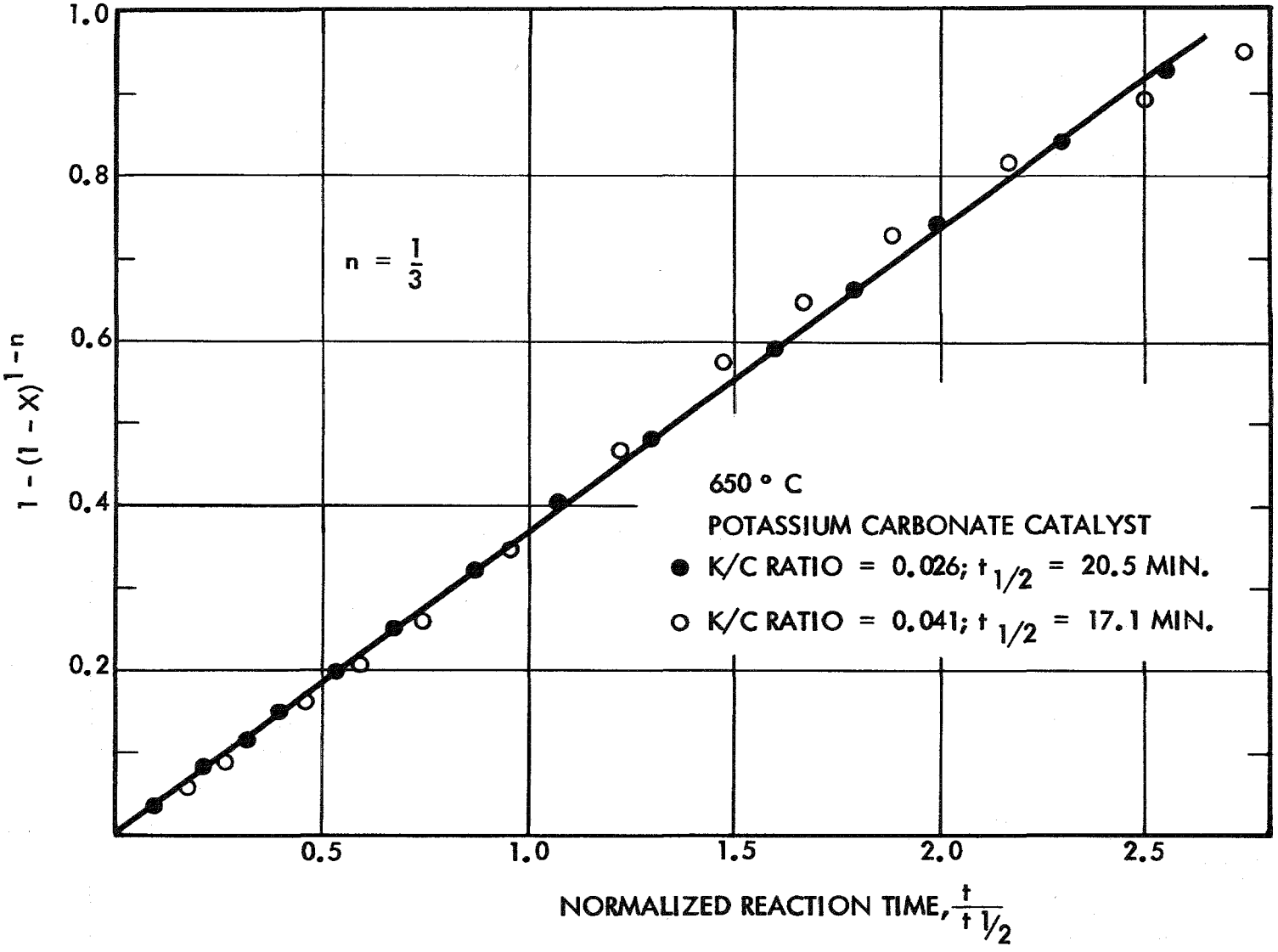

Figure 5-8. Dependence of Char Conversion Extent on Reaction Time for Low Catalyst Concentrations.

dioxide reaction, another means of supplying reaction heat is needed. One approach that is commonly taken in many of the gasification processes currently being developed, is to introduce air or oxygen along with the steam fed to the gasifier reactor. Partial combustion of the char or coal takes place and since the carbon-oxygen reaction is exothermic, heat is furnished for the char-steam reaction. It was an objective of this catalytic gasification effort to determine whether alkali salts were also effective catalysts for the char-oxygen-steam reaction. If effective and able to lower gasification temperature, catalytic gasification could offer the possible advantage of substantially increasing the methane yield in primary gasifier reactors and subsequently reducing the amount of downstream processing for producing a high Btu content product gas. The net effect as in the case of a catalytic hydrogen generation process, would be to reduce the cost of the fuel product.

The effectiveness which alkali catalysts have in promoting the char-oxygen-steam reaction was studied with the fixed-bed reactor. Solid reactant mixtures consisting of COED char, alkali catalysts and calcium carbonate were dry mixed and reacted with steam at temperatures ranging from 300° to 650°C. Calcium carbonate was added to test mixtures as a sulfur absorber and not as a carbon dioxide acceptor. A reactant feed gas of 0.023 mole min^{-1} steam and 0.0012 mole min^{-1} oxygen was used for the char-oxygen-steam reaction experiments. Total reactor pressure was approximately one atmosphere. Product gas was collected and the volume measured by means of an automatic flowmeter. Gas samples were regularly withdrawn during reaction and analyzed by means of a gas chromatography for hydrogen, methane, carbon monoxide and carbon dioxide. Carbon dioxide and carbon monoxide were the only product gases detected from char-oxygen-steam reactions. Hydrogen and some methane were probably produced in the char gasification reactions, but were likely combusted with the excess oxygen fed to the reactor. The theory that the lack of any appreciable hydrogen or methane in the product gas is due to combustion with excess oxygen is supported by the observation that carbon dioxide is the principle gaseous product and that carbon monoxide is present at much lower concentrations. In the absence of oxygen, hydrogen is a major product. Under the experimental conditions employed for the char-

oxygen-steam reaction studies, conversion product gas composition did not appear to vary significantly with reaction temperature or catalyst. For reaction conditions in which an excess oxygen is not present, these observations would likely not apply.

The effectiveness which alkali catalysts have in promoting the char-oxygen-steam reaction can be seen from the Arrhenius curves plotted in Figure 5-9. Plotted in this figure for each of the reaction systems studied, are the specific gasification rates (moles carbon gasified per hour per mole carbon in the bed) observed versus the reciprocal of reaction temperature. As can be seen from the curves, potassium carbonate which was an effective catalyst for the char-steam and char-acceptor-steam reaction, is also an active catalyst for the char-oxygen-steam reaction. For reaction temperatures between approximately 300° and 500°C, the specific gasification rate of the K_2CO_3 catalyzed reaction is a factor of two to three higher than the uncatalyzed char-oxygen-steam reaction. At temperatures above approximately 500°C the difference in rates diminishes and actually become inverted. Sodium carbonate at 15% concentration appears from the rate curves to be much less effective in promoting the char-oxygen-steam reaction than potassium carbonate. As for the char-steam reaction calcium carbonate does not show any activity in promoting the char-oxygen-steam.

As is evident from the results presented in the Figure, the effect of alkali catalysts in promoting the char-oxygen-steam reaction is to shift the reaction curves to lower temperatures rather than change significantly the slope of the curves. This is to say that alkali catalysts promote reaction by increasing the pre-exponential or frequency factor in the Arrhenius rate equation rather than by reducing reaction activation energy. The activation energy for the catalyzed char-oxygen-steam reactions appears to be slightly less than 44 Kcal observed for the catalyzed char-steam reaction, though at higher reaction temperatures this is not the case. How alkali catalysts function chemically or physically in the char-oxygen-steam reaction and in other gasification reaction is unresolved. They are active catalysts and have a wide applicability in promoting char gasification reactions, thus warranting further study and developmental effort in using them in catalytic coal conversion processes.

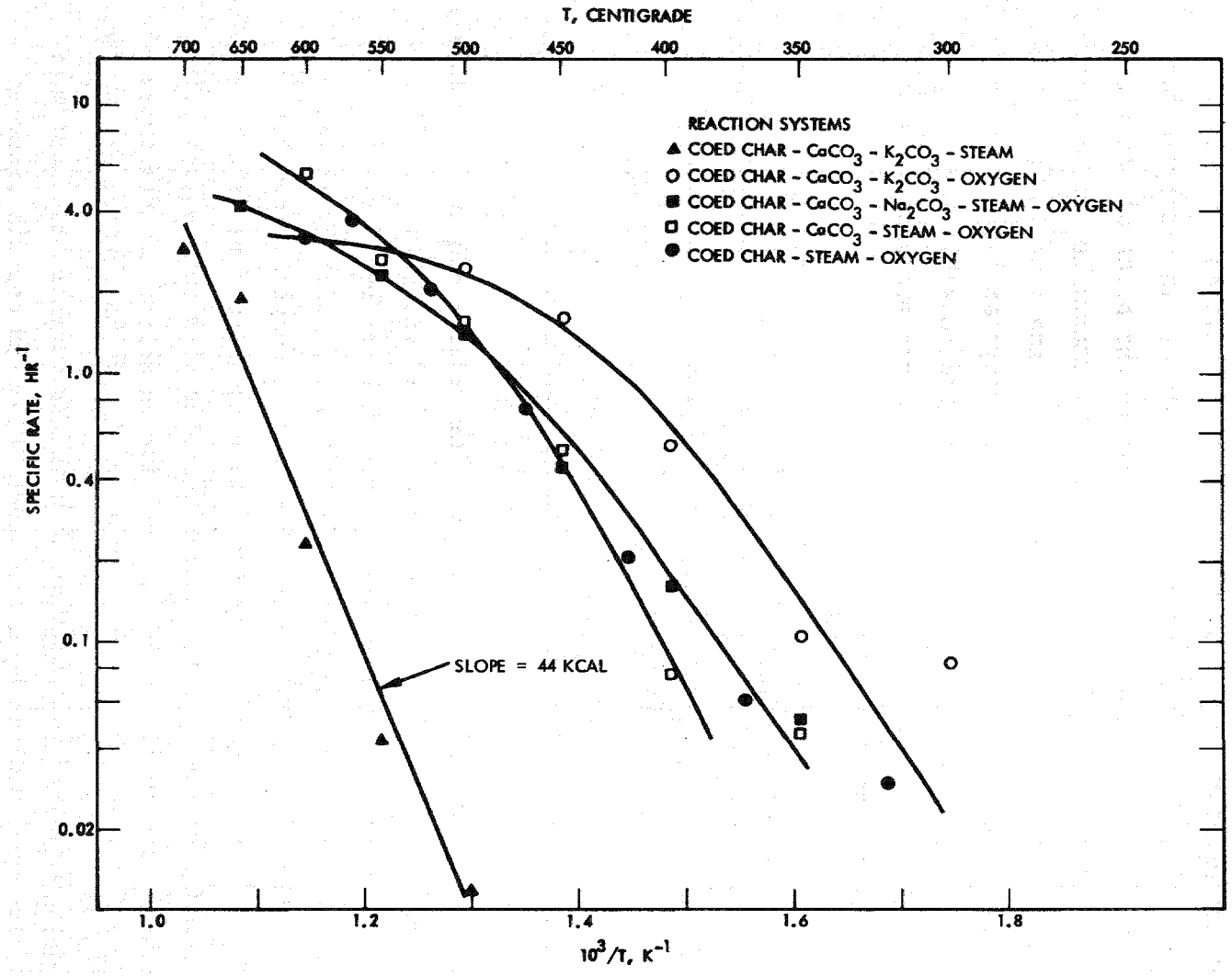

Figure 5-9. Arrhenius Rate-Temperature Plots for the Char-Steam and Char-Oxygen-Steam Reactions

5.3 RECYCLABILITY PERFORMANCE OF ALKALI CATALYST SYSTEMS

In addition to activity or effectiveness, catalyst life or recyclability is another performance property which must be carefully considered in selecting catalyst systems for use in catalytic conversion processes. While abundant in nature and processed in large quantities for industrial use, the costs of alkali salts are such that their use in catalytic conversion processes could add a significant cost to the price of the fuel product if as catalysts they are short-lived and cannot be used to produce a large volume of product. It was a major goal of the experimental effort to begin to assess alkali catalyst lifetimes or recyclabilities, the effects of various reaction conditions on recyclability and possible ways of extending it. It was of interest also to determine the eventual fate of catalysts in char gasification reactions.

Catalyst lifetime or recyclability performances were evaluated with the fixed-bed reactor by reacting test mixtures with steam to gasify char and then mixing fresh char with the reaction residues and rereacting the reconstituted mixtures with steam. After each steam reaction residues were exposed to air at high temperature to burnoff unreacted and/or to regenerate acceptor. During steam gasification product evolution rate and composition were measured so that changes in reaction rate or catalyst effectiveness with recycle could be determined. The measure adopted to quantify catalyst lifetime or recyclability was the catalyst usage ratio. Catalyst usage ratio is defined as the weight of char that can be catalytically gasified per unit weight of catalyst initially used. Char gasification in order to be termed "catalytic" needed to exhibit a reaction rate that was at least one-half the reaction rate observed during the first steam reaction cycle. A summary of the results obtained for the catalyst recyclability studies is presented in Tables A-4 and A-5 in the Appendix. Presented below in the remainder of this section is a discussion of the results of the FBR catalyst recycle experimentation. Results of the recycle tests performed using fluidized-bed reaction conditions are presented and discussed in Section 6.

5.3.1 Dependence on Catalyst Type and Acceptor Regeneration

Perhaps the most significant finding of the FBR studies has been the observation that alkali catalyst recyclabilities vary substantially with the particular catalyst system. The degree of variation can be seen from the summary results presented in Tables 5-3 and 5-4 for the char-acceptor-steam and the nonacceptor char-steam reactions. From the results obtained sodium carbonate shows the highest recyclability performance under all of the variable test conditions employed. For the COED char-acceptor-steam reaction Na_2CO_3 can be used to catalytically gasify between 27 to 30 times its weight of char. For comparison with reaction cycles which include a 950°C acceptor regeneration treatment, other single based alkali catalysts such as NaF, K_2CO_3 and $Na_2B_4O_7$ are able to catalytically gasify, 19, 8 and 8 times their weight of char,respectively. The nonacceptor char-steam reaction differences in catalyst recyclabilities are not as definitive. As the results in Table 5-4 show, under the condition employed for the non-acceptor char-steam reactions only two to three reaction cycles could be completed before significant loss of catalyst activity was incurred. This is believed to be due to the greatly increased amount of char that is gasified in each reaction cycle compared with reactions in which a carbon dioxide acceptor was used. It appears from the results however that N_2CO_3 and K_2CO_3 have usage ratios between 16 and 32. Results for Na_2CO_3 are consistent with those obtained for this catalyst in the char-acceptor-steam reaction. Potassium carbonate shows a definite improvement in recyclability performance where the acceptor does not need to be regenerated. As with the catalyzed char-acceptor-steam reaction, $Na_2B_4O_7$ appears to be the least recyclable, able to catalytically gasify only 16 times its weight of char. The much poorer performance of $Na_2B_4O_7$ catalysts for char gasification reactions has also been confirmed in fluid-bed reaction tests. On the basis of the poorer recycle performance of $Na_2B_4O_7$ and its lower activity than either Na_2CO_3 or K_2CO_3, it would appear that this material is the least attractive catalyst for use in catalytic char gasification reactions.

Table 5-3. Variation of Catalyst Recyclability Performance with Catalyst Type

System	Experimental Conditions		Catalyst Recyclability Performance	
	Steam Reaction Temperature, °C	Acceptor Regeneration Temperature, °C	Reaction Cycles[a]	Char: Catalyst Usage Ratio[b]
FMC COED Char-K_2CO_3 (80%, 20%)	650	500	2	8
FMC COED Char-CaO-K_2CO_3 (19%:76%:5%)	650	500	4-5	19
FMC COED Char-CaO-$Na_2B_4O_7$ (19%:76%:5%)	650	500	2-3	10
FMC COED Char-CaO-Na_2CO_3 (19%:76%:5%)	650	500	8	30
FMC COED Char-CaO-$Na_2B_4O_7$-CaF_2 (18%:72%:5%:5%)	650	500	5	18
FMC COED Char-CaO-K_2CO_3 (19%:76%:5%)	650	950	2	8
FMC COED Char-CaO-Na_2CO_3 (19%:76%:5%)	650	950	7	27
FMC COED Char-CaO-K_2CO_3-CaF_2 (18%:72%:5%:5%)	650	950	2	7
FMC COED Char-CaO-NaF (19%:76%:5%)	650	950	5	19
FMC COED Char-CaO-$Na_2B_4O_7$ (19%:76%:5%)	650	950	2	8
FMC COED Char-CaO-$Na_2B_4O_7$-CaF_2 (18%:72%:5%:5%)	650	950	3	11
FMC COED Char-K_2CO_3 (95%:5%)	750	750	1	19
FMC COED Char-K_2CO_3-CaF_2 (90%:5%:5%)	750	750	1	18
NORIT "A" Char-CaO-K_2CO_3 (19%:76%:5%)	650	1000	2	8

[a]Number of reaction cycles through which catalyst remained effective.

[b]Ratio of weight char catalytically gasified to weight of alkali salt used.

[c]Catalyst active through reaction cycle completed. Additional reaction cycles need to be completed in order to establish recyclability performance.

Table 5-3. Variation of Catalyst Recyclability Performance with Catalyst Type (Continued)

System	Experimental Conditions		Catalyst Recyclability Performance	
	Steam Reaction Temperature, °C	Acceptor Regeneration Temperature, °C	Reaction Cycles[a]	Char: Catalyst Usage Ratio[b]
NORIT "A" Char-CaO-K_2CO_3-CaF_2 (18%:72%:5%:5%)	650	1000	2	8
NORIT "A" Char-Hollister Dolomite-K_2CO_3 (13%:82%:5%)	650	900	4	10
NORIT "A" Char-Hollister Dolomite-K_2CO_3-CaF_2 (12%:78%:5%:5%)	650	900	>3[c]	>7
Synthane Char-Hollister Dolomite-K_2CO_3 (16%:79%:5%)	650	900	>4[c]	>13
Synthane Char-Hollister Dolomite-K_2CO_3-CaF_2 (15%:75%:5%:5%)	650	900	>4[c]	>12
Colstrip Char-Hollister Dolomite-K_2CO_3 (12%:83%:5%)	650	900	3	7
Colstrip Char-Hollister Dolomite-K_2CO_3-CaF_2 (12%:78%:5%:5%)	650	900	4-5	11

[a]Number of reaction cycles through which catalyst remained effective.

[b]Ratio of weight char catalytically gasified to weight of alkali salt used.

[c]Catalyst active through reaction cycle completed. Additional reaction cycles need to be completed in order to establish recyclability performance.

Table 5-4. Summary of Catalyst Performance Results for 650°C Nonacceptor, Char-Steam Reaction

Reaction System			Product Evolution Rate[a] Reaction Cycle			Usage Ratio[b]
Char	Sulfur Acceptor	Catalyst	1	2	3	
80% COED	15% $CaCO_3$	5% K_2CO_3	0.40	0.22	0.33	16 32
80% COED	15% $CaCO_3$	5% Na_2CO_3	0.47	0.20	0.10	16 32
80% COED	15% $CaCO_3$	5% $Na_2B_4O_7$	0.16	0.09	0.09	16
80% COED	10% $CaCO_3$	5% K_2CO_3-5% CaF_2	0.62	0.23	-	16 32
80% COED	15% MgO	5% K_2CO_3	0.47	0.16	0.16	16
80% COED	20% CaO (or $CaCO_3$)	No Catalyst	0.09			-

[a] Moles product gas evolved per mole of carbon per hour.

[b] Weight char catalytically gasified per unit weight alkali catalyst employed.

As can be seen from the collected results presented in Table 5-5, inclusion of a high temperature, 900°C or greater, acceptor regeneration step in the reaction cycle can significantly reduce catalyst recyclability. The magnitude of the reduction however appears to be very dependent on the particular catalyst and char employed in the reaction. For the catalyzed COED char-CaO-steam reaction, increasing the regeneration or burnoff temperature from 500°C to 950°C reduces the usage ratio of Na_2CO_3 and $Na_2B_4O_7$ catalyst by 10% and 20% respectively, while for K_2CO_3, approximately a 60% reduction is incurred. With Norit char and K_2CO_3 catalyst no loss in catalyst recyclability is observed through seven reaction cycles. However in acceptor regeneration temperature to 1000°C, K_2CO_3 remains active through only two reaction cycles for a reduction in usage ratio of approximately 70%. Reduction in the recyclability performance of $Na_2B_4O_7$ is of little consequence since this catalyst's recyclability is poor even without high temperature acceptor regeneration. The slight reduction observed for Na_2CO_3 is probably not significant enough to be concerned with. The reduction in K_2CO_3 catalyst recyclability with acceptor regeneration is important. If indeed K_2CO_3 suffers such a large reduction in performance, this catalyst may not be suitable for an acceptor based catalytic process in which catalyst is circulated along with an acceptor between a low temperature gasifier reactor and an elevated temperature acceptor regenerator. Sodium carbonate in this case would then be the most attractive catalyst system.

In the area of catalyst recycle performance, results obtained with the fixed-bed and fluid-bed reactor are somewhat in disagreement. While results from both reactors agree that with and without acceptor regeneration, sodium carbonate is significantly more recyclable than potassium carbonate, fluid bed tests, however, show that for both alkali carbonate catalysts, recycle performance is not degraded with acceptor regeneration, but improved between 30% and 40%. No explanation for this observed difference can be offered at this time; resolution of the differences will have to wait further experimentation.

5.3.2 Effect of Acceptor and Char Type

Calcium and magnesium oxide, while originally included in reaction mixtures to provide carbon dioxide absorption and sulfur retention, have been

Table 5-5. Effect of Acceptor Regeneration Temperature on Catalyst Recyclability Performance in 650°C Char-Acceptor Steam Reaction

Reaction System	Acceptor Regeneration[a] Temperature, °C	Catalyst Recyclability Performance	
		Reaction Cycles[b]	Char: Catalyst Useage Ratio[c]
COED Char-CaO-K_2CO_3 (19%,76%,5%)	500	5	19
	900	3	11
	950	2	8
COED Char-CaO-$Na_2B_4O_7$ (19%,76%,5%)	500	2-3	10
	950	2	8
COED Char-CaO-Na_2CO_3 (19%,76%,5%)	500	8	30
	950	7	27
Norit Char-CaO-K_2CO_3 (19%,76%,5%)	500	>7[d]	>27
	900	>7[d]	>27
	1000	2	8

[a]Air treatment temperatures below 900°C used to burnoff unreacted char and not for acceptor regeneration.

[b]Number of reaction cycles through which catalyst maintained 50% of the activity shown on first reaction cycle. For FBR experiments activity remained relatively constant throughout its life and became deactivated usually in one reaction cycle.

[c]Ratio of weight char catalytically gasified to weight potassium carbonate employed.

[d]Catalyst active through reaction cycle completed.

observed to serve another important function in catalytic char gasification. While observed to be an ineffective catalyst for the char-steam reaction, the presence of lime and magnesia appears to significantly extend the recyclability of potassium carbonate catalyst. As can be seen from Table 5-6, the presence of MgO and CaO increased the char : catalyst usage ratios by factors of 1.3 and 2.4 respectively over the corresponding cases where no alkaline earth salt is used. For the purposes of extending catalyst life it is not currently known whether such large concentrations of alkaline earth salt are necessary to obtain this effect. Further work to determine whether lower concentrations of acceptor have this beneficial effect needs to be performed. As shown below, small additions of other materials such as fluorspar can be effective in improving catalyst recyclability. For process considerations, even if necessary at high concentrations, lime, dolomite, and other natural alkaline earth minerals are considerably cheaper than alkali catalysts on a unit weight basis and could thus still provide a more economical method of obtaining catalyst performance than increased alkali usage.

Table 5-6. Effect of Lime and Magnesia on Potassium Carbonate

System	Catalyst Recyclability Performance	
	Reaction Cycle	Char : Catalyst[a] Usage Ratio
COED Char - K_2CO_3 (80%, 20%)	2	8
COED Char - MgO-K_2CO_3 (19%, 76%, 5%)	3	10
COED Char - CaO-K_2CO_3 (19%, 76%, 5%)	5	19

[a] Ratio of weight char catalytically gasified to weight potassium carbonate catalyst employed.

While only one series of recyclability experiments has been completed in which only the carbon source has been varied, results indicate that char type can significantly affect catalyst recyclability. In recycling reaction residues from test mixtures consisting of COED and NORIT chars with CaO acceptor and K_2CO_3 catalyst, char : catalyst usage ratios of 11 and something greater than 22 were obtained for COED and NORIT chars respectively. When adjusted for carbon content the usage ratios for COED and NORIT chars (expressed in terms of grams carbon catalytically gasified per gram of catalyst) are 8.5 and 19, respectively. The difference in catalyst recyclability obtained for the two chars supports the hypothesis that catalyst deactivation occurs at least partially through a combination of catalyst with char ash constituents. COED char has twice the ash content of NORIT char (Table A-1 in the Appendix) and catalysts would thus tend to deactivate faster upon recycle. These recycle results were obtained for a reaction cycle which included a 900°C acceptor regeneration treatment. Omission of this elevated temperature treatment would greatly improve the recyclability of K_2CO_3 with COED char; it remmains to be determined whether char type would significantly influence catalyst recyclability without elevated temperature treatment.

5.3.3 Effectivenss of Fluorspar and Phosphate Salts as Alakli Catalyst Stabilizers

The affect which small additions of fluorspar and phosphate salts have on alkali catalyst recyclability can be seen in the results presented in Tables 5-3 and 5-4. As the data show,the effectiveness which these additives have in improving catalyst recycle performance is mixed. For the catalyzed char-acceptor-steam reaction in which a 500°C char burnoff treatment is included in the reaction cycle, addition of fluorspar improves the usage ratio for $Na_2B_4O_7$ catalyst with COED char by 80%. And for the Colstrip char-Hollister acceptor-steam reaction with a 900°C acceptor regeneration treatment, flurospar addition improves K_2CO_3 recyclability by approximately 60%. On the other hand for recycle tests using 950°C and 1000°C acceptor regeneration treatment, no improvement in K_2CO_3 catalyst recyclability is observed. For nonacceptor based gasification reactions, the effect of fluorspar addition on catalyst stability is more consistent.

As can be seen from the results in Table 5-7, addition of 5% CaF_2 to the test mixture increases recyclability performance for K_2CO_3, Na_2CO_3 and $Na_2B_4O_7$ by 111%, 57% and 64% respectively. In the case of K_2CO_3 catalyst, CaF_2 increases the recyclability of this catalyst to where it is longer lived than Na_2CO_3. The improvement in alkali catalyst recyclability achieved with phosphate salt addition is also substantial though the degree is dependent on the particular phosphate salt used. Addition of 5% and 10% calcium phosphate to reaction mixtures containing potassium carbonate resulted in modest 16% and 26% increases in catalyst usage over the unamended catalyst while addition of 10% sodium phosphate approximately doubled catalyst usage. Calcium and sodium phosphate by themselves are not effective catalysts for the char-steam reaction. Thus it is clear that combining these materials with alkali catalysts is resulting in extention of stabilization of catalyst activity.

Table 5-7. Effect of Stabilizer Addition on Catalyst Usage for 650°C Nonacceptor COED Char-Steam Reaction

Catalyst System	Useage Ratio[a]	% Improvement Over Single Catalyst
5% K_2CO_3	19	—
5% K_2CO_3 + 5% CaF_2	40	111
5% K_2CO_3 + 5% $Ca_3(PO_4)_2$	22	16
5% K_2CO_3 + 10% $Ca_3(PO_4)_2$	24	26
5% K_2CO_3 + 10% NaH_2PO_4	37	95
5% Na_2CO_3	30	—
5% Na_2CO_3 + 5% CaF_2	47	57
5% $Na_2B_4O_7$	11	—
5% $Na_2B_4O_7$ + 5% CaF_2	18	64
5% NaF	46	—

[a]Weight char catalytically gasified per unit weight alkali catalyst employed.

In summary, FBR results generally show that alkali catalyst recyclability can be significantly improved through fluorspar and/or phosphate addition. As will be discussed below, fluidized-bed reactor tests also tend to confirm the beneficial effect that these additives can have in improving catalyst recycle performance. There appears from the results to be some variability in the degree of improvement with certain catalysts and reaction conditions under which stabilization is attained. Additional experimental work is needed to better define the limits of improvement and exact conditions under which these stabilizer additives are effective before an assessment of their benefit to catalytic gasification can be made. The use of combinational catalyst system or catalyst-stabilizer systems is an interesting approach to making alkali catalysts more economical for catalytic conversion processes. The potential advantage appears at this time to be large enough to justify further research in the area.

5.3.4 Fate of Alkali Catalysts and Mechanism of Deactivation

That alkali catalysts lose their effectiveness in promoting char gasification reactions with recycle has been clearly demonstrated. The rates at which catalyst systems become deactivated appear to vary with the particular catalyst and to depend on various reaction conditions. On the basis of the results obtained two processes or mechanisms whereby catalyst activity is lost can be postulated. The first is that active alkali catalyst is physically lost from the reaction residue. This could occur through either volitilization in a reaction cycle or by inadvertent mechanical loss during experimentation. The second process involved retention of alkali but conversion to a less or noncatalytic form during char gasification or in subsequent acceptor regeneration. To determine which of these processes were possibly responsible for catalyst deactivation and to learn something about the nature of the deactivation process(es), selected recycled reaction residues were analyzed for their alkali contents and examined by X-ray diffraction and differential thermal analysis to identify the alkali compounds present. Summarized below in the remainder of this section are the results obtained from these studies.

Presented in Table 5-8 is a summary of the results obtained from alkali analyses performed on recycled reaction residues and the reaction treatment conditions to which the samples were exposed. All of the residues were recycled several times so that the catalyst systems were no longer active. The residues were treated and extracted with a mixture of hydrofluoric and nitric acid using a pressure digestion technique[22] recommended for the analysis of coal ash constituents. Acid extraction solutions and residue washings were neutralized, diluted and analyzed by atomic absorption spectroscopy for calcium and alkali content. As can be seen from the results, the amount of alkali found in recycled reaction residues was generally considerably less than the amount initially used. The percentage alkali recovered or retained in the residue ranged between 40 and 62% except for one case where the apparent recovery was greater than 100%. Contamination of the sample during analysis is suspected. To confirm that the loss of alkali from the reaction residues is real and not due to inadvertant mechanical losses in handling or ash entrainment during gasification, the observed and expected alkali metal : calcium weight ratios were computed for each sample. As can be seen from the tabluation of results presented in Table 5-8, the observed alkali : calcium ratios are less than the expected values confirming that preferential volatilization or loss of alkali from the reaction residue is occuring. The percentage loss of alkali from the reaction residues, corrected for mechanical losses by this ratioing technique, indicates that the magnitude of the volatilization loss ranges from 13 to 37% depending on the catalyst and reaction conditions employed.

The observed partial loss of alkali from test mixtures can possibly be explained by the mechanism proposed in Section 5.1.3 for explaining the apparent mobility of catalysts during gasification. It is also possible that alkali volatilization losses are incurred during acceptor regeneration or char burnoff. The limited data presented in Table 5-8 indicate that possibly higher alkali losses are sustained in reaction cycles with 950°C acceptor regeneration treatments. The data is insufficient at present to firmly establish whether alkali loss is incurred during steaming or acceptor regeneration. Analyses of additional reaction residues need to be performed, using perhaps a non extractive or whole sample analysis technique such as

Table 5-8. Reaction Recycle Test Conditions and Observed Residue Alkali Losses.

Original Reaction Test Mixture Composition[a]				Reaction Cycles[b]	Acceptor Regeneration/ Char Burnoff Temperature	% Alkali Recovery	Alkali: Calcium Weight Ratio		% Reduction in Alkali: Ca Ratio
Catalyst	Char	Acceptor	Stabilizer				Observed	Expected	
10% Na_2CO_3	24% COED	62% CaO	4% CaF_2	11	500	62	0.081	0.093	13
10% K_2CO_3	24% COED	62% CaO	4% CaF_2	10	500	46	0.105	0.120	13
10% K_2CO_3	24% COED	62% CaO	4% CaF_2	9	950°C	45	0.0907	0.119	24
10% K_2CO_3	25% COED	65% CaO	—	9	950°C	40	0.0788	0.126	37
10% Na_2CO_3	25% COED	65% CaO	—	12	500	>99	0.157	0.0972	(-62)[c]

[a] Compositions expressed in terms of weight percentage.

[b] Reaction-regeneration cycles completed before analysis of reaction residue performed.

[c] Observed increase in alkali: calcium ratio. Result considered to be spurious due to a possible contamination problem.

neutron activation or proton induced x-ray emission analysis inorder to definitively establish the extent of loss and the reaction step in which the loss is incurred.

The magnitude of alkali loss, 38 to 60%, would not appear to explain the entire loss of catalyst activity. Results from studies of the effect of concentration on catalyst activity show that a 50% reduction in catalyst concentration should not result in loss of essentially all catalyst activity. The magnitude of the reduction in activity suggests that a second method, conversion of active catalyst to a less active or non catalytic form is also occuring. Results of x-ray diffraction analysis of recycled test mixtures from fluidized bed experiments which were reported on earlier (19), were not successful in positively identifying the chemical forms in which deactivated alkali catalyst might exist. All that could be concluded from the x-ray results were that: (1) alkali carbonates if present in residues were there at less than approximately the two weight percent level, (2) silicates, aluminates, alumino-silicates, sulfates, sulfites and some complex calcium-alkali carbonates were possible chemical forms in which alkali could possibly exist (spectral overlap and instrument resolution problems precluded positive confirmation of these compounds), and (3) deactivated alkali catalysts do not exist as sulfides at any appreciable concentrations. Differential thermal analysis of recycled residues showed that alkali catalysts initially added as carbonate salts do not exist in the deactivated state as hydroxide or oxide compounds. Further catalyst performance work, particularly with a wider selection of chars varying in ash and sulfur contents, need to be performed to reveal correlations and establish catalyst conversion as a partial deactivation mechanism.

6. FLUID BED REACTOR STUDIES

Catalyzed char gasification reactions were studied in two laboratory scale fluidized-bed reactors under varying reactor conditions. The objective of the fluid-bed studies were to demonstrate catalyst performance properties, particularly activity, recyclability and product composition, under conditions which more closely approximate the anticipated operations of a commercial catalytic conversion process. The results obtained were intended to serve as preliminary input to an engineering effort aimed at developing and evaluating a conceptual catalytic char conversion process for hydrogen production. In the fluid-bed experiments, catalyst performance in two char conversion processing concepts were investigated. One concept involved use of a carbon dioxide acceptor together with an alkali catalyst to produce hydrogen and the second involved a resident catalyst in which only a sulfur absorber such as calcium carbonate is present with the catalyst and used to produce methane. In this second concept investigated, no regeneration or recalcination at temperatures above the steam gasification temperature are required. Two fluid-bed reactor systems were used to study catalyst performance. One was used to study performance at or near atmospheric reaction pressures while the second reactor was used for studies at elevated pressures up to 6 atmospheres. The results obtained from these studies are presented and discussed below in the remainder of this section.

6.1 CATALYST PERFORMANCE IN ATMOSPHERIC PRESSURE GASIFICATION REACTIONS

6.1.1 Catalyst Recyclability

Four catalyst systems, Na_2CO_3, K_2CO_3, Na_2CO_3 with CaF_2 and K_2CO_3 with CaF_2 were tested to determine their performance. An additional series of experiments using $Na_2B_4O_7$ catalyst were initiated, but this material showed only minimal catalyst activity and the series of experiments with this catalyst were not continued. The recycle experiments consisted of reacting dry mixed power mixtures with steam until essentially all of the char had been gasified, and then in the case of the acceptor gasification concept, exposing the reaction residues at 950°C to air for twelve to fourteen hours to decompose any calcium carbonate that was formed during steam gasification. Fresh

char was added to the calcined residue to reconstitute the test mixture and the mixture re-reacted with steam. This cycle was completed until the catalyst system was no longer active. In determining catalyst recycle performance for the resident catalyst or nonacceptor gasification, the 950°C recalcination treatment was omitted from the reaction cycle. The composition of initially prepared test mixtures were: 25% COED char, 65% calcium oxide and 10% catalyst. For experiments where fluorspar was used, test mixtures consisted of 24% COED char, 62% calcium oxide, 10% alkali catalyst and 5% calcium fluoride. The figure of merit used in measuring catalyst recycle performance was the same as that used in the fixed-bed reactor experiments, namely catalyst usage ratio, or the weight char that could be catalytically gasified over the number of reaction cycles completed per weight of alkali catalyst used.

The results obtained for the catalyst recycle performance tests are summarized in Table 6-1. As can be seen from the results sodium carbonate has the highest recyclability for both the calcined and noncalcined cases, and is able to catalytically gasify 25 and 33 times its weight of char for the resident catalyst and acceptor gasification concepts, respectively. Potassium carbonate on the other hand shows approximately half of the recyclability performance as the sodium salt. The superior recycle performance observed for Na_2CO_3 agrees with results obtained from the fixed-bed tests. As mentioned, the $Na_2B_4O_7$ series of recycle experiments were not completed since the catalyst showed only minimal activity in char gasification reactions. The effect on catalyst recyclability of exposing reaction residues containing catalyst to 950°C acceptor regeneration treatments seems to differ from that observed in fixed-bed experiments. For Na_2CO_3 and K_2CO_3 catalyst there appears to be a moderate improvement in recyclability rather than any reduction. Not enough reaction cycles were completed with the Na_2CO_3-CaF_2 catalyst system to determine the effect of acceptor regeneration and the slight decrease in usage observed for the K_2CO_3-CaF system is within the limits of experimental error. No explanation for the difference in observed results from the fixed-and fluid-bed reactor tests can be advanced at this time. Fluorspar addition also does not show a consistent effect in stabilizing alkali catalyst activity. For Na_2CO_3 a

Table 6-1. Fluid Bed Reactor Catalyst Recycle Performance for 650°C, Atmospheric Pressure Gasification Reactions

REACTION SYSTEM	USAGE RATIO[a]	
	NONCALCINED	950°C CALCINED
Na_2CO_3 - COED Char - CaO (10%, 25%, 65%)	25	33
Na_2CO_3 - CaF_2 - COED Char - CaO (10%, 5%, 24%, 62%)	20	12[b]
K_2CO_3 - COED Char - CaO (10%, 25%, 65%)	13	18
K_2CO_3 - CaF_2 - COED Char - CaO (10%, 24%, 62%)	23	20
$Na_2B_4O_7$ - COED Char - CaO (10%, 25%, 65%)	0[c]	-

[a] Weight char catalytically gasified per weight alkali catalyst used.

[b] Series incompleted; catalyst still active last reaction cycle completed.

[c] Catalyst showed no activity in four experiments.

small decrease in catalyst recyclability is observed with CaF_2 addition for the noncalcining case while for K_2CO_3, CaF_2 approximately doubles catalyst activity. Little improvement is observed for K_2CO_3 catalyst with 950°C acceptor regeneration. While additional work appears needed to confirm and square some of the fluid-bed results with those obtained from fixed-bed experiments, catalyst recycle performance results from both studies show generally that high catalyst usage ratios and activities can be obtained through use of simple admixed catalyst systems and may recycle without resorting to solution extraction procedures for recovery of catalyst.

6.1.2 Product Gas Composition and Approach to Water-Gas Equilibria For Alkali Catalyzed Gasification Reactions

Data from the atmospheric pressure fluid-bed gasifier experiments were reduced to obtain the specific gasification rates (grams char gasified per gram char in bed per hour), specific water feed rates (grams water per gram char per hour), steam utilizations (%) and the apparent water gas equilibrium constant. These data, together with the gasifier product composition, provide considerable information on the performance of the catalytic fluid-bed reactor. These factors are discussed below.

Figures 6-1 through 6-4 show the H_2, CH_4, CO, and CO_2 product gas composition (volume percent on a dry basis) from the reactor as a function of carbon utilization and the specific steam rate (gms steam/hr/gm carbon in the bed). The specific steam rate is related to the carbon utilization by the equation:

$$Sp_{H_2O} = H_2O_{in}/(1-X)\cdot W\cdot \xi)$$

where

Sp_{H_2O} = specific steam rate (gm/gm-hr)

H_2O_{in} = steam feed rate (gm/hr)

X = fraction of char reacted

W = initial weight of char in the bed (gms)

ξ = weight percent of carbon in the char

For the particular experimental arrangement used in these experiments the specific steam rate is inversely proportional to the carbon utilization. A continuously fed fluid-bed reactor experiment would have a different form for this equation.

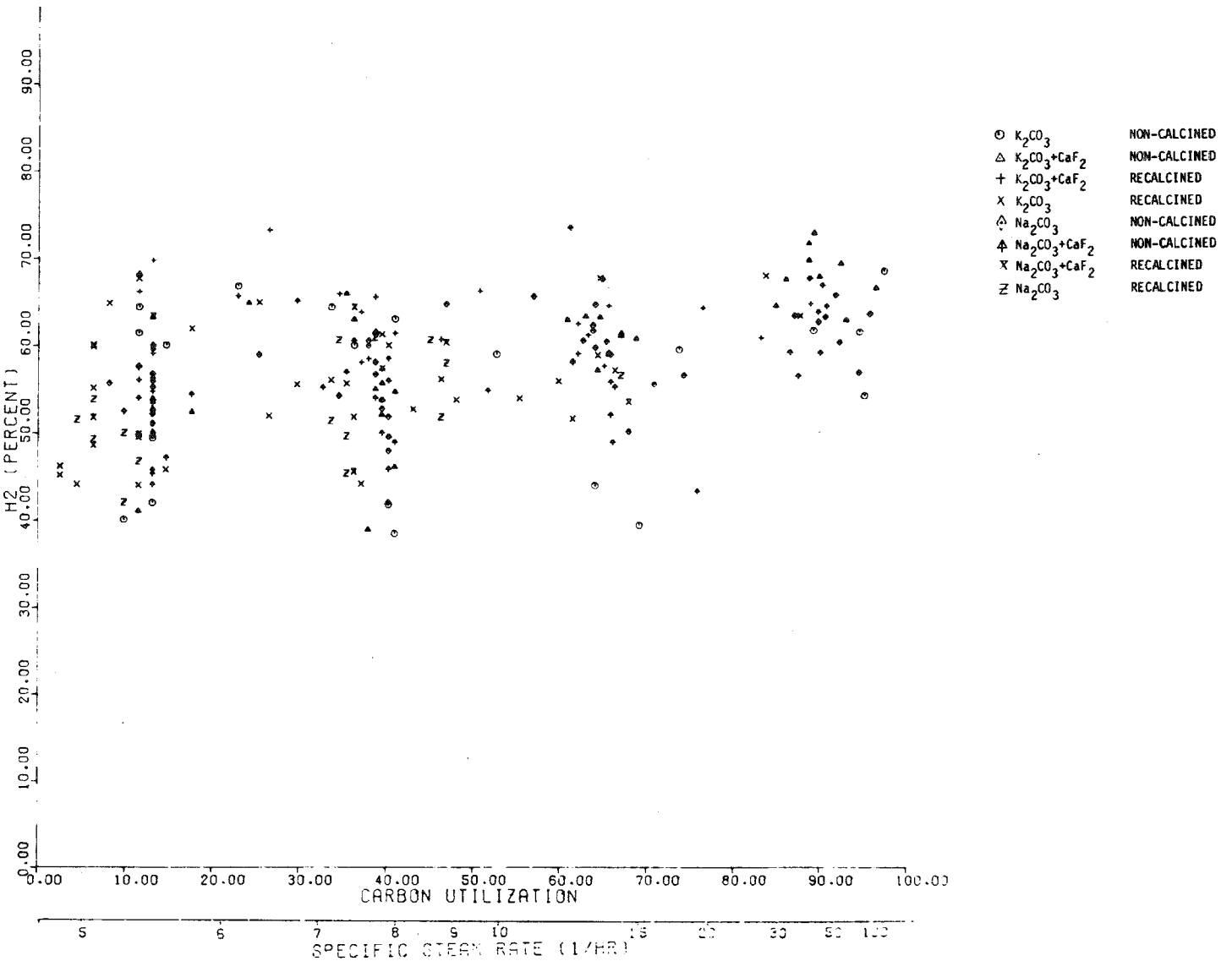

Figure 6-1. H_2 Percent As a Function of Carbon Utilization and Specific Steam Rate

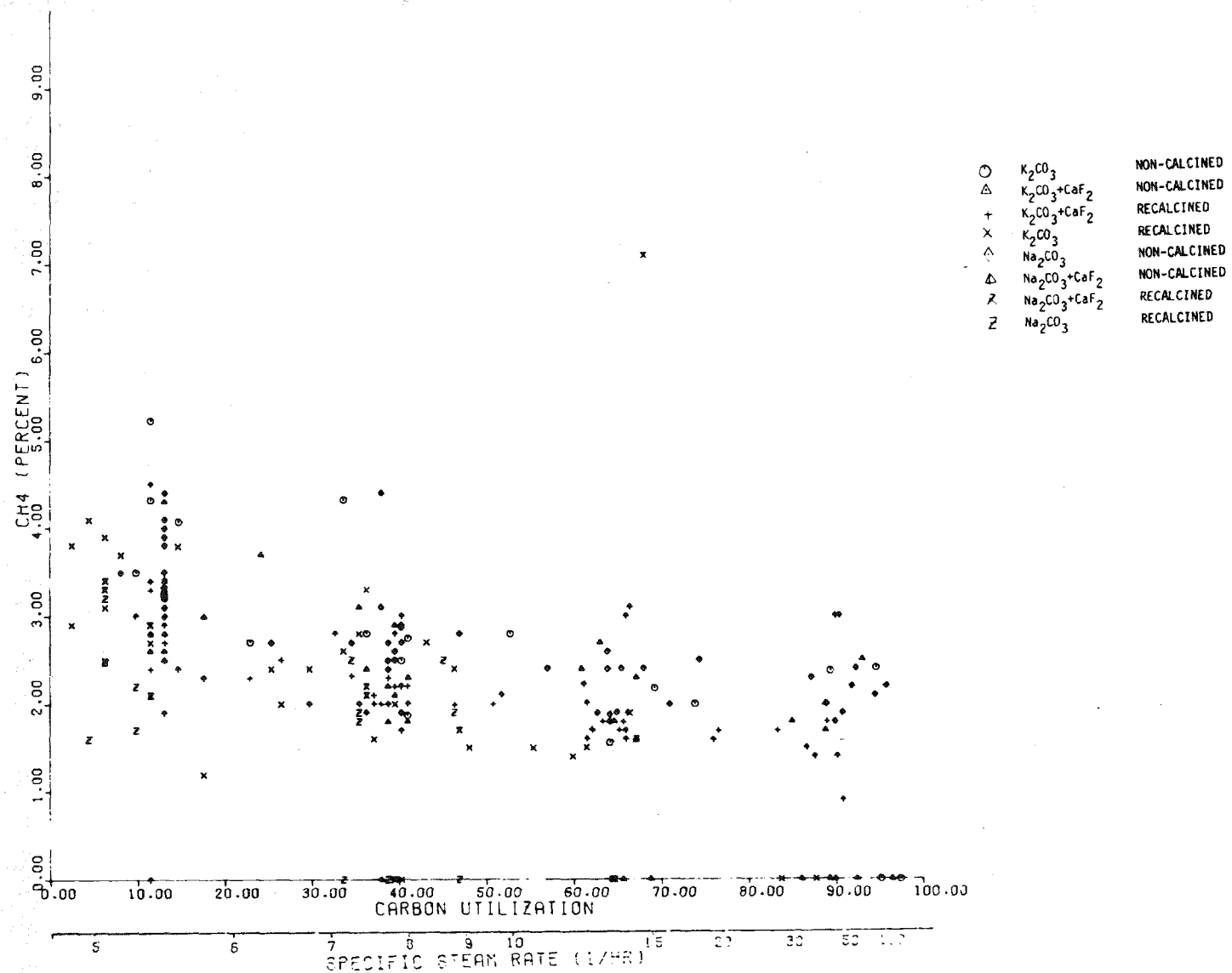

Figure 6-2. CH_4 Concentration as a Function of Carbon Utilization and Specific Steam Rate

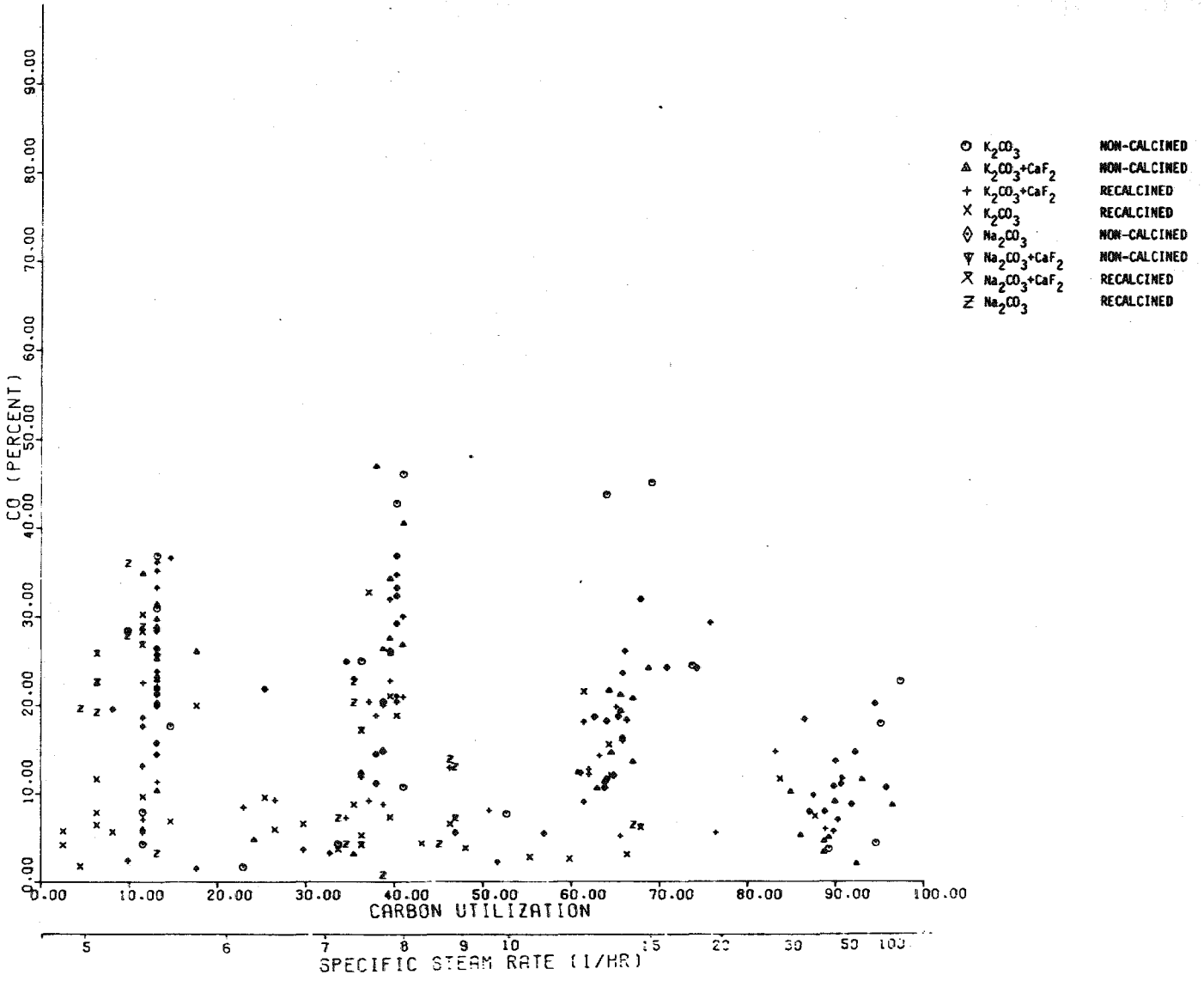

Figure 6-3. CO Concentration as a Function of Carbon Utilization and Specific Steam Rate

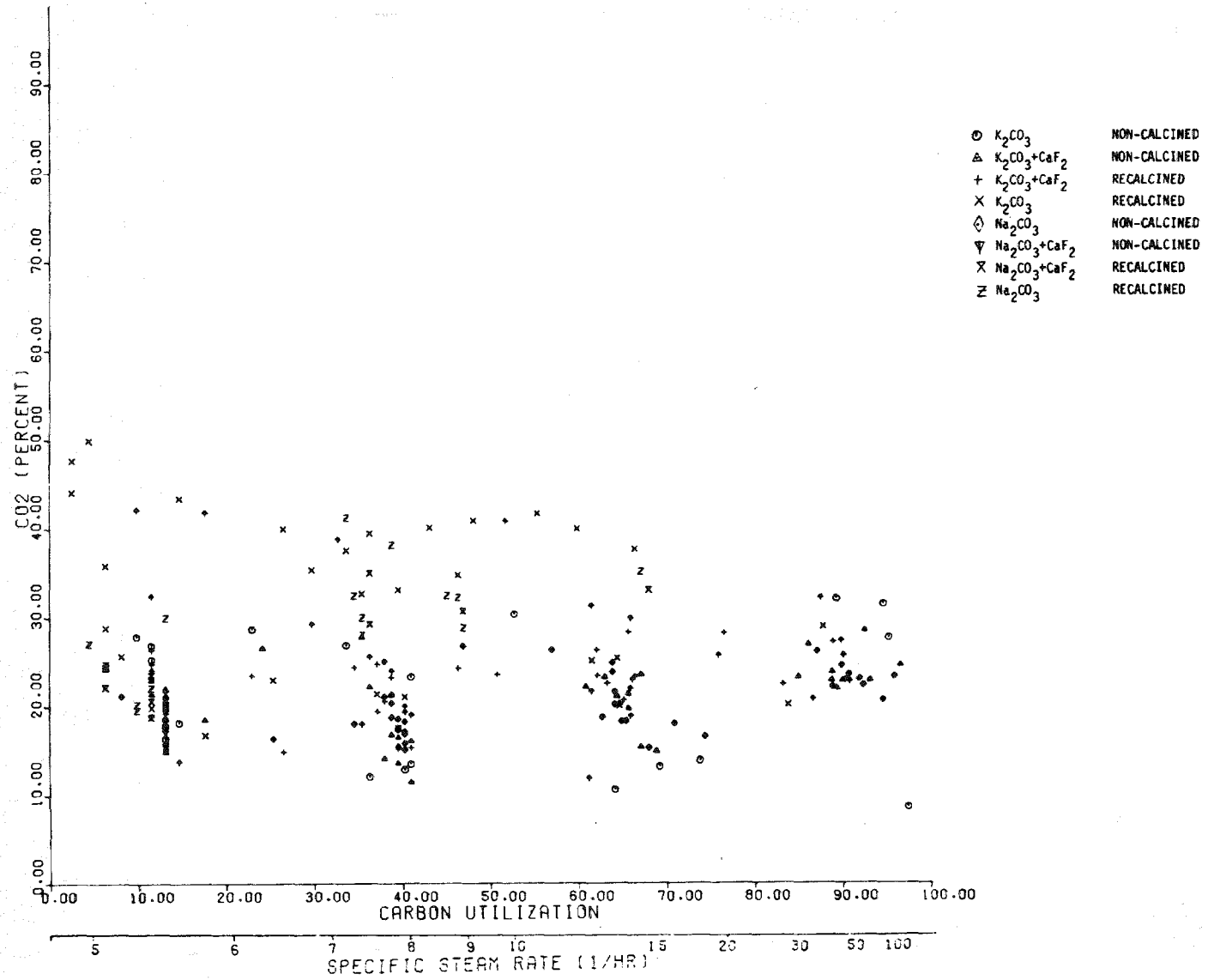

Figure 6-4. CO_2 Concentration as a Function of Carbon Utilization and Specific Steam Rate

For all catalysts and both conversion process concepts the gas composition is similar with the exception of the experimental series using recalcined K_2CO_3 catalyst. In this series the concentrations of CO are too low while those of CO_2 are too high in comparison to the other series. A gas chromatograph calibration error is suspected. With the exception of this series a fairly consistent pattern emerges. In Figure 6-1 the hydrogen percent in the gasification products is seen to increase from a mean value of 55% to a mean value of 65% as the carbon utilization changes from 5% to 95%. This change in the carbon utilization corresponds to a change in the specific steam rate of 5 to 100 (hr^{-1}). Figure 6-2 shows that the mean methane concentration varies from 3.5% to 2% for the same range of carbon utilization.

Figures 6-3 and 6-4 show that the carbon monoxide and carbon dioxide concentrations, unlike the H_2 and CH_4 composition curves, have a fair degree of scatter in the observed values. Much of the variation as previously mentioned is due to the series using K_2CO_3 with recalcining. Neglecting this series reduces the scatter and mean values for CO show a decrease from 25% to 10% as the carbon utilization increases from 5% to 95%. At the same time the CO_2 concentration, shown in Figure 6-4, increases from 20% to 25%. This observed behavior is consistent with the increasing unreacted steam in the reactor effluent which occurs with increasing specific steam rate. In other words with an increasing excess of steam available for the water gas shift reaction more CO is shifted to CO_2 thus lowering the CO content in the product gas while increasing the H_2 and CO_2 concentrations.

These data show very little difference in ability of the acceptor to remove CO_2 from the gasification products between the calcined and uncalcined experiments. Indeed, for most of the recalcining experiments, calculations based on the CO and CO_2 contents in the effluent gas indicate about 5%-10% removal. This small CO_2 removal is not consistent with the pressurized experiments in which 60% or more of the CO_2 is removed. This inconsistency is discussed further below. The major effect on the gas composition is governed by the acceptor performance. When the acceptor is removing CO_2 as was the case at elevated pressure, very high purity hydrogen, 95% and higher,

is obtained. With low acceptor performance, as was observed in these initial atmospheric pressure experiments, the hydrogen yield is around 60%. Clearly, obtaining high acceptor performance is important in order to obtain high H_2 yields.

It is interesting to compare the gas composition measured in these experiments with those reported for several uncatalyzed commercial scale reactors. Figures 6-5, 6-6 and 6-7 show the calculated equilibrium constant as a function of temperature and measured values for the reactions:

$$CO + H_2O \leftrightarrows CO_2 + H_2 \qquad K_1 = \frac{[CO_2]\,[H_2]}{[H_2O]\,[CO]}$$

$$CO_2 + C \leftrightarrows 2CO \qquad K_2 = [CO]^2/[CO_2]$$

$$2H_2 + C \leftrightarrows CH_4 \qquad K_3 = [CH_4]/[H_2]^2$$

These data were compiled by Crawford et al[10] and taken from 63 IGT tests on Illinois No. 6 char and 32 ESSO tests on Disco (Pittsburgh) char. The range of ratios found in this investigation are also shown in the figures. The mean value for K_1 computed from these experiments was one-half of the equilibrium value and is very close to that reported in the other work. The range of K_1 values from these experiments is rather large since no attempt was made to smooth and screen the data. This result suggests that it may be beneficial to incorporate a shift catalyst in order to improve the hydrogen yield.

The mean value of K_2 is about equal to the calculated equilibrium value, although at high specific steam rate it decreases to 20% of the equilibrium value. This is much higher than the IGT and ESSO data. This implies that the catalysts accelerate the carbon-dioxide-carbon reaction. This is consistent with acceleration of steam-carbon reaction. One expects both reactions to be accelerated since a similar kinetic mechanism is probably involved.

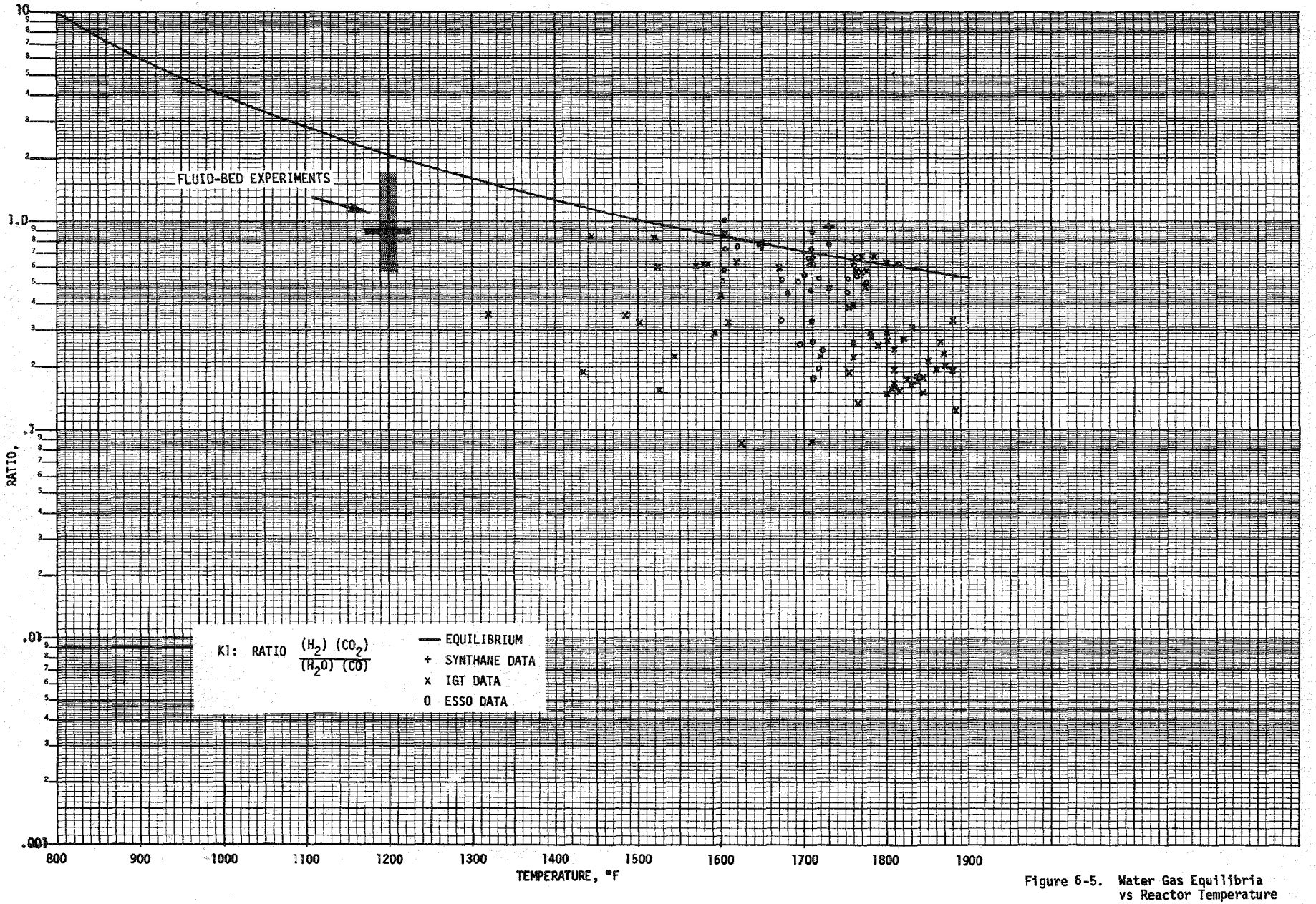

Figure 6-5. Water Gas Equilibria vs Reactor Temperature

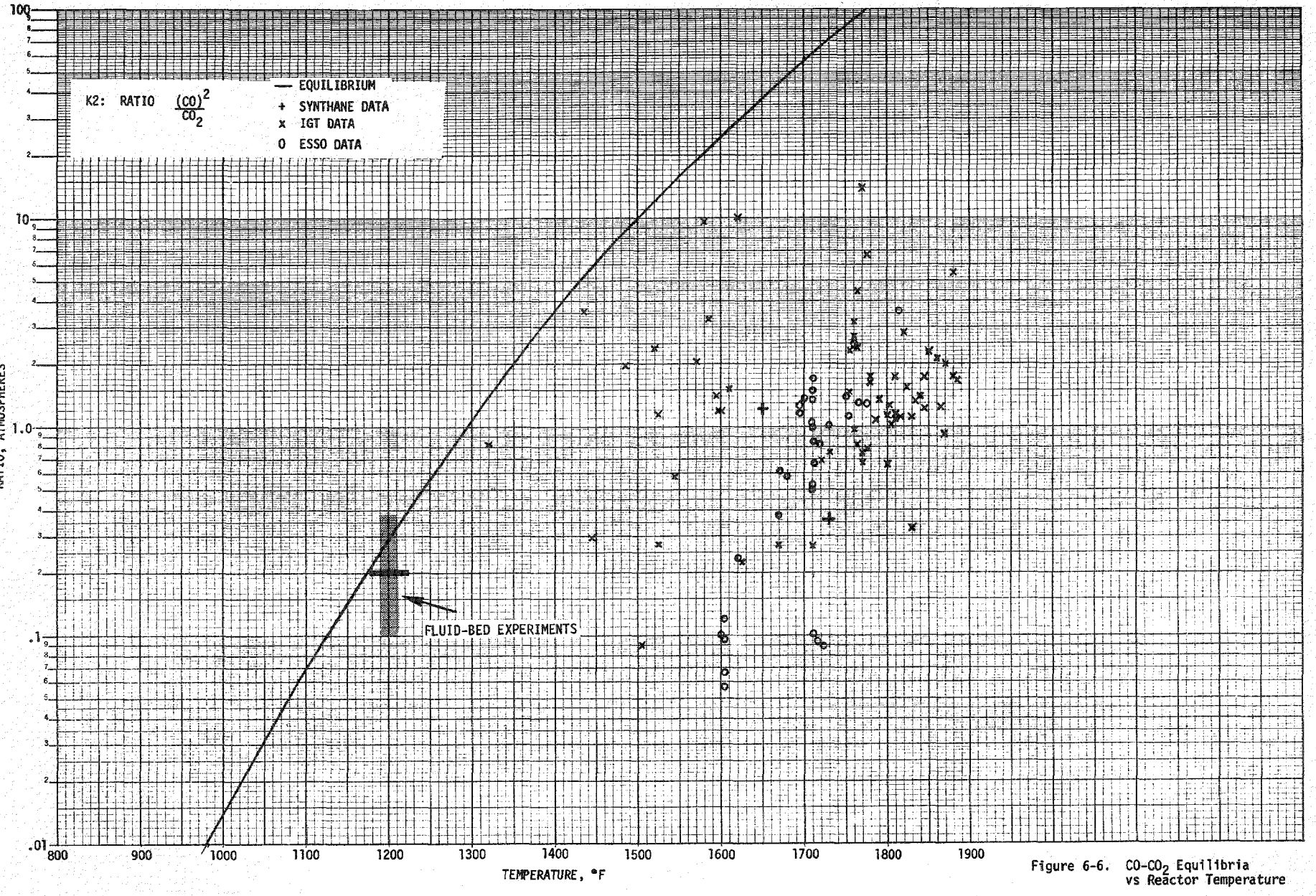

Figure 6-6. $CO-CO_2$ Equilibria vs Reactor Temperature

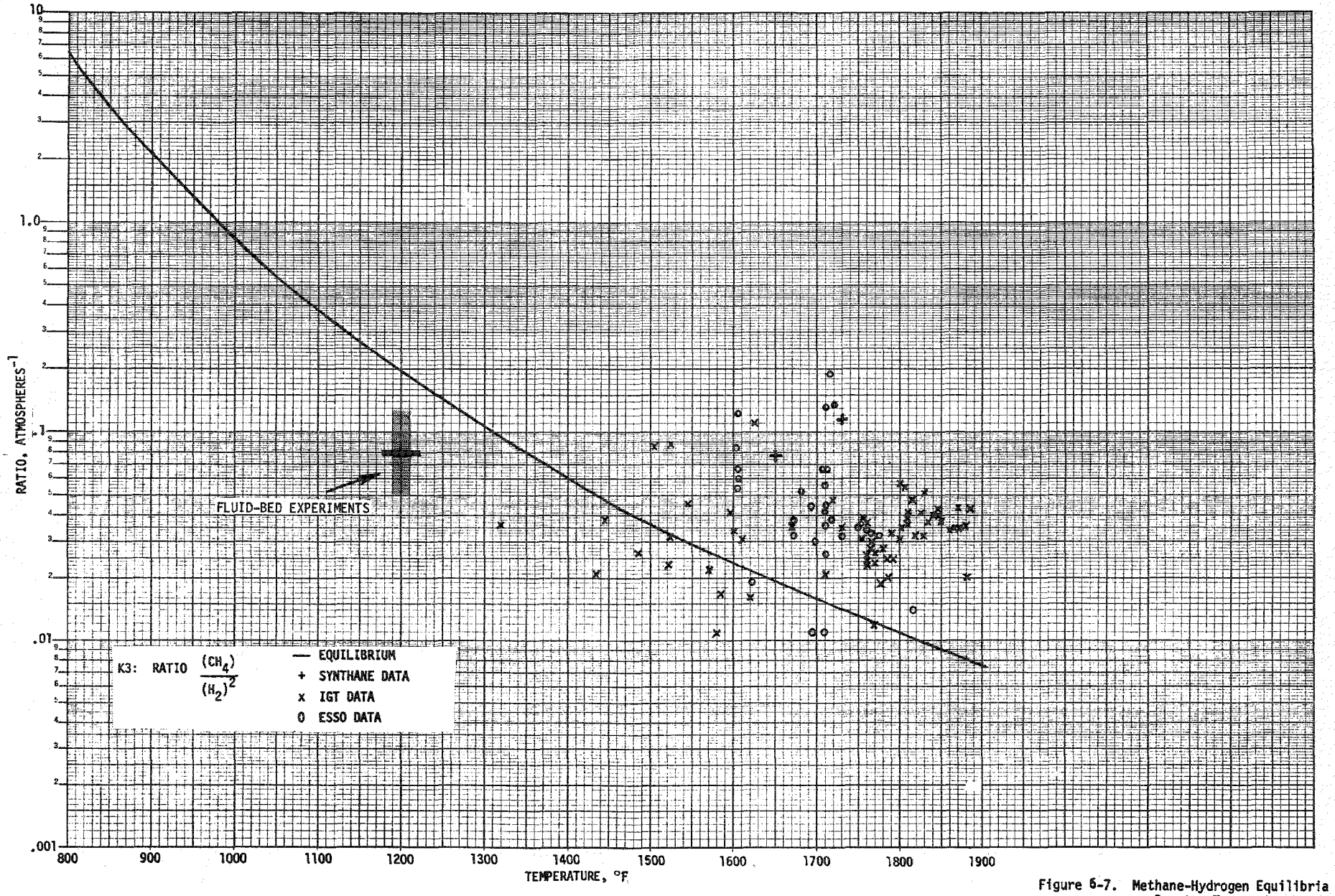

Figure 6-7. Methane-Hydrogen Equilibria vs Reactor Temperature

The observed value for the ratio of CH_4/H_2^2 approaches the equilibrium value initially but decreases as the gasification reaction progresses. This is in contrast to IGT and ESSO data which generally tend to get greater than equilibrium methane concentrations. One possibility here is that for the IGT and ESSO data, methane is formed by hydrogen position shift during the carbon ring fracture rather than the reaction of gaseous H_2 with graphite carbon. In the absence of a catalyst the methane could then persist in above equilibrium concentrations. Alkali catalysts are known to be good reforming catalysts. This may explain why greater than equilibrium concentrations of methane are not observed in these catalytic gasification experiments.

6.1.3 Catalyst Effect on Gasification Rates and Steam Utilization

The calculated specific gasification rates and the percent steam utilization for the K_2CO_3 + CaF_2 catalyst with recalcining are shown in Figures 6-8 and 6-9 as a function of carbon utilization. Curves presented for this catalyst are typical of the results obtained for other systems. The gasification rate for all experiments is seen to rise during the transient heat up of the reactor for both the catalyzed and uncatalyzed char. At about 10%-20% carbon utilization, the uncatalyzed rate becomes stable and then decreases to zero around 60% carbon gasification. The catalyzed rate however, never goes to zero and is alway greater than the uncatalyzed rate. Despite considerable variation in the catalyzed rate, it is seen that the trend is toward stable or increasing gasification with increasing carbon utilization. (This variation in the gasification rate may result from bubbling or slugging in the fluid-bed.) A conclusion to be drawn from a comparison of the catalyzed and uncatalyzed rates is that for the char and temperature selected, gasification beyond 60% of the original carbon present is not possible without a catalyst at the temperatures employed in these experiments. Chars of different reactivity may show different maximum uncatalyzed utilizations.

Another useful way to examine the rate data is to plot $\ell n\ C/C_o$ versus time, where C is carbon present at time T and C_o is the initial carbon inventory. In cases in which the gasification reaction is not steam limited but is a first order reaction in the carbon concentration a straight line

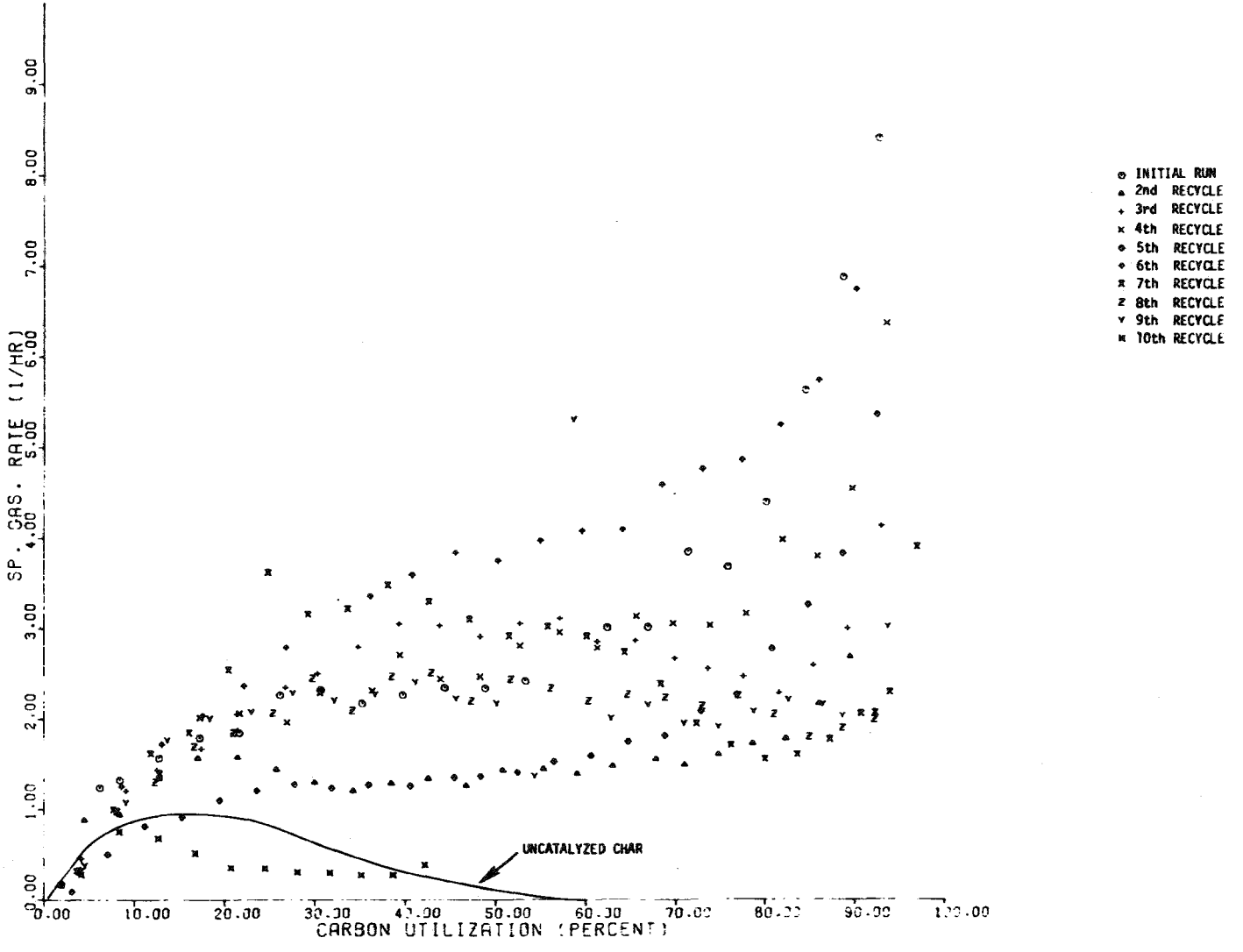

Figure 6-8. Specific Gasification Rate Versus Carbon Utilization for $K_2 CO_3$ + CaF_2 Catalyzed Reaction (Nonrecalcining Case).

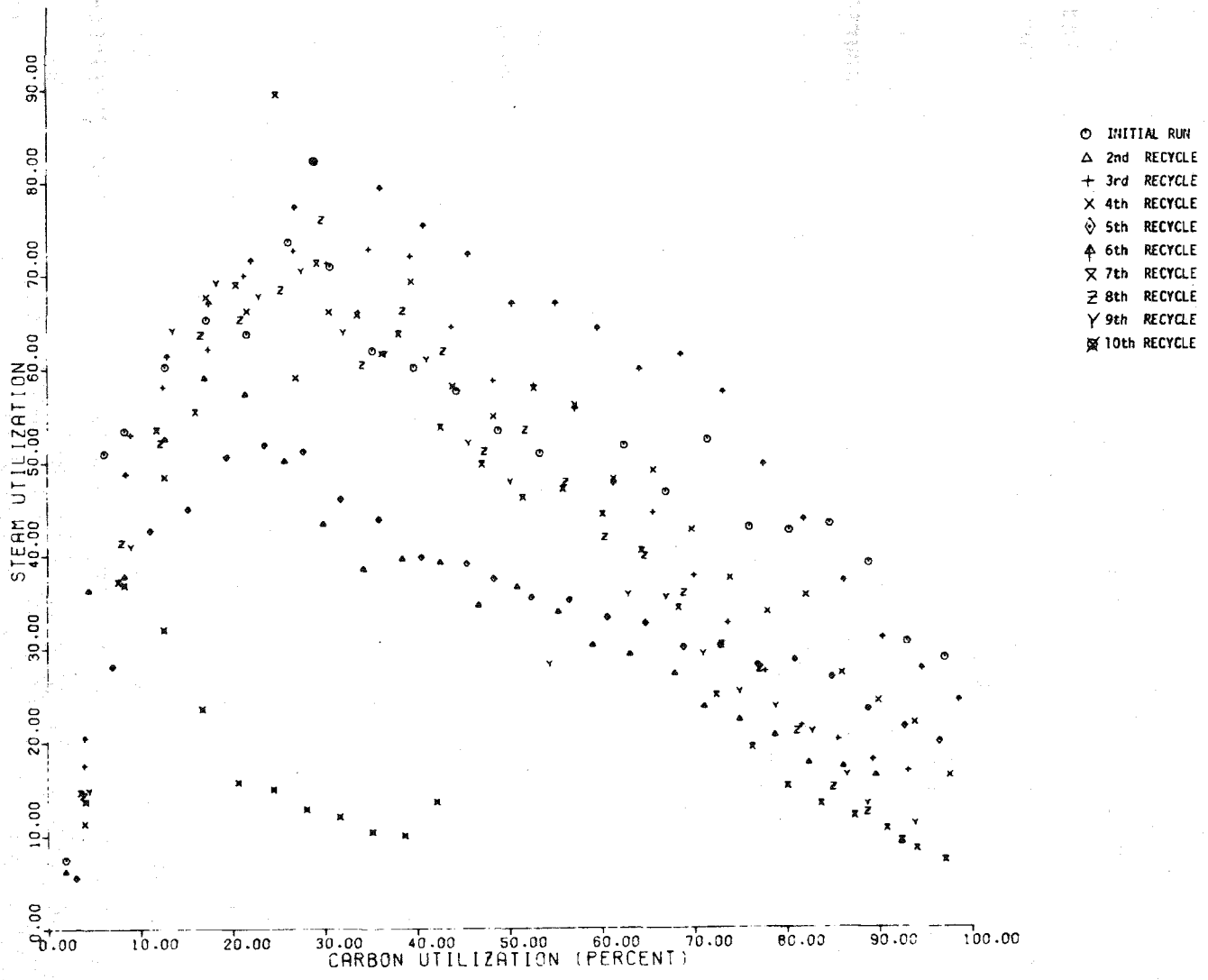

Figure 6-9. Steam Utilization Versus Carbon Utilization for K_2CO_3 + CaF_2 Catalyzed Reactor (Nonrecalcining Case).

will result with the slope equal to the specific gasification rate. The data of Figure 6-8 is replotted in this fashion in Figure 6-10.

A typical steam utilization vs carbon utilization curves are plotted in Figure 6-9 for the K_2CO_3 - CaF_2 catalyzed reaction. For all experiments steam utilization is seen to increase early in the reaction and then decrease during the later stages of gasification. This result is expected from considerations of the specific gasification rate. The gasification rate is constant or slightly increasing (in the catalyzed case), but the amount of char present in the bed decreases in relation to the fraction char remaining. Since the amount of steam fed to the system is constant, the amount reacted or the utilization should decrease as observed. Of course when the gasification rate goes to zero, as in the uncatalyzed case, the steam utilization also goes to zero.

The very high utilization early in the experiment indicates that the steam feed rate was just barely enough to ensure that the reactions were not steam feed limited. In the pressurized experiments the steam feed rate was increased to achieve good fluidization, and considerably lower steam utilizations were obtained. This is discussed in Section 6.2.2. Steam utilization data for other series have been reported earlier.[11]

6.1.4 Char Sulfur Retention

In addition to activity and recyclability another performance property that was assessed for catalyst-acceptor systems using a fluidized-bed reaction medium, was system sulfur retention capability. In order for catalytic gasification to be an economically viable approach for deriving synthetic fuels from coal, catalyst systems are going to have to perform multiple functions. Sulfur retention is an important auxiliary catalyst-acceptor performance function for a conversion process since post gasification cleanup operations of product gas streams will be energy inefficient and add a significant cost to the price of the desired product. While complete retention of char sulfur as a solid product by an absorber-catalyst system during gasification can probably never be achieved, retention of the bulk of the sulfur at this stage can greatly reduce the energy inefficiency

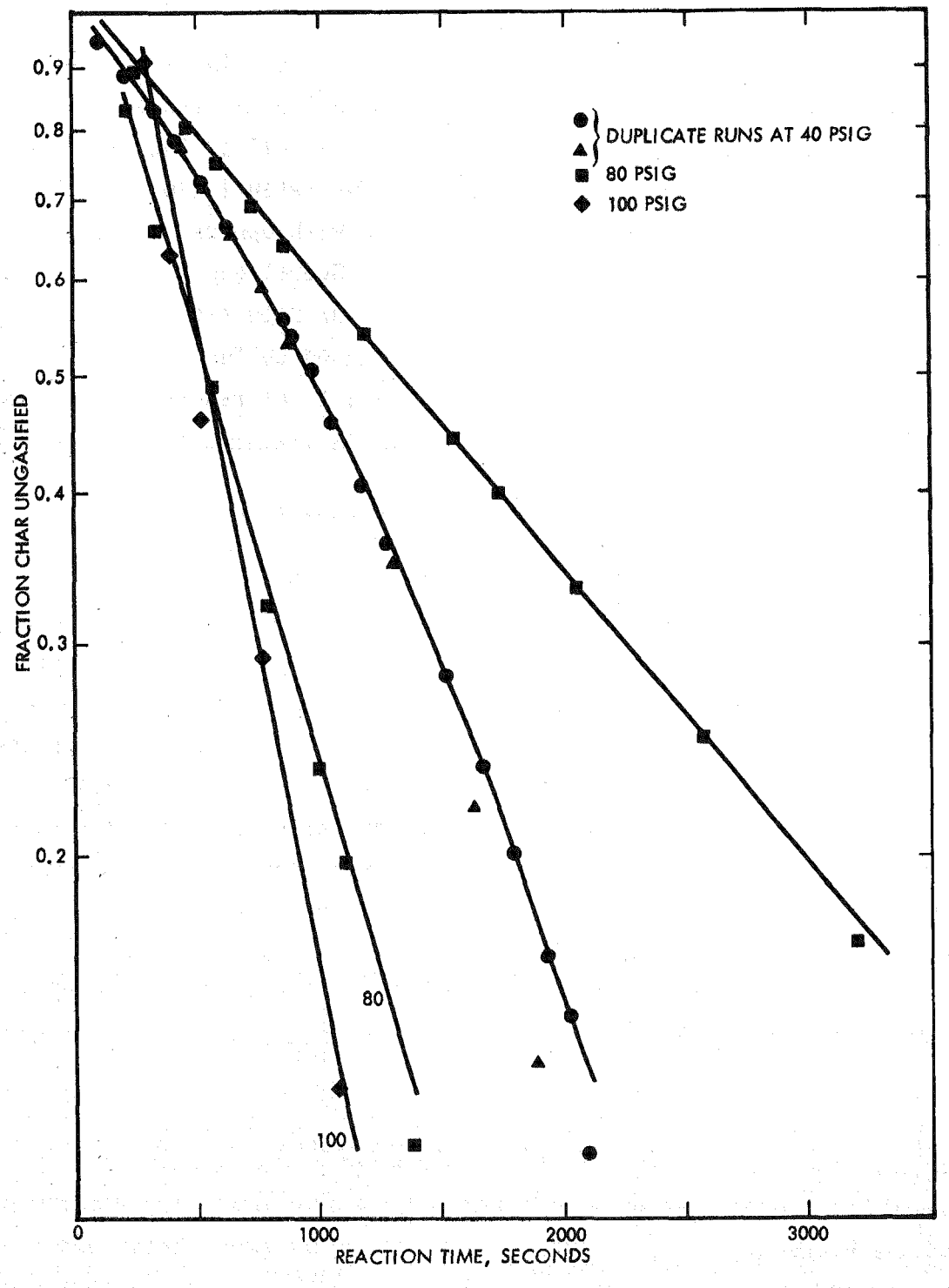

Figure 6-10. Carbon Content Versus Reaction Time for K_2CO - CaF_2 Catalyzed Gasification Reaction

of post gasification sulfur removal and minimize its cost impact on the product.

The high sulfur retentions achieved using a batch fluid-bed reactor with several different catalyst systems are summarized in Table 6-2. A steam gasification temperature of 650°C was used in all of the experiments. As can be seen from the results presented, sulfur retention by acceptor-catalyst systems was generally greater than 50% with approximately 11% utilization of acceptor for sulfur absorption. Operations at elevated pressure can be expected to further improve sulfur retention and acceptor utilization. These results not only show that good sulfur retention can be obtained with these catalyst-acceptor systems, but the results also demonstrate catalyst activity and recyclability in the presence of sulfur.

6.2 CATALYST PERFORMANCE IN ELEVATED PRESSURE GASIFICATION REACTIONS

Two series of experiments were performed to show the effects of elevated reaction pressure on char gasification kinetics, product composition and catalyst recyclability. For the elevated pressure experiments fresh mixtures of 6.25 g of COED char, 16 g of CaO acceptor, and 2.5 g of K_2CO_3 catalyst were used for each experiment. In the recycling experiments the material in the reactor from the previous run was recalcined at 950°C and fresh char was added to achieve the same weight ratio of char to mixture as in the original experiment. The steam reaction temperature was 650°C in all cases and steam flow rate was adjusted with pressure to provide a superficial fluidizing velocity of 0.5 fps. The steam mass flow rates needed to achieve this fluidizing velocity and the initial specific steam rate for various reaction pressures are summarized in Table A-7 in the Appendix.

It should be noted that the fluidizing velocity of .5 fps is 2.5 times larger than that used in the smaller atmospheric pressure reactor. The greater disengagement height in the larger (elevated pressure) reactor permitted the higher velocity. Better fluidization and more consistent results were obtained at the higher fluidizing velocity using the same sample size as was used in the atmospheric pressure reactions.

Table 6-2. Char Sulfur Retention for Catalyst-Acceptor System Using Fluid-Bed Gasifier

Catalyst-Acceptor System	950°C Acceptor Regeneration	Number of Reaction Cycles	% Sulfur Retention[a]	% Acceptor Utilization[b]
Na_2CO_3 - CaO	No	12	56	13
Na_2CO_3 - CaF_2-CaO	No	11	68	14
K_2CO_3 - CaO	Yes	9	60	10
K_2CO_3 - CaF_2- CaO	No	10	36	7
K_2CO_3 - CaF_2 - CaO	Yes	9	50	9

[a] Computed as ratio of weight sulfur found in reaction residue after nth reaction cycle to weight sulfur fed from char times 100. FMC COED char used all cases (ultimate analysis: 2.83% total sulfur).

[b] Computed as ratio moles sulfur retained after nth reaction cycle to moles lime charged times 100.

6.2.1 Product Gas Composition and Acceptor Utilization

Figure 6-11 shows the composition of the product gas as a function of the percent carbon gasified. It is seen in all cases that the hydrogen content is initially high and then drops off to 60-70% as the CaO absorber saturates with CO_2. Increasing reaction pressure increases substantially the hydrogen yield owing to increased absorption of CO_2 by the acceptor. At 100 psig 98% H_2 is obtained during gasification of 70% of the carbon charged to the reactor. Examining hydrogen and CO_2 composition of the product gas for the different pressures, it is seen that the knee in the H_2 curves shifts to higher reaction extents with increased pressure. At atmospheric and 40 psig pressure the knee occurs 40% carbon gasified, at 80 psig 50%, and at 100 psig at 70%. Thus increasing the pressure to 100 psig doubled the amount of CO_2 free H_2 that could be obtained. This change in the hydrogen concentration reflects an increase in acceptor performance with pressure, and not a change in the equilibrium gas compositions. Once the acceptor saturates and no longer removes CO_2 the gas composition is approximately the same as for the atmospheric experiments when no recalcining is employed. As previously discussed, performance of the acceptor is not consistent between identical experiments conducted in the large and small fluid-bed reactors. More CO_2 removal is obtained in the larger reactor even when operated at atmospheric pressure. The improvement in carbon dioxide absorption is probably due to a longer gas residence time in the larger reactor.

As can be seen from Figure 6-11, reactor pressure has little or no effect on the product gas methane and carbon monoxide compositions. The constant methane composition in the product gas is somewhat unexpected since higher reaction pressures should favor high methane yields from both char and carbon monoxide hydrogenation reactions. Since the methane yields do not increase with pressure, methane production from these reactions can be assumed to be rate limited and insignificantly affect product composition under the experimental conditions employed. By contrast, the water gas shift reaction should be unaffected by pressure and a reasonably constant value of carbon monoxide should be expected in the product gases. This is indeed observed. A level between 5 to 10% CO is always present. The

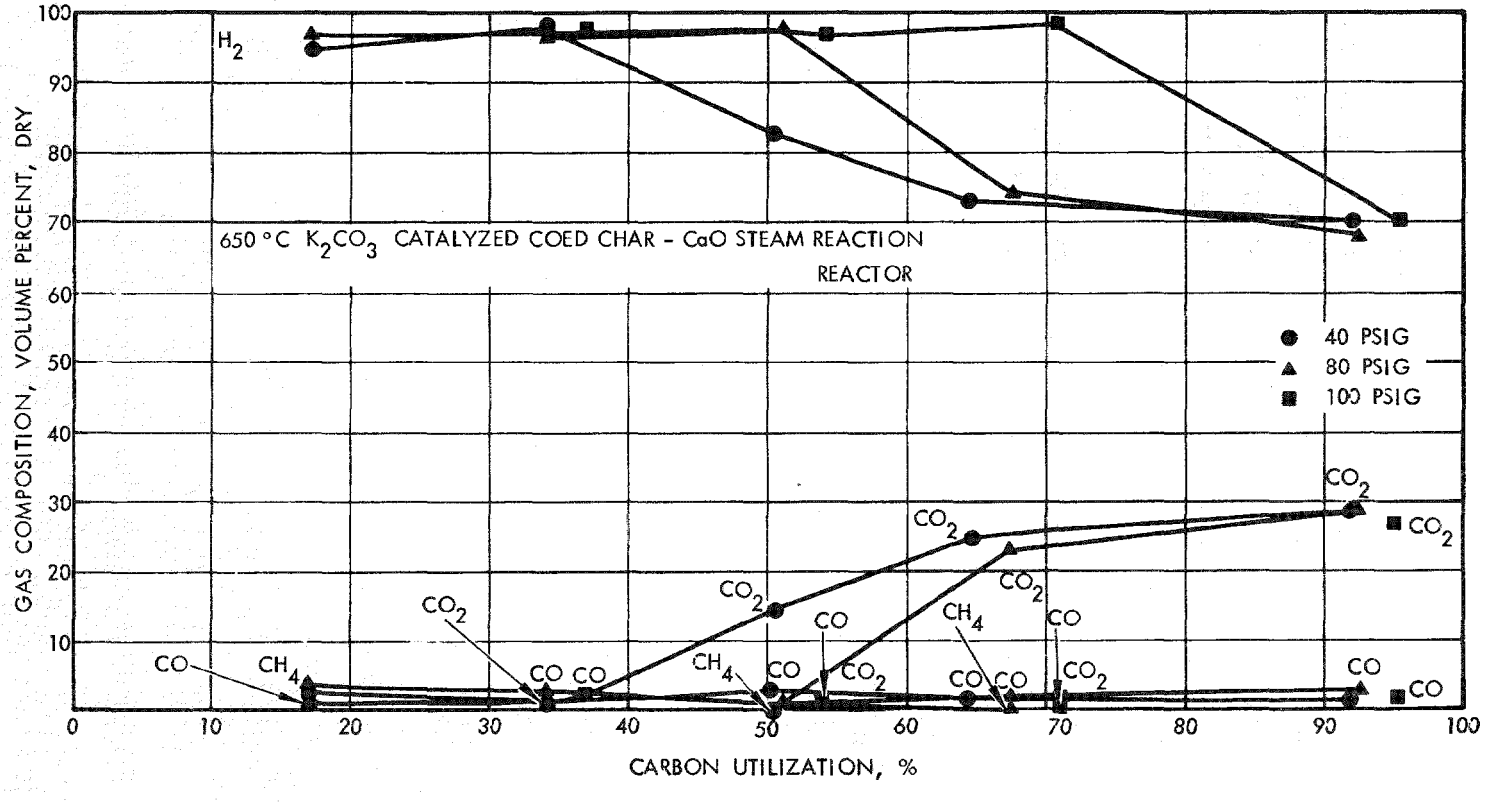

Figure 6-11. Product Gas Composition Versus Carbon Utilization Curves for Elevated Pressure Gasification Reactions.

level of carbon monoxide, however in the product gas stream is not solely determined by the water gas reaction. While the carbon dioxide acceptor is functioning, the CO_2 level should be established by decomposition pressure of calcium carbonate. At 650°C, CO_2 pressure above $CaCO_3$ is only a few torr, thus the water gas shift reaction should be driven far to the right, favoring increased H_2 production. This is generally what is being observed while the acceptor is absorbing well. The residual level of CO_2 found in the product gas is due to either a kinetically limited shift reaction which occurs downstream of the fluidized-bed reactor zone, or by a limited uptake rate of CO_2 by the acceptor.

The effects of elevated reaction pressure on the K_2CO_3 catalyzed gasification rate can be seen in Figure 6-12 where specific gasification rate is plotted as a function of the fraction of carbon gasified for various reaction extends. It is seen that the specific gasification rate increases from around 2.5 hr^{-1} to about 7 hr^{-1} as the reactor pressure is increased from atmospheric to 80 psig. It is generally accepted that the uncatalyzed specific gasification rate may be expressed by the equation:

$$\frac{1}{C}\frac{dC}{dt} = \frac{k_1 P_{H_2O}}{1 + K_2 P_{H_2O} + k_3 P_{H_2}}$$

Where C equals carbon inventory.

In a fluidized-bed, such as was used in these experiments, the recirculation coal char encounters an almost pure steam environment at the bottom of the bed. Thus the inhibiting effect of the hydrogen is not present, and the hydrogen term in the above expression may not be important. The form of the specific gasification expression neglecting the hydrogen inhibition suggests that the gasified rate should be proportional to the steam partial pressure when $k_2 H_2O << 1$, and approach a constant value of k_1/k_2 when $k_2 << 1$. The data presented in Figure 6-12 are really insufficient to evaluate the applicability of this equation quantitatively, but the increase of reaction rate observed with increasing reactor pressure is consistent with the uncatalyzed rate expression.

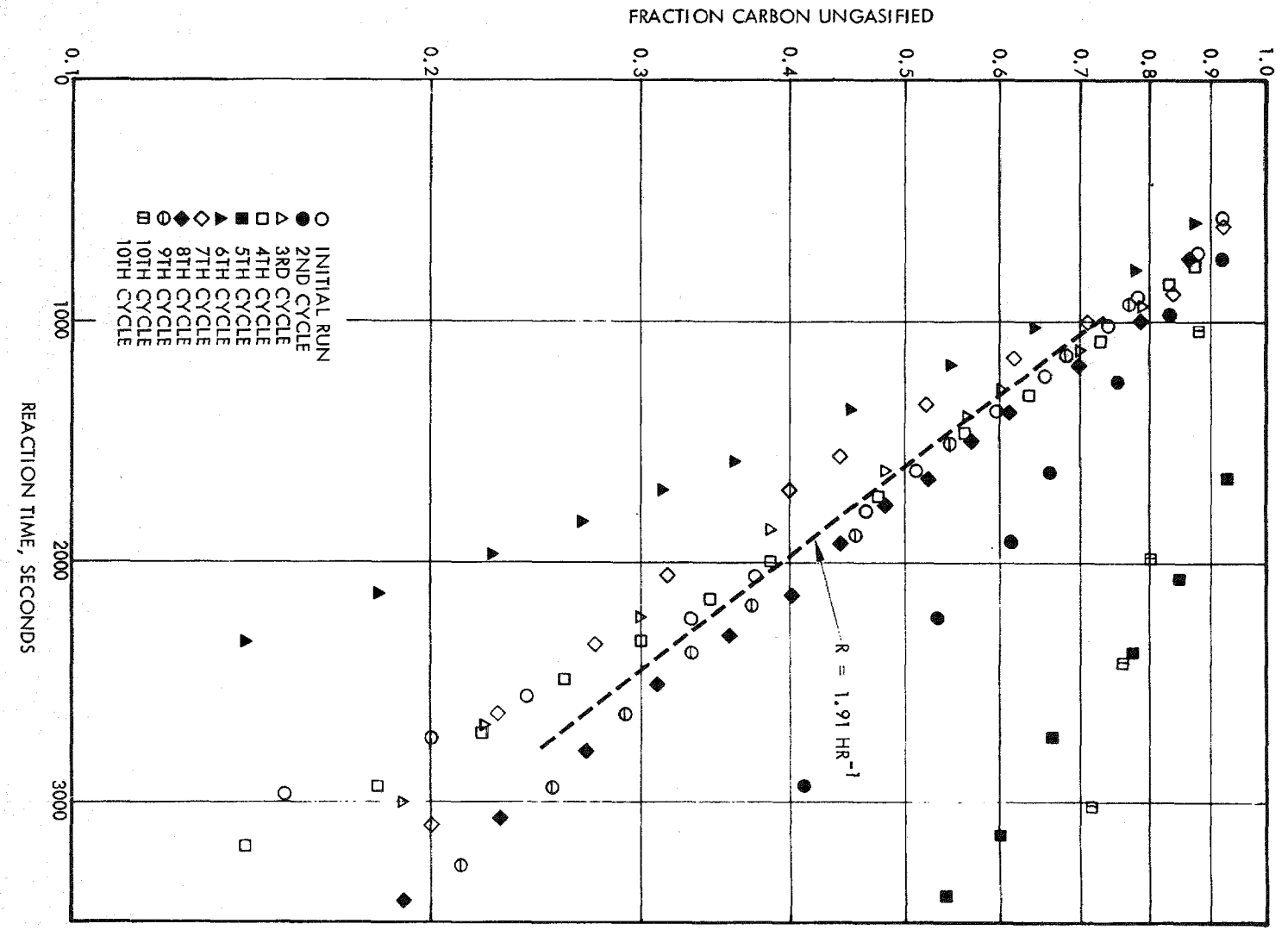

Figure 6-12. Variation of Specific Gasification Rate with Reaction Extent for Elevated Pressure Reactions

Figure 6-12 also shows the baseline uncatalyzed reaction rates for three different pressures. In each case a similar behavior is seen. Initially the gasification is high and appears to be the same order of magnitude as the catalyzed rate. After 10 to 20% of the char has been gasified the uncatalyzed reaction drops to very low values. The reaction rates are so low for this remaining char fraction that it is virtually unreactable at these conditions. To gasify this remaining char fraction would require considerably higher reaction temperatures.

6.2.2 Gasification Rates and Steam Utilizations

The integrated form of the first order rate expression is

$$\frac{C}{C_o} = e^{-kt}$$

where C/C_o equals the fraction of carbon remaining and k equals the specific gasification rate constant. Thus, as shown with the atmospheric data, a semi-log plot of C/C_o vs t (time) should be a straight line with the slope equal to -k. This plot is shown in Figure 6-13, and it is seen that a reasonable approximation to this expression is obtained. At high utilizations, i.e., with small amounts of the original carbon remaining in the bed, the curves tend to bend downward which implies increasing reaction rates as the carbon is depleted. This could in fact be the case owing to an increasing catalyst : char ratio or it could result from errors in calculating the carbon utilization. Errors in calculating the carbon utilization, especially near the end of the reaction, would cause the calculated specific gasification rate to be too high.

It is interesting to note that the specific gasification rate, measured in the fixed-bed experiments, was found to be a 2 hr^{-1}. This was at atmospheric pressure and compares quite closely with the value of 2 to 3 hr^{-1} measured in these experiments for the same conditions.

Steam utilizations are shown in Figure 6-14 as a function of reaction extent for various reaction pressures. The curves are similar to those observed for the atmospheric experiments performed using the smaller reactor except that value of the utilizations are lower due to the higher fluidizing velocities and greater steam densities employed at elevated pressure.

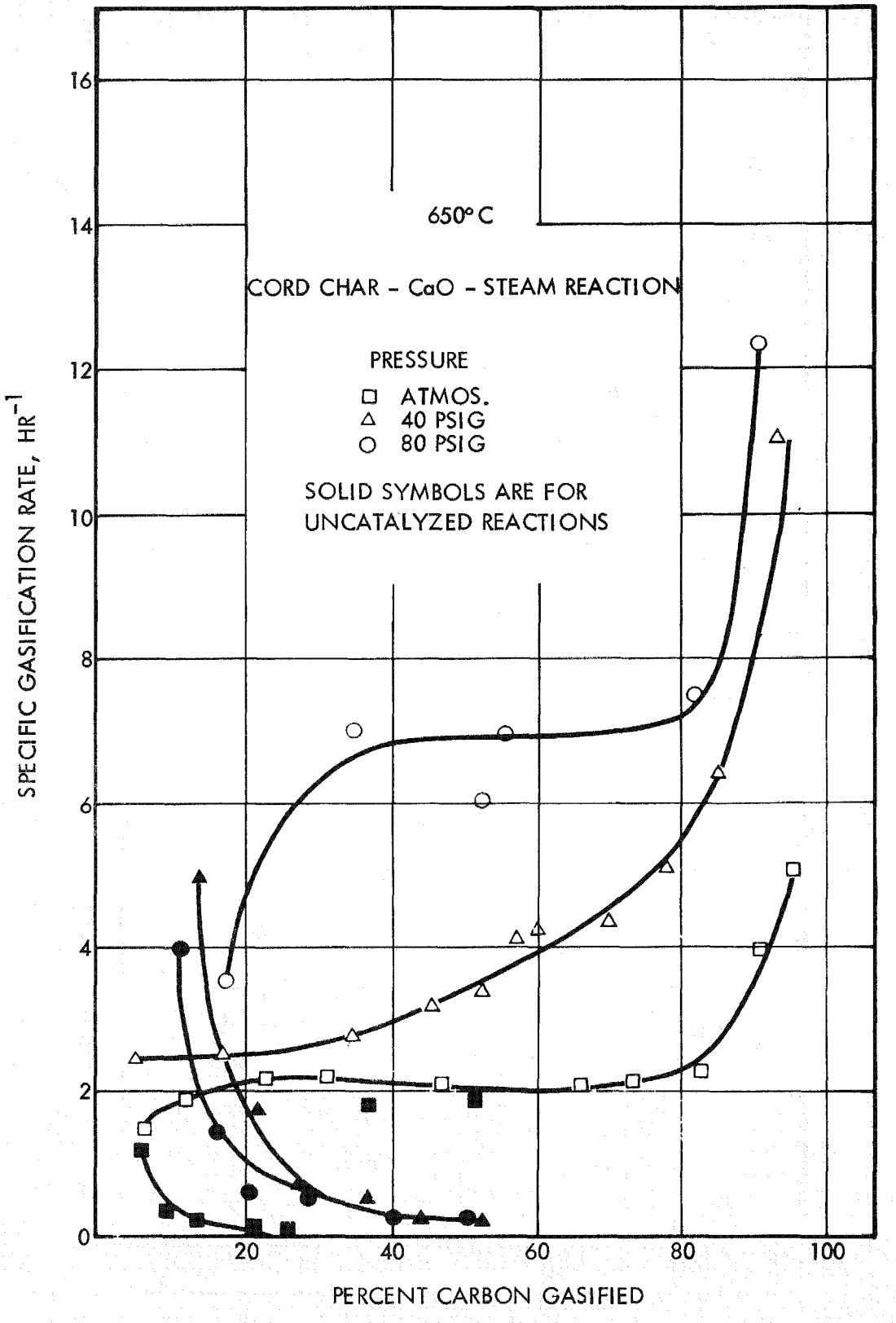

Figure 6-13. Reaction Extent Versus Time Plots for K_2CO_3 Catalyzed COED Char-CaO-Steam Reaction for Various Reaction Pressures.

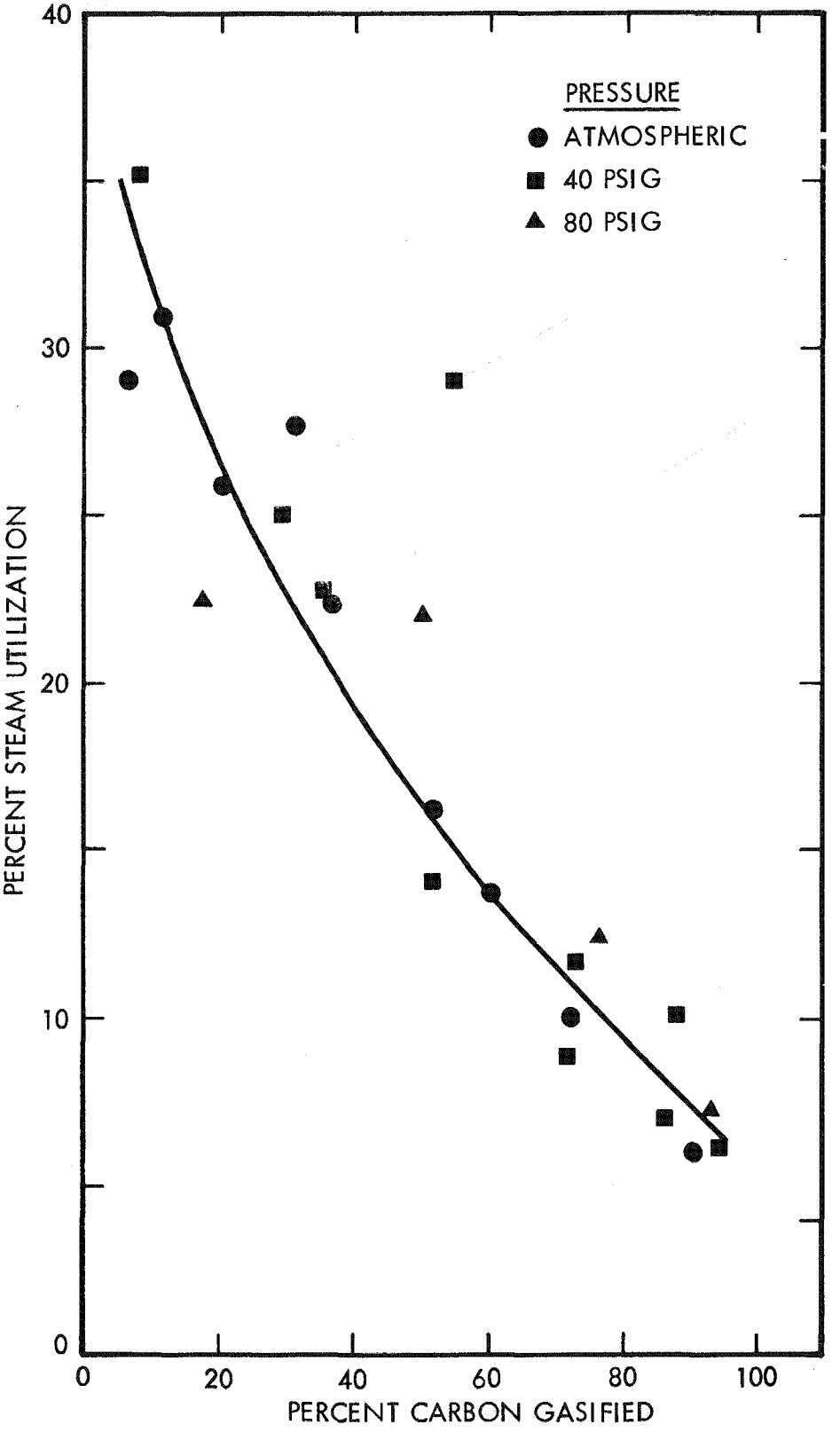

Figure 6-14. Steam Utilization Versus Reaction Extent Curves for K_2CO_3 Catalyzed Gasification Reactions at Atmospheric and Elevated Reaction Pressures.

The effects of elevated reaction pressure on gasification rates may be summarized as follows:

- The catalyzed gasification rates show a marked increase with increasing reactor pressure. This result is consistent with the acceptor model for carbon gasification with steam.
- Over a fairly broad range of reaction extents, the specific char gasification is relatively constant and for a given steam partial pressure the rate appears to be first order with respect to carbon.
- The uncatalyzed gasification is extremely slow at a 650°C reaction temperature such that only 10% to 20% of the char charged to the reactor can be gasified.

6.2.3 Catalyst Recyclability

Figure 6-15 shows the specific gasification rate curves obtained for five reaction cycles for the K_2CO_3 catalyzed COED char-CaO-steam reactor. The reaction pressure for those tests were 100 psig. The fluid-bed material was recalcined at 950°C between steam gasification reactions in order to regenerate the acceptor. The gasification rate is seen to be quite reproducible except for the initial run which falls slightly below successive runs. It was observed that the material became more free-flowing and less agglomerating after the first recalcining treatment. Thus, the improved gas rate may be due to improved material gasification fluidization properties. As can be seen from the curves, no apparent reduction in catalyst activity is observed in the five recycles completed. Too few reaction/regeneration cycles were completed to determine catalyst recycle performance and acceptor absorptivety degradation at elevated reaction pressures. From the five reaction cycles completed, a lower limit in the usage ratio for K_2CO_3 would have to be 13. While additional recycle tests need to be completed with K_2CO_3 and other alkali catalysts systems to determine upper limits for recycle performances, it appears from these initial results that usefully long lived catalysts for hydrogen production from coal char-acceptor-steam will be attainable.

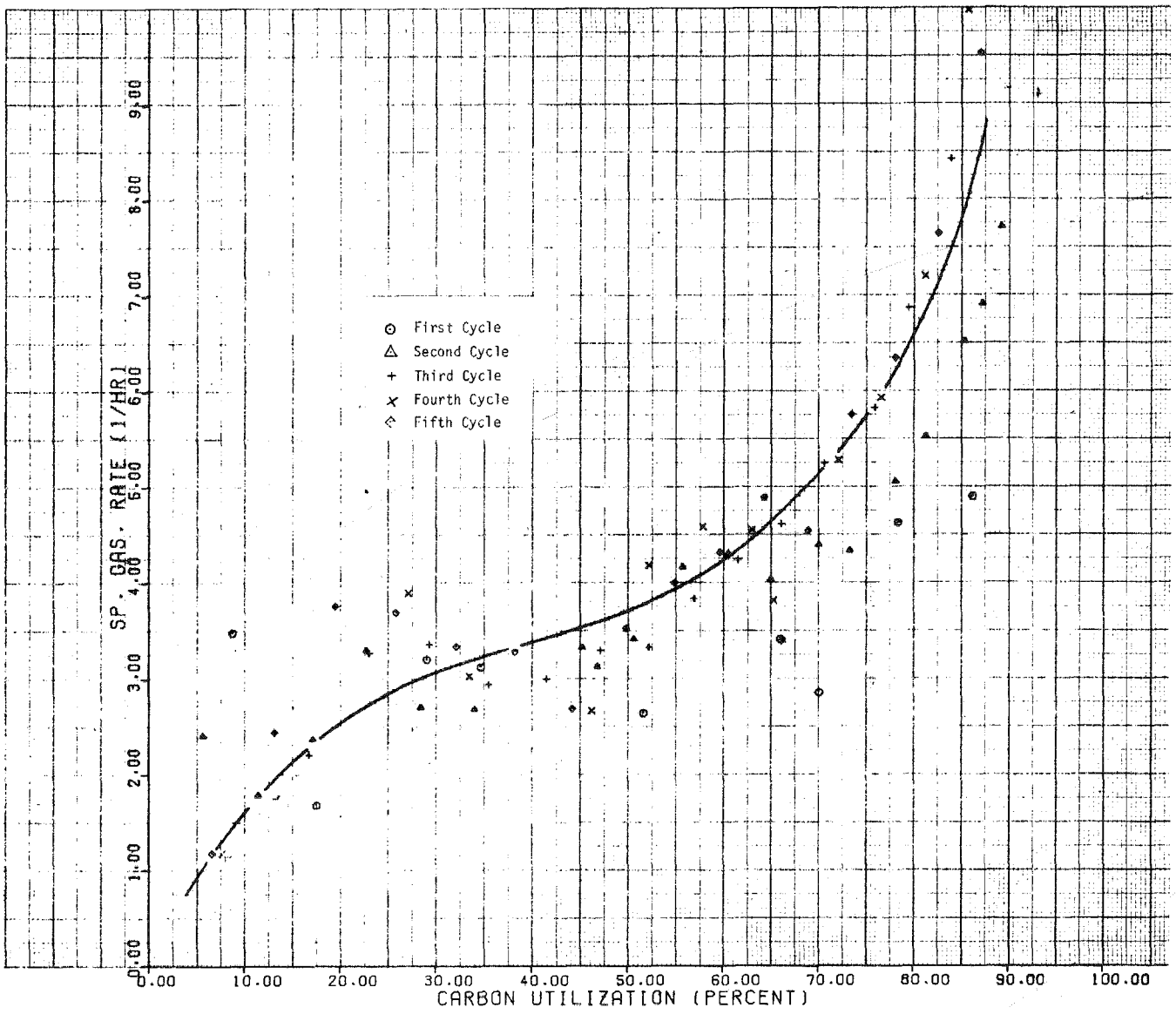

Figure 6-15. Specific Gasification Rate Curves Obtained with Recycled K_2CO_3 Catalyst.

7. DESIGN AND ECONOMIC EVALUATION OF A CONCEPTUAL CATALYTIC CHAR CONVERSION PROCESS FOR HYDROGEN PRODUCTION

This section of the report presents and discusses the results obtained from the engineering study effort performed under the program. The objectives of the study effort were to develop a conceptual design for a commercial scale plant for producing a high purity hydrogen product based on catalyzed coal char-carbon oxide acceptor-steam reactions, and to prepare an economic estimate and comparisons for producing this product by means of such a catalytic conversion process. The process design is based on TRW laboratory data and is augmented where necessary, with reasonable engineering assumptions. The laboratory data utilized as design criteria included: catalyst deactivation rate; maximum acceptor to catalyst ratio; and product composition at specific carbon and steam utilization rates at the temperature (1200°F) of envisioned commercial plant operation. These laboratory data were, however, acquired at reactor pressures somewhat lower than those expected in commercial plant operation, 15 psia as opposed to 150 psia. To reflect improved reaction efficiencies expected at higher system pressures, adjustments were made in the product gas composition for the conceptual commercial plant design.

A summary description of the process and results of the economic evaluation are presented in Section 7.1. The design basis for the conceptual process and a more detailed description of the operating process are presented in Sections 7.2 and 7.3. Process material and utility balances are summarized in Section 7.4 and a discussion of process thermal efficiency presented in Section 7.5. The major pieces of equipment required in the process are summarized in Section 7.6. Fixed capital investment and net operating cost projections are presented in Section 7.7, and economic comparisons of the catalytic hydrogen process with other coal conversion processes presented in Section 7.8.

7.1 SUMMARY PROCESS DESCRIPTION AND ECONOMIC ANALYSIS

A conceptual plant design and product cost evaluation of a process has been completed which utilized coal, char, lime and alkali salts in the production of hydrogen. The designated plant produces 200 million (MM) standard cubic feet per day (SCFD) of ninety-five percent hydrogen gas at a 40°F dew point for a utility financing cost of three dollars per million British thermal units (Btu).

The process is based on two reactions. The first is the hydrogen generation reaction in which steam reacts with the carbon in char in the presence of lime to produce hydrogen and limestone,

$$C + CaO + 2H_2O(steam) + catalyst \rightarrow CaCO_3 + 2H_2$$

The sulfur in the char also reacts to produce calcium sulfide,

$$H_2 + 1/2\ S_2 \rightarrow H_2S$$

$$H_2S + CaO \rightarrow CaS + H_2O$$

The overall hydrogen generation reaction can be written,

$$CaO + char + H_2O + catalyst \rightarrow CO_2 + CO + CH_4 + H_2 + H_2O + CaS + CaCO_3 + residue + catalyst$$

For this design, the nitrogen content of the char was ignored.

The other basic reaction is the lime regeneration reaction,

$$CaCO_3 \rightarrow CaO + CO_2$$

The calcium sulfide present is also converted to calcium sulfate,

$$CaS + 2O_2 \rightarrow CaSO_4$$

The heat required for the lime regeneration reaction is supplied by both the calcium sulfide conversion and the combustion of char with air. The overall regeneration reaction can be written:

$$CaCO_3 + char + residue + air + CaS + catalyst \rightarrow CaO + CO_2 + NO + O_2 + N_2 + H_2O + CaSO_4 + catalyst + residue$$

The specific design information derived from extrapolations of TRW laboratory data were as follows:

Catalyst deactivation rate = 1 lb/20 lbs of coal char processed

Maximum acceptor to catalyst ratio = 6.6:1, lb/lb

Product gas composition from hydrogen generator reactor

	Volume %, dry
H_2	80
CO_2	5
CO	12
CH_4	3

The product requirement was 200 MM SCFD of gas containing 95 percent hydrogen at a 40°F dew point. The raw materials were Illinois #6 coal char and Hollister dolomite. The selection of Hollister dolomite was not intended to affect the selection of a plant site, but to represent a typically usable dolomite composition. The plant location was chosen to be Southern Illinois. This site meets the criteria of availability of large resources of coal char and a large potential industrial market for product hydrogen.

The resulting 200 MM SCFD hydrogen plant requires 4,700 tons per day of char, 1,500 tons per day of dolomite, 200 tons per day of sodium carbonate and 1,100,000 gallons per day of water. The annual operating cost of hydrogen production was estimated to be 53 million dollars. This figure was calculated based on coal char at $15 per ton, dolomite at $11.50 per ton [6], and catalyst at $84 per ton[7]. The total capital investment was estimated to be 130 million dollars. The total capital and operating costs were used to estimate the gas price utilizing both utility and twelve percent discounted cash flow (DCF) financing methods[8]. The calculated gas price ranged from $3.00/MM Btu for utility financing to $3.51/MM Btu for DCF financing.

A block diagram of the conceptual process appears in Figure 7-1. Coal is transported from a char source to the hydrogen generator reactors where it is fluidized with steam and mixed with calcined dolomite or calcined

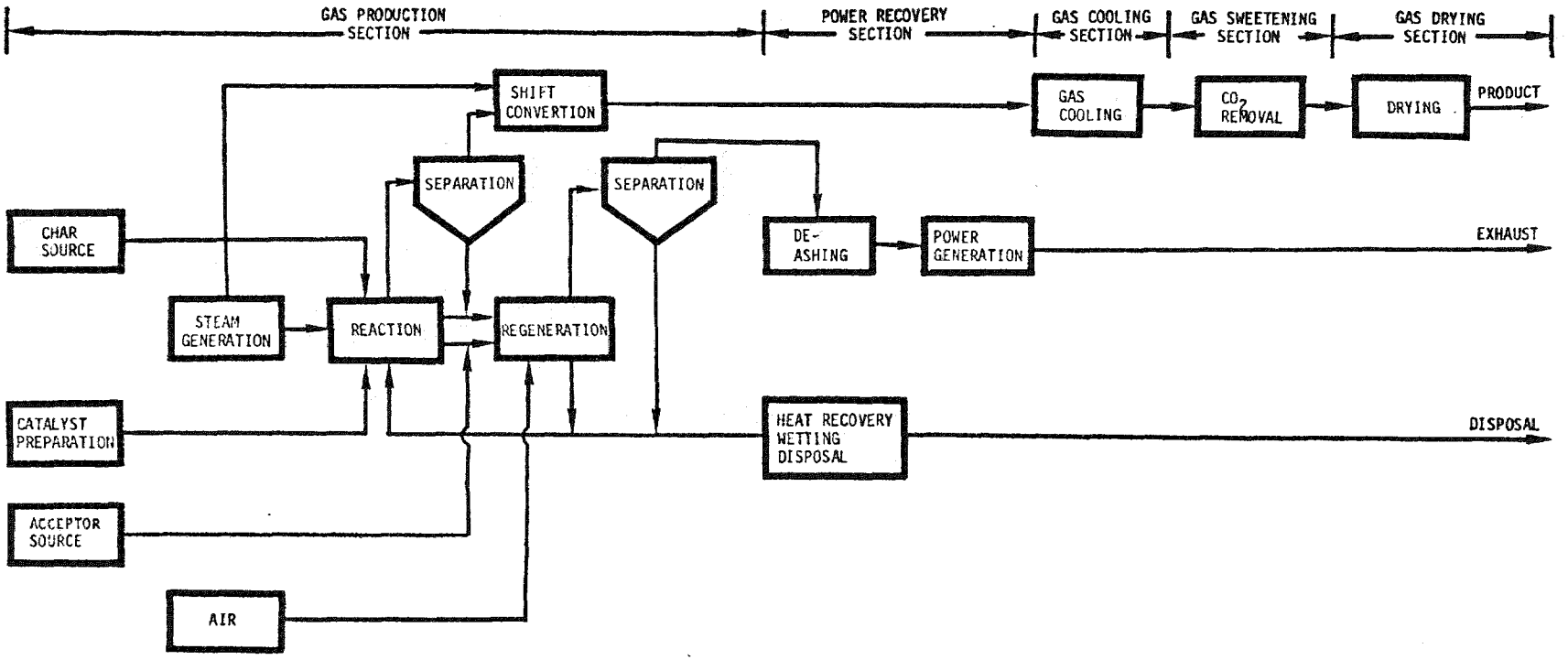

Figure 7-1. TRW Catalytic Coal Char to Hydrogen Process Block Diagram

limestone and a solid alkali metal catalyst. The reaction produces a gaseous product which is 80 percent hydrogen on a dry basis. These effluent gases flow through gas-solids separators to shift conversion reactors. The carbon monoxide in the reactor effluent gases reacts with steam over iron oxide catalyst to produce hydrogen and carbon dioxide. The product of shift conversion is cooled in the gas cooling operation to the temperature required by the CO_2 removal operation. The effluent gases from the CO_2 removal operation flow to gas drying where sufficient water is removed to meet a 40°F dew point product gas specification. The solid products of the hydrogen generation reaction are limestone, calcium sulfide, char residue and catalyst. These solids are transported to the regenerator where limestone is calcined with unreacted char and air to produce the lime required in the reactors. Makeup acceptor is transported from the acceptor source to the regenerators. Gaseous products from the regenerators flow through gas-solids separators and deashers where particulates are sufficiently removed to allow exhaustion of the gas through power generation turbines. A portion of the solid products from the regenerators are transported to heat recovery equipment prior to wetting and final disposal. The process requires no oxygen plant or special sulfur gas cleanup operation.

A parametric study was made to evaluate the effects of variations in the price of char, sodium carbonate and the total plant capital investment on the price of hydrogen production. When char prices ranged from $7.50 to $22.50 per ton, or when total plant investment ranged from 49.5 million to 148.5 million dollars, the utility financing price of hydrogen ranged from $2.49 to $3.55 per million Btu. Changes in the price of sodium carbonate from $42 to $127 per ton affected the utility price of hydrogen by 27 cents per million Btu, from $2.88 to $3.15 per MM Btu.

The economic competiveness of the catalytic process was assessed by comparing the bottom line product prices on a BTU basis with six coal conversion processes producing different fuel products. Because of the different design bases used for each of the processes and the large errors associated in projecting the economics of advanced conversion processes at this early stage of development, product cost comparisons should be used

to determine only whether new process concepts represent reasonable, economically viable conversion alternatives. Results of the comparison of the catalytic hydrogen process with other conversion approaches show that catalytic hydrogen production represents a competitive alternative conversion process. Specifically the economics of the catalytic hydrogen process were compared with those for H-Coal Liquefaction[1], Synthane[2], Lurgi[3], Kopper-Totzek[4] and IGT Steam-Iron HYGAS[5] processes. On a cost per million Btu basis, assuming a char cost of $15.00/ton, dolomite at $11.50/ton and Na_2CO_3 catalyst at $84/ton, the TRW process is competitive with the Synthane, Lurgi, IGT Steam-Iron HYGAS, and Kopper-Totzek processes while being somewhat less competitive with the H-Coal hydrocarbon production process when compared on similar bases.

The economics of hydrogen production were also evaluated with shift conversion eliminated to determine the effect of greater reaction extents. In other words, the gaseous product from hydrogen generation was assumed to be 95 percent hydrogen on a dry basis thus eliminating several of the elements of the process design. The result is a 10% reduction in product cost, or a hydrogen gas price of $2.70/MM BTU on a utility financing basis.

7.2 PROCESS DESIGN BASIS

Primary characteristics and products of the TRW Catalytic Coal Energy to Hydrogen Process are listed in this section. The basis for this design is a manufacturing complex located in southern Illinois. The complex receives Illinois #6 coal and produces a coal char which is utilized as feed to the hydrogen plant. The hydrogen plant contains all necessary supporting facilities to serve the needs of operating, maintenance, development, administrative and service personnel independent of the other plants in the complex.

Specific elements of the design basis are as follows:

Products

(1) Hydrogen. The plant will produce a minimum of 19000 pound moles per hour of hydrogen in a gas stream which is 95 percent pure. The final product gas stream will have a dew point of 40°F. The capacity is sufficient to supply the hydrogen requirements of a 250 million (MM) Btu per day HYGAS pipeline gas generating plant.[9] The purity is acceptable for most industrial hydrogen uses.

(2) Solids. The plant will produce a solids stream which is a mixture of ash, lime and gypsum. Provisions will be made for the safe disposal of these solids.

Raw Materials

(3) Coal Char. The feed char composition on a dry basis is assumed to be as follows:

	weight percent
Carbon	64.16
Hydrogen	2.94
Oxygen	1.78
Sulfur	3.93
Ash	27.19

This char composition was taken from a Coalcon design for Illinois #6 coal.[10] It is assumed that this char composition is not a function of particle size and that the size of the char delivered to the hydrogen plant will be that required for reactor operability. It is also assumed that this char is delivered at the pressure, 150 psia, temperature, 80°F, and rate, consistent

with the requirements of the hydrogen generation plant. This final assumption is reasonable since it is assumed that the char is produced in a 150 psia gasifier. It is then transported, using dense phase fluid transport techniques, through solids coolers (for waste heat recovery) and finally to the hydrogen generation plant.

(4) Dolomite. Holister dolomite was the acceptor material utilized in the TRW laboratory experiments that were used as the basis for this conceptual process design. The composition of this material is as follows:[11]

	weight percent
$CaCO_3$	56.11
$MgCO_3$	42.27
CaO	31.4*
MgO	20.2*
SiO_2, Al_2O_3, Fe_2O_3	.93
Acid Solubles	.69
LOI (Loss on ignition)	46.8

(5) Catalyst. The catalyst is assumed to be commercially available sodium carbonate (58% pure).

Process

(6) Hydrogen Generation. The hydrogen generator reactor will be designed for the following operating conditions:

T = 1200°F
P = 150 psia above the bed
Gas residence time = 10 sec
Superficial Gas Velocity = 2 FPS

The gas produced will have the following composition:

	Vol %, dry basis
H_2	80
CO_2	5
CO	12
CH_4	3

* Calculated on basis of carbonate present in material.

The amount of water in this gas will adjust with the CO, CO_2 and H_2 content to one half the equilibrium ratio for the water gas shift reaction at 1200°F. The TRW laboratory data which is the basis for this conceptual design was obtained at 1200°F and 15 psia. The hydrogen content of the product gas was 65 to 70 mole percent on a dry basis. Based on early experimental data increases in pressure favor hydrogen generation. An increase in hydrogen composition from 70 to 80 percent appears justified by a pressure increase of tenfold, 15 psia to 150 psia. The gas residence time was calculated from CO_2 acceptor published laboratory data.(12) A superficial gas velocity of approximately 2 feet per second (FPS) was considered to be in the range of commercial fluidized-bed reactors.

The Residue char produced in the reactor is assumed to be composed of only ash: the char which is gasified reacts completely. The char which passes through the reactor is completely unchanged. The catalyst replacement rate will be based on a deactivation rate of 20 pounds of char reacted per pound of catalyst utilized. The maximum amount of acceptor in the reactor is 6.6 lbs of acceptor per pound of catalyst. These two values were based on results of TRW experimentation.

(7) Acceptor Regeneration. The acceptor regeneration reactor will be designed to operate at the following conditions:

T = 1800°F

P = 150 psia above the bed

Gas residence time = 10 sec
Superficial Gas Velocity = 3 FPS

The temperature level was selected to be consistent with TRW laboratory investigation. The pressure was selected to avoid pressuring and depressuring the circulating solids stream. The superficial gas velocity of 3 FPS was chosen to justify the assumption that fifty percent of the char ash generated in the reactor and regenerator per cycle would be entrained in the regenerator exhaust gases. The residence time was calculated from CO_2 Acceptor published laboratory data.(12)

(8) Steam Generation. Plant and process steam generation will be considered an integral part of the hydrogen generation process.

7.3 PROCESS DESCRIPTION

The process configuration is depicted in the Process Flow Diagrams, shown in Figure 7-2 and 7-3 For convenience of explanation, the flow diagram divided into five sections: gas production, power recovery, gas cooling, gas sweetening and gas drying.

GAS PRODUCTION

The gas production section consists of solids - coupled fluidized bed reactors and regenerators, fixed-bed gas-water shift reactors, and the necessary hoppers, compressors and pumps to allow for the pressurized transport of solids, slurries and gases. Two gas production trains comprise this 200 MM SCFD hydrogen plant. Coal char (1) is received at a rate of approximately 4,700 tons per day from a coal utilization facility. It is fed to the hydrogen generation reactors (R-1102), at room temperature, 150 psia and at a size that will be fluidized at a gas velocity of 2-3 FPS. The means of char transport to the plant is external to the considerations of this design. Approximately fifty percent of this char is used for hydrogen generation in these reactors. The remainder is used in the regenerator for the regeneration of spent acceptor. The hydrogen reactor design incorporates two separate fluidized-beds. The upper bed is the char bed. The lower bed is made up of the product limestone, gypsum and CaS that falls through the fluidized char bed. Feed dolomite is sized to fluidized at 3-4 FPS. Calcined dolomite, lime, is transported from the regenerator (5) to the upper reactor bed by means of dense phase fluid transport with a portion of the water required for the reaction. Liquid water, fed to the reactors to absorb the generated heat and control the reaction temperature, is vaporized by contact with hot solids to generate the steam needed for fluidization and reaction. Specially designed nozzles in coned bottom reactors and transport pipes are used to achieve this effect. Makeup solid catalyst (4) is fed using a sequential lock hopper system that can be depressurized, loaded, pressurized and dumped. The reactors operate at 1200°F and 150 psia. Each upper portion is 19' ø x 40' T-T (tangent to tangent) and each lower portion is 13'6"ø x 16' T-T.

Hot char, ash (6) and spent acceptor (7) are transported from the reactor to the regenerator using dense phase fluid transport. Regenerator off gases (18) (17) that have been cooled (E-1110) and recompressed (C-1102) are the transport mediums. Makeup dolomite (8) is transferred by a belt conveyor to a sequential lock hopper feed system similar to the catalyst feed system and is added to the spent acceptor transport pipes. Combustion air (9) is compressed to 190 psia and fed to the regenerator. The regenerator is designed to operate at 1800°F and 150 psia with a gas velocity of 3 FPS. This gas rate will fluidize the mixed solids and presumably entrain fifty percent of the ash generated during each reactor-regenerator cycle. Ninety-seven percent of regenerated solids are recycled to the upper reactor bed. The other three percent (10) are transported with steam and combined with recovered ash (12) in the bleed solids cooler (E-1103). These solids flow through lock hoppers (B-1101), bleed solids moistening drums (E-1104), bleed solids lock hoppers (B-1102), and onto the wet solids disposal belt for transport to disposal. Because the bleed solids and ashes enter the moistening drum at 400°F, sprayed cooling water vaporizes, requiring condensation (E-1105) and return to the drum. Sufficient water is recycled to the bleed solids moistener that disposal solids contain approximately fifteen percent moisture.

Heat energy is recovered from the regenerator product gases by generating and superheating steam in heat exchangers located above the disengaging section of the regenerator vessels (E-1107 and E-1108).

POWER RECOVERY

The power recovery section consists of sand filter systems, gas expanders, electric generators, and small gas coolers. Entrained solids not removed in the regenerator cyclones from the hot regenerator effluent gases are recovered in the sand filter system (S-1110). The particulate free gases from the sand filters are divided into two streams. Approximately ninety-six percent of these gases (14) are exhausted through power turbines which generate the following: power needed to run the regenerator air compressors for one of the production trains (D-1101); the power required for the lift gas compressors (D-1102); and seventy-four percent

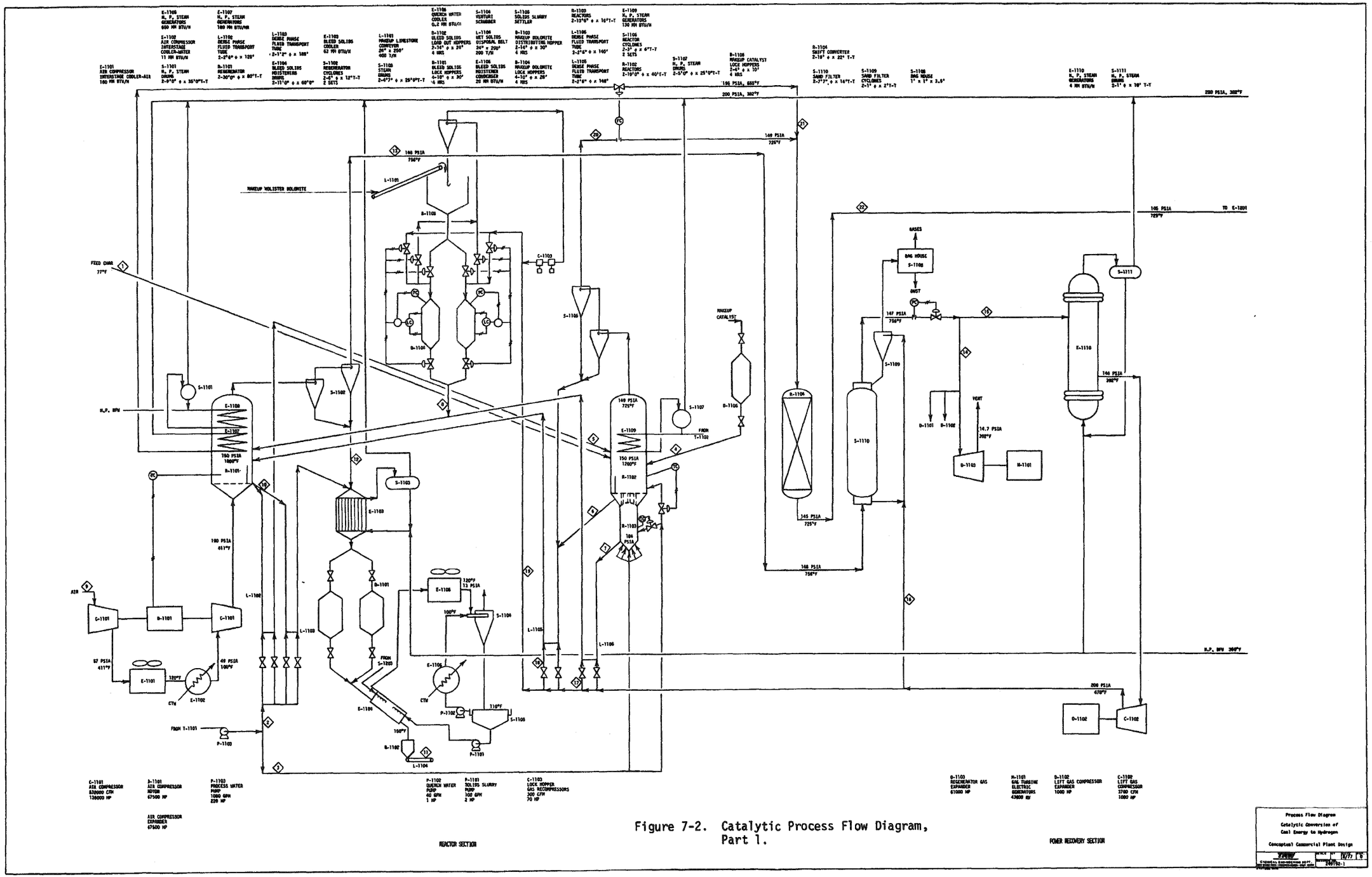

Figure 7-2. Catalytic Process Flow Diagram, Part 1.

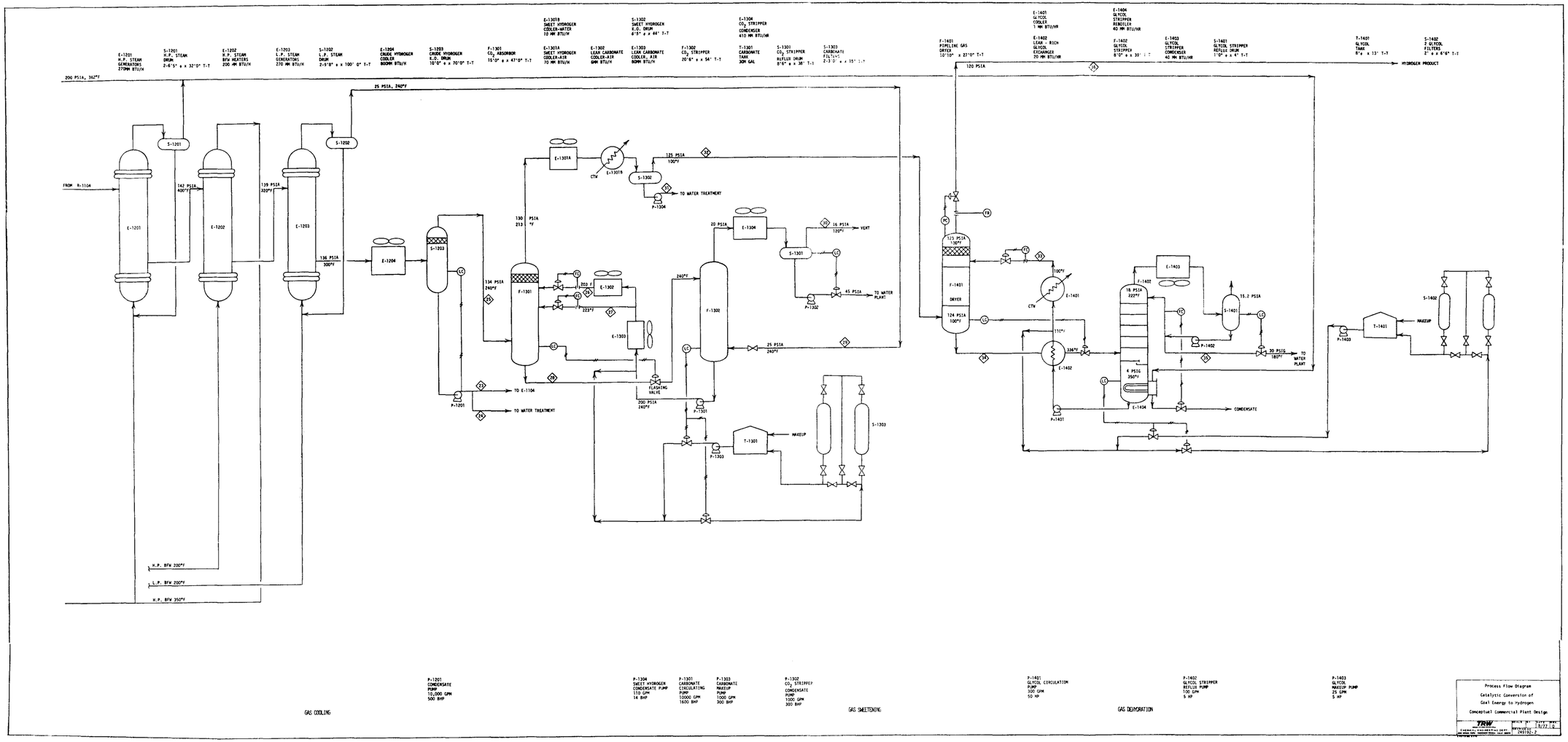

Figure 7-3. Catalytic Process Flow Diagram, Part 2.

of the electricity required for the entire production process (D-1103 and M-1101). Heat is recovered from the other four percent of effluent gases (15) to generate process steam prior to gas recompression (C-1102). This 200 psia gas is recycled to serve as the transport medium for hot char and spent acceptor feeds to the regenerators.

GAS COOLING

The reactor product gas is cooled to 725°F, in steam generators located above the disengaging sections of the reactor upper beds (E-1109). That gas (20) is assumed to be of the following composition:

	Volume %
CO_2	3.8
CO	9.0
CH_4	2.3
H_2	60.4
H_2O	24.5

This gas composition is consistent with the dry gas composition stated in the design basis and supported by TRW laboratory data. The concentration of water was calculated assuming a fifty percent approach to the equilibrium product constant for the water gas shift reaction at 1200°F. The reactor effluent gases contain only eleven percent of the water required for the water gas shift conversion reaction. The additional water (21) is supplied in the form of 655°F superheated steam. These two reactors, designed to operate at 140 psia and 725°F, are 19' ø x 22' T-T each. The product gas from the shift conversion reactor has the following composition:

	Volume %
CO_2	4.2
CO	.1
CH_4	.7
H_2	22.9
H_2O	72.1

This product gas composition was calculated using a 93 percent approach to the water gas shift reaction equilibrium product at 725°F based on design information obtained from the open literature.[13]

Heat is recovered from these gases (22) to generate process steam; to heat boiler feed water; and to generate low pressure steam (E-1201, E-1202 and E-1203, respectively). The 300°F two-phase hydrogen stream is then further cooled to 240°F in an air cooler (E-1204). Condensed water, containing dissolved carbon dioxide is recovered at drum S-1203. At drum S-1203, the two processing trains become one. A portion of the recovered carbonated water from S-1203 (23) is used to wet the regenerator bleed solids. The other portion (24) is pumped to the complex water treatment facility and recovered to meet plant water requirements.

GAS SWEETENING

More than ninety-four percent of the carbon dioxide in the raw hydrogen stream is removed by reaction with a 35 percent potassium carbonate solution in a split stream 20-tray absorber (F-1301). The vessel dimensions are 15' ø x 47' T-T. It is designed for a gas velocity of 5 FPS. The initial absorber section is designed to absorb 1.5 MM SCFH of CO_2 with a 17°F temperature rise. The topping section has a design absorbtion rate of 0.09 MM SCFH of CO_2 at a 10°F temperature rise.

The 240°F rich potassium carbonate solution (28), containing 3.48 SCF of CO_2 per gallon of solution, flashes through a letdown valve into the CO_2 stripper. The solution pressure is reduced from approximately 134 to 20 psia. Water and CO_2 are recovered as stripper overhead products. These flow through the air cooler (E-1304) to the K.O. drum where 678 gpm of 0.08 percent carbonated water is recovered and pumped to water treatment. Carbon dioxide is vented from the reflux drum to the atmosphere. Stripping steam is used at a rate of more than 292,000 pounds per hour. The 20-tray stripping tower is designed for a 9 FPS gas velocity and is 20'6"ø x 54' T-T. The stripper bottoms product is lean carbonate solution containing 2 SCF CO_2 per gallon of solution. It is pumped to solution cooler E-1303 where the temperature is reduced from 240°F to 223°F. Ninety-two percent of the cooled solution (27) is used for the initial absorbing stage. The remainder of the solution (26) is further cooled to 203°F (E-1302), and used for the topping stage.

"Sweet" hydrogen is the overhead product from the CO_2 absorber. It is cooled from 213°F to 100°F in air and water coolers E-1301A and E-1301B. Approximately 100 gpm of water condenses from the sweet hydrogen gas and is recovered in the K.O. drum (S-1302). This water is also pumped to the plant water treatment facility.

GAS DRYING

The 100°F hydrogen gases from K.O. drum S-1302 are fed to the gas dryer F-1401. Triethylene glycol solution (97.2 wt. %) is used to reduce the water content of the gas to a 40°F dew point. The 11' ø x 27' T-T dryer contains six bubble cap trays and a demister pad. It is designed to operate at 100°F, 123 psia and absorb 2,800 lb/H of water. Rich TEG solution is the bottom product from the absorber (34). It is heated to 336°F in the lean-rich glycol heat exchanger (E-1402) and flashed through a pressure letdown valve into the glycol stripper. Rich solution pressures are reduced from 125 to 19 psia. The glycol stripper operates at 18 psia and 222°F. The 10-tray vessel is 8' ø x 34' T-T. Water vapor is the stripper overhead product. It is condensed at 180°F. More than ninety percent of the condensate is returned to the stripper as reflux. The remainder is pumped to the complex water treatment facility.

The gas dryer overhead product is 200 MM SCFD of gas that is more than 95 percent hydrogen at 123 psia and 40°F dew point. The gas composition is as follows:

	Volume %
H_2O	.1
CO_2	1.0
CO	.4
CH_4	3.1
H_2	95.4

The heating value of this product gas is 343 Btu/SCF.

7.4 MATERIAL AND UTILITY BALANCES

The flow rate in pounds per hour of each of the numbered streams on the process flow diagram, Section 7.3, is given in Table 7-1, As shown, the material requirements for a 200 MM SCFD hydrogen capacity plant are approximately 4,700 tons per day of coal char, 1,500 tons per day of dolomite, 200 tons per day of catalyst and 1 MM gallons per day of water.

The process utility requirements are summarized in Table 7-2. Process heat recovery and power generation accounts for over ninety percent of the process energy requirements. The total connected horsepower required for the 200 SCFD hydrogen plant is 130,000 HPH. The regenerator exhaust gas expanders provide ninety percent of this requirement. The remaining 14,000 megawatts are purchased from the coal utilization complex. The steam consumption for the total process is also listed in Table 7-2. Required steam is generated by heat recovered directly from process streams. The steam is generated at two levels, 200 psia and 25 psia.

TABLE 7-1. MATERIAL BALANCE

Stream No.	1	2	3	4	5	6	7	8	9	10	11	12
Name	Char Feed	Lifting Medium	Water	Makeup Catalyst	Regenerator Recycle	Char and Residue to Reg	Spent Acceptor	Makeup Dolomite	Air	Bleed Solids	Solids to Disposal	Ash
Component	Flow Rate, Lb/H											
Char												
C	251,226					123,368						
H	11,512					5,653						
O	6,970					3,423						
S	15,388					7,557						
Ash	106,466					52,281						
CaO					394,144		39,414			12,190	12,190	
Catalyst				9,964	322,169		332,133			9,964	9,964	
$CaCO_3$							608,673	69,789				
$MgCO_3$								52,575				
MgO					812,766		812,766			25,137	25,137	
Other				7,215	298,437		307,667	2,015		9,230	9,230	
Ca$							17,621					
$CaSO_4$					2,112,547		2,112,546			65,336	65,336	
H_2O		39,147	397,072		37,814				25,570	1,333	29,624	
CO_2											14	
CO												
CH_4												
H_2												
N_2									1,539,197			
O_2									467,337			
NO												
Residue					1,721,193	1,775,378				53,233	53,233	53,233
Total, lb/H	391,562	39,147	397,072	17,179	5,699,070	1,967,660	4,230,820	124,380	2,032,104	176,423	204,728	53,233

TABLE 7-1. (Continued)

Stream No.	13	14	15	16	17	18	19	20	21	22	23
Name	Regenerator Exhaust	To Gas Turbines	To Heat Recovery	Sand Lift Gases	Spent Acceptor Lift Gases	Char Residue Lift Gases	Lock Hopper Pressurizing Gases	Hydrogen To Shift	Steam	Crude Hydrogen	Condensate to E-1104
Component	Flow Rate, Lb/H										
Char											
C											
H											
O											
S											
Ash											
CaO											
Catalyst											
$CaCO_3$											
$MgCO_3$											
MgO											
Other											
CaS											
$CaSO_4$											
H_2O	79,017	76,000	3,017	49	1,370	1,558	40	133,718	1,099,523	1,185,283	28,291
CO_2	807,750	776,903	30,847	505	14,008	15,930	404	80,212		167,870	14
CO								76,705		2,140	
CH_4								10,983		10,983	
H_2								36,799		42,165	
N_2	1,598,286	1,537,248	61,038	1,000	27,717	31,521	800				
O_2	72,799	70,018	2,781	46	1,262	1,437	36				
NO	334	321	13	-	6	7	-				
Residue											
Total, lb/H	2,558,186	2,460,490	97,696	1,600	44,363	50,453	1,280	308,417	1,099,523	1,407,941	28,305

TABLE 7-1. (Continued)

Stream No.	24	25	26	27	28	29	30	31	32	33	34	35	36
Name	Condensate to Water Treatment	Sour H_2	Lean Carbonate Stage 2	Lean Carbonate Stage 1	Rich Carbonate	Stripping Steam	Carbon Dioxide	Condensate	Sweet Hydrogen	Lean Glycol	Rich Glycol	Water	H_2 Product
Component	Flow Rate, Lb/H												
Char													
C													
H													
O													
S													
Ash													
CaO													
Catalyst													
$CaCO_3$													
$MgCO_3$													
MgO													
Other													
CaS													
$CaSO_4$													
H_2O	1,051,919	105,073			53,652	292,436	7,603	48,394	3,027		2,649	32,276	378
CO_2	526	166,830			157,207		156,943		9,623				9,623
CO		2,140							2,140				2,140
CH_4		10,983							10,983				10,983
H_2		42,165							42,165				42,165
N_2													
O_2													
NO													
Solution			378,000	4,320,000	4,320,000					129,100	129,100		
Residue													
Total; lb/H	1,052,445	327,191	378,000	4,320,000	4,908,859	292,436	164,546	48,394	67,938	129,100	131,749	32,276	65,289

TABLE 7-2. UTILITY BALANCE

	Power Balance	
Generation, HP	Source	Unit
117,400	Regenerator Gas Expander	D-1101, 2 & 3
Consumption, HP		
122,650	Air Compressors	C-1101
920	Lift Gases Compressors	C-1102
6,600	Miscellaneous Pumps, Blowers and Motors	
130,170	TOTAL	
12,770	Purchased Power, HP	
14,095	Purchased Power, KW (average efficiency = 68%)	

	200 PSIA Steam Balance	
Generation, LB/H	Source	Unit
65,340	Bleed Solids Coolers	E-1103
666,870	Steam Generators	E-1108
123,160	Steam Generators	E-1109
10,610	Steam Generators	E-1110
275,350	Steam Generators	E-1201
1,141,330	TOTAL	
Consumption, LB/H		
1,099,520	Shift Conversion Reactors	R-1104
41,810	Glycol Stripper Reboiler	E-1404
1,141,330	TOTAL	

	25 PSIA Steam Balance	
Generation, LB/H	Source	Unit
292,440	Steam Generators	E-1203
Consumption, LB/H		
292,440	CO_2 Stripper	F-1302

7.5 PROCESS THERMAL EFFICIENCY

The thermal efficiency of a process is defined as the percentage of heat input that is efficiently utilized in the desired manner.[14] Because this definition is somewhat arbitrary, three different methods were used in an effort to present a meaningful thermal efficiency for this process which utilizes coal char energy at a rate of 0.07 tons char/MM Btu of 95.4 percent hydrogen gas product. The three thermal efficiencies are presented in Table 7-3.

The first thermal efficiency is generally called the cold gas efficiency. It is calculated by dividing the heating value of the hydrogen product by the heating value of the coal char feed. In this case, the cold gas efficiency does not represent the process efficiency. This process has a fuel deficiency that must be made up in electric power. The second efficiency reported is the thermal efficiency. It is lower than the cold gas efficiency by the heating value of the electric power which must be supplied to this process. The third thermal efficiency reported is the fuel equivalent efficiency. This value is the cold gas efficiency reduced by the fuel value, at 33 percent efficiency, of the additional 14 megawatts per hour of electric power required by this process.

TABLE 7-3. THERMAL EFFICIENCY OF TRW COAL CHAR TO HYDROGEN PLANT

$$\text{Cold Gas Efficiency} = \frac{\text{Hydrogen Product Gas-Btu/D}}{\text{Char Feed - Btu/D}} \times 100 = 59\%$$

$$\text{Thermal Efficiency} = \frac{\text{Hydrogen Product Gas-Electric Power Requirement-Btu/D}}{\text{Char Feed - Btu/D}} \times 100 = 55\%$$

$$\text{Fuel Equivalent Efficiency} = \frac{\text{Hydrogen Product Gas-Electric Power Fuel Equivalent}^{*}\text{-Btu/D}}{\text{Char Feed - Btu/D}} = 48\%$$

* The electric power fuel equivalent is the quantity of fuel a 33 percent efficient power plant consumes with an output equal to 14 megawatts.

7.6 MAJOR EQUIPMENT SUMMARY AND COSTS

Presented in this section is a summary of the major equipment needed to carry out the various processing operations for this plant. The equipment list presented in Table 7-4 briefly describes each piece of equipment and also presents both a FOB and installed equipment cost.

The bare equipment cost of processing vessels are calculated on a weight basis. An allowable stress of 13,750 PSI was used to calculate required vessel wall thicknesses. Carbon steel was priced at $1.25 per pound. The volume of required refractory was estimated. Costs are based on a price of $0.10 per pound and a density of 200 lb per cu ft. Equipment cost of motors are estimated at $75 per horsepower, installed. Cost of compressors, turbines and expanders are estimated at $30 per horsepower, installed. Bare equipment costs of pumps and conveyors are taken from Gutnrie.[15] Cost of heat exchangers are calculated for the surface area required. Prices range from $8 per sq ft for bare carbon steel tube vacuum condensers to approximately $15 per sq ft for high pressure gas to high pressure steam generators with low alloy tubes. Cost of air coolers are calculated at $12 per sq ft of bare surface required based on a $75,000 6 row, 16' x 48' air cooler.

The installed cost of all equipment is four times the estimated bare equipment cost. Installed equipment costs include the cost of engineering, design, construction and erection of processing and attendant equipment (e.g., lube oil systems, seal flush systems, blowdown systems, purge gas systems). This cost also includes the cost of instrumentation, piping, electrical and insulation and all contractor direct and indirect charges, fees and contingencies. The total installed equipment cost for this 200 MM SCFD plant is 83 million dollars.

TABLE 7-4. EQUIPMENT LIST

Item Number	Description	Equipment Cost $M	Total Installed $M
B-1101	4-Bleed Solids Lock Hoppers Size: 10' ø x 30' T-T Holdup: 4 HRS W/60° Cone Bottoms 3/8" Shell thickness 22,000 lbs each	109	437
B-1102	2-Bleed Solids Load Out Hoppers Size: 14' ø x 24' T-T Holdup: 4 HRS W/60° Cone Bottoms 3/8" Shell thickness 20,000 lbs each	51	204
B-1103	2-Makeup Limestone Distributing Hoppers Size: 14' ø x 30' T-T Holdup: 4 HRS W/60° Cone Bottoms 3/4" Shell thickness 44,000 lbs each	109	435
B-1104	4-Makeup Limestone Lock Hoppers Size: 10' ø x 28' T-T Holdup: 4 HRS W/60° Cone Bottoms 3/4" Shell thickness 42,000 lbs each	209	836
B-1105	2-Makeup Catalyst Lock Hoppers Size: 4' ø x 10' T-T Holdup: 4 HRS W/60° Cone Bottoms 3/4" Shell thickness 5,000 lbs each	13	53
C-1101	2-Regenerator Air Compressors Capacity: 532,000 CFM Gas MW: 28.6 Inlet Pressure: 14.7 PSIA Exit Pressure: 190 PSIA Inlet Temperature: 100°F Efficiency: 84% HP: 67,500 each		4,050
C-1102	2-Lift Gas Compressors Capacity: 3,700 CFM Gas MW: 32 Inlet Pressure: 144 PSIA Exit Pressure: 200 PSIA Inlet Temperature: 392°F Efficiency: 60% HP: 500 each		30

TABLE 7-4. (Cont'd)

Item Number	Description	Equipment Cost $M	Total Installed $M
C-1103	2-Lock Hopper Gas Recompressors Capacity: 300 CFM Gas MW: 32 Inlet Pressure: 14.7 PSIA Exit Pressure: 205 PSIA Inlet Temperature: 100°F Efficiency: 84% HP: 35 each		2
D-1101	Regenerator Air Compressor Expander HP: 67,500		2,025
	Regenerator Air Compressor Motor HP: 67,500		5,062
D-1102	2-Lift Gas Compressor Expanders HP: 500 each		30
D-1103	1-Regenerator Gas Expander HP: 61,000		1,830
E-1101	2-Regenerator Air Compressor Interstage Coolers, Air Heat Load: 160 MM Btu/H U: 50 Btu/hr sq ft °F Area: 49,456 ft^2 total No. of bays: 8 Power: 480 HP	600	2,400
E-1102	2-Regeneration Air Compressor Interstage Coolers, Water Heat Load: 11 MM Btu/H U: 14 Btu/hr sq ft °F ΔTLM: 11°F Area: 55,556 ft^2 Cooling Water: 900 GPM Dim: 6'0"ø x 32' T-T each	444	1,776
E-1103	2-Bleed Solids Coolers Heat Load: 63 MM Btu/H U: 8.4 Btu/hr sq ft °F ΔTLM: 338°F Area: 22,190 ft^2 Dim: 7'8"ø x 25' T-T each	178	710

TABLE 7-4. (Cont'd)

Item Number	Description	Equipment Cost $M	Total Installed $M
E-1104	2-Ash Cooler-Moisteners Dim: 11' ø x 60' Rotary Drums each	352	1,408
E-1105	Bleed Solids Moistener Condenser Heat Load: 20 MM Btu/H U: 130 Btu/hr sq ft °F Area: 4,121 ft^2 No. of bays: 1 Power: 40 HP	50	200
E-1106	Quench Water Cooler Heat Load: 0.2 MM Btu/H U: 28 Btu/hr sq ft °F ΔT AVE: 30°F Area: 238 ft^2 Cooling Water: 40 GPM Dim: 0'8"ø x 20' T-T	2	8
E-1107	2-High Pressure Steam Superheaters Heat Load: 180 MM Btu/H U: 42 Btu/hr sq ft °F ΔT AVE: 1,144°F Area: 3,754 ft^2 total	34	136
E-1108	2-High Pressure Steam Generators Heat Load: 650 MM Btu/H U: 188 Btu/hr sq ft °F ΔTLM: 692°F Area: 4,996 ft^2	75	300
E-1109	2-High Pressure Steam Generators Heat Load: 130 MM Btu/H U: 144 Btu/hr sq ft °F ΔTLM: 550°F Area: 1,641 ft^2	25	100
E-1110	High Pressure Steam Generator Heat Load: 10 MM Btu/H U: 25 Btu/hr sq ft °F ΔTLM: 112 Area: 3,528 ft^2	54	216
L-1101	Makeup Dolomite Conveyor Size: 24" x 250' Set: 45° Angle 400 T/H	123	492

TABLE 7-4. (Cont'd)

Item Number	Description	Equipment Cost $M	Total Installed $M
L-1102	2-Dense Phase Fluid Transport Tubes Dim: 30" ø x 128'l w/4" refractory	44	176
L-1103	Dense Phase Fluid Transport Tube Dim: 14" ø x 188'l w/4" refractory	29	116
L-1104	Wet Solids Disposal Belt Size: 24" x 200' 200 T/H	103	412
L-1105	Dense Phase Fluid Transport Tube Dim: 30" ø x 148' w/4" refractory	50	200
L-1106	Dense Phase Fluid Transport Tube Dim: 30" ø x 140' w/4" refractory	48	192
M-1101	Gas Turbine Electric Generators Size: 43,000 KW		4,575
P-1101	2-Solids Slurry Pumps Size: 100 GPM each 2 HP each	2	8
P-1102	2-Quench Water Pumps Size: 40 GPM each 1 HP each	2	8
P-1103	2-Process Water Pumps Size: 1,000 GPM each 220 HP each	30	120
R-1101	2-Regenerators Size: 30' ø x 80' T-T W/9" refractory + 3" Gunnite 2-1/2" Shell thickness Operating Pressure: 150 PSIA Operating Temperature: 1800°F Weight: Vessel 1,527,000 lbs Refractory 1,476,000 lbs	2,056	8,224
R-1102	2-Reactors Size: 19' ø x 40' T-T W/4" refractory + 2" Gunnite 2" Shell thickness Operating Pressure: 150 PSIA Operating Temperature: 1200°F Weight: Vessel 748,000 lbs Refractory 828,000 lbs	1,018	4,071

TABLE 7-4. (Cont'd)

Item Number	Description	Equipment Cost $M	Total Installed $M
R-1103	2-Reactors Size: 13'6"ø x 16' T-T W/4" refractory + 2" Gunnite 2" Shell thickness Operating Pressure: 175 PSIA Operating Temperature: 1200°F Weight: Vessel 274,000 lbs Refractory 174,000 lbs	360	1,440
R-1104	2-Shift Conversion Reactors Size: 19' ø x 22' T-T 1-9/16" Shell thickness Operating Pressure: 145 PSIA Operating Temperature: 725°F Weight: 261,000	326	1,305
S-1101	2-High Pressure Steam Drums Size: 9' ø x 35' T-T Weight: 93,000 lbs	116	465
S-1102	Regenerator Cyclones 2-sets 2-stages Size: 6' ø x 12' T-T Weight: 34,000 lbs	42	170
S-1103	2-High Pressure Steam Drums Size: 4'7"ø x 25' T-T Weight: 20,000 lbs	25	100
S-1104	Venturi Scrubber	5	20
S-1105	Solids Slurry Sittler Size: 40' ø x 20'	37	148
S-1106	Reactor Cyclones 2-sets 2-stages Size: 3' ø x 6' T-T Weight: 8,000	10	40
S-1107	2-High Pressure Steam Drums Size: 5' ø x 25' T-T Weight: 22,000 lbs	28	112

TABLE 7-4. (Cont'd)

Item Number	Description	Equipment Cost $M	Total Installed $M
S-1108	Bag House Size: 1'w x 1'l x 3'6"h Weight: 240 lbs	1	4
S-1109	Sand Filter Cyclones 2-sets Size: 1' ø x 2' T-T Weight: 400 lbs	1	4
S-1110	2-Sand Filters Size: 7'7"ø x 14' T-T 7/8" Shell thickness Weight: 32,000 lbs	40	160
S-1111	2-High Pressure Steam Drums Size: 1' ø x 10' T-T Weight: 1,000 lbs	1	4
T-1101	Process Water Tank Size: 1,382,000 gal	157	628
E-1201	2-High Pressure Steam Generators Heat Load: 270 MM Btu/H U: 36 Btu/hr sq ft °F ΔTLM: 118°F Area: 63,384 Dim: 5' ø x 60' T-T each	963	3,852
E-1202	2-Boiler Feed Water Heaters Heat Load: 200 Btu/H U: 32 Btu/hr sq ft °F ΔTLM: 80°F Area: 78,124 ft^2 Dim: 5'2"ø x 60' T-T each	1,109	4,436
E-1203	2-Low Pressure Steam Generators Heat Load: 270 MM Btu/H U: 27 Btu/hr sq ft °F ΔT AVE: 74°F Area: 135,136 ft^2 Dim: 6'10"ø x 60' T-T each	1,811	7,244
E-1204	2-Crude Hydrogen Coolers Heat Load: 800 MM Btu/H U: 60 Btu/hr sq ft °F Area: 123,648 No. of bays: 20 Power: 1200 HP	1,500	6,000

TABLE 7-4. (Cont'd)

Item Number	Description	Equipment Cost $M	Total Installed $M
P-1201	2-Crude Hydrogen Condensate Pumps Size: 10,000 GPM HP: 500	63	252
S-1201	2-High Pressure Steam Drums Size: 6'5"ø x 32" T-T Weight: 44,000 lbs	55	220
S-1202	2-Low Pressure Steam Drums Size: 9'8"ø x 100' T-T Weight: 98,000	122	488
S-1203	Crude Hydrogen K. O. Drum Size: 10' ø x 70' T-T Weight: 85,000 lbs	106	424
E-1301A	Sweet Hydrogen Cooler-Air Heat Load: 70 MM Btu/H U: 70 Btu/hr sq ft °F Area: 37,094 ft^2 No. of bays: 6 Power: 360	450	1,800
E-1301B	Sweet Hydrogen Cooler-Water Heat Load: 10 MM Btu/H U: 58 Btu/lb sq ft °F ΔT AVE: 18°F Area: 9,678 ft^2 Dim: 3' ø x 42' T-T	132	528
E-1302	Lean Carbonate Cooler-Air Heat Load: 6 MM Btu/H U: 80 Btu/hr sq ft °F Area: 1,150 ft^2 No. of bays: 1 Power: 11	14	56
E-1303	Lean Carbonate Cooler-Air Heat Load: 80 MM Btu/H U: 80 Btu/hr ft sq °F Area: 12,364 ft^2 No. of bays: 2 Power: 120 HP	150	600
E-1304	CO_2 Stripper Condenser-Air Heat Load: 410 MM Btu/H U: 60 Btu/hr sq ft °F Area: 129,822 ft^2 No. of bays: 21 Power: 1260 HP	1,575	6,300

TABLE 7-4. (Cont'd)

Item Number	Description	Equipment Cost $M	Total Installed $M
F-1301	CO_2 Absorber Size: 15' ø x 47' T-T 1-3/8" Shell thickness Operating Pressure: 130 PSIA Operating Temperature: 213°F Weight: 149,000 lbs	180	744
F-1302	CO_2 Stripper Size: 20'6"ø x 54' 1-3/8" Shell thickness Operating Pressure: 20 PSIA Operating Temperature: 240°F Weight: 228,000	285	1,140
P-1301	2-Carbonate Circulating Pumps Size: 10,000 GPM 1600 HP	263	1,052
P-1302	CO_2 Stripper Condensate Pump Size: 1000 GPM 300 HP	22	88
P-1303	2-Carbonate Makeup Pump Size: 1000 GPM 300 HP	107	214
P-1304	2-Sweet Hydrogen Condensate Pumps Size: 110 GPM 14 HP	6	24
S-1301	CO_2 Stripper Reflux Drum Size: 8'6"ø x 38' T-T Weight: 18,000 lbs	22	44
S-1302	Sweet Hydrogen Condensate Drum Size: 6'5"ø x 44' T-T Weight: 15,000 lbs	19	76
S-1303	2-Carbonate Filters Size: 3' ø x 15' T-T Weight: 5,000	6	24
T-1301	Carbonate Tank Size: 30,000 GAL Weight: 13,000 lbs	16	64

TABLE 7-4. (Cont'd)

Item Number	Description	Equipment Cost $M	Total Installed $M
E-1401	Lean Glycol Cooler, Water Heat Load: 1 MM Btu/H U: 50 Btu/lb sq ft °F ΔTLM: 11°F Area: 1,818 ft^2 Dim: 2' ø x 20' T-T	25	100
E-1402	Lean-Rich Glycol Exchanger Heat Load: 20 MM Btu/H U: 70 Btu/lb sq ft °F ΔT AVE: 12°F Area: 23,810 ft^2 Dim: 4' ø x 60' T-T	324	1,296
E-1403	Glycol Stripper Condenser, Air Heat Load: 40 MM Btu/H U: 130 Btu/hr sq ft °F Area: 4,599 ft^2 No. of bays: 2 Power: 68HP	56	224
E-1404	Glycol Stripper Reboiler Heat Load: 40 MM Btu/H U: 100 Btu/hr sq ft °F ΔT AVE: 32°F Area: 12,500 ft^2 Dim: 7'2"ø x 10' T-T	150	600
F-1401	Pipeline Gas Dryer Size: 10'10"ø x 27' T-T 1-1/8" Shell thickness Operating Pressure: 130 PSIA Operating Temperature: 100°F Weight: 53,000 lbs	66	264
F-1402	Glycol Stripper Size: 8' ø x 39' T-T 1" Shell thickness Operating Pressure: 18 PSIA Operating Temperature: 222°F Weight: 56,000 lbs	70	280
P-1401	2-Glycol Circulation Pumps Size: 300 GPM 50 HP	8	24

TABLE 7-4. (Cont'd)

Item Number	Description	Equipment Cost $M	Total Installed $M
P-1402	2-Glycol Stripper Reflux Pumps Size: 100 GPM 5 HP	3	12
P-1403	2-Glycol Makeup Pumps Size: 25 GPM 5 HP	3	12
S-1401	Glycol Stripper Reflux Drum Size: 1' ø x 4' T-T Weight: 200 lbs	1	4
S-1402	2-Glycol Filters Size: 2' ø x 6'6" T-T Weight: 2,000 lb	2	8
T-1401	Glycol Tank Size: 5,000 GAL Weight: 18,000 lbs	22	88

7.7 FIXED CAPITAL INVESTMENT AND NET OPERATING COST

An estimate of the fixed capital investment and net operating cost for the TRW hydrogen from coal char plant at the 200 MM SCFD plant size is presented in this section.

The total capital investment is estimated at 130 MM dollars. The components of this estimate are shown in Table 7-5. Three quarters of this cost is the total plant investment. The total plant investment is the sum of the installed equipment cost plus the offsites. The sum of the installed equipment cost is the 83 million dollar battery limits figure in Table 7-5. Broken down by processing section, this cost is as follows:

Section	Cost, $MM
Gas Production	39
Power Recovery	7
Gas Cooling	22
Gas Sweetening	12
Gas Drying	3
Battery Limits	83
Offsites	16
Total Plant Investment	99

The service facilities included in the 16 million dollar offsites cost include the following: steam distribution, water supply, cooling and pumping, water treatment, water distribution, sanitary waste disposal, communications, raw-materials storage, finished product storage and fire-protection system. The 16 MM dollar offsite cost is twelve percent of the total capital investment (offsite costs usually range from 6 to 25 percent of total capital investment).[16] Other elements of the total capital requirement estimate were calculated using the BRAUN gas cost guidelines.[8]

TABLE 7-5. CAPITAL REQUIREMENTS

	MM$
Total Plant Investment	
Battery Limits* - $MM 83	
Offsites - $MM 16	
	99
Initial Charge of Catalyst and Chemicals	.7
Allowance for Funds During Construction (total plant investment x 1.87 x 9 percent interest)	17
Startup Cost (20 percent of total annual gross operating cost)	10
Working Capital (sum of [1] Raw Materials Inventory of 14 days at full rate, [2] Materials and Supplies at 0.9 percent of total plant investment, and [3] Net Receivables at 1/24 annual gas at $1.00/MM Btu and by-product revenue at calculated sales price)	3
Total Capital Requirement	130

* The battery limits capital requirement includes the cost of engineering, design, construction and erection battery limits processing and attendant equipment. Also included are costs of instrumentation, piping, electrical, and insulation, all contractor direct and indirect charges, fees and contingencies.

The net operating cost is estimated at $52 MM per year. Table 7-6 shows the items that make up this cost. The method of estimating these elements varies from the BRAUN guidelines only in the cost of maintenance labor and supplies. Maintenance cost, estimated by the BRAUN procedure, is a percentage of the plant investment for certain types of processing equipment. This cost is then divided sixty-forty between maintenance labor and maintenance supplies. The methodology utilized in the cost estimate presented in Table 7-5 was to estimate maintenance labor at 2.7 percent of the total plant investment. Maintenance supplies were estimated at 1.5 percent of the total plant investment.

The amount of process materials required are based on the material balance presented in Section 7.4. A ninety percent plant operating factor was used to calculate annual requirements. By definition, the only process raw material is coal char. The char value is based on a 12,341 Btu per pound heating value as compared to 11,420 Btu per pound for Illinois #6 Coal. Seventy-five percent of this ratio times $18 per ton of Illinois #6 Coal resulted in a char valued at $15 per ton.[8] The other process feedstocks are included as catalyst and chemicals. Dolomite is priced at $11.50 per ton.[6] The sodium carbonate catalyst is $48 per ton for 58 percent Na_2CO_3 FOB Green River, Wyoming. Transportation adds $36 per ton.[7] A price of $84 per ton of Na_2CO_3 was utilized. Eighty-five percent potassium carbonate is priced at $9.75 per 100 pounds. Triethylene glycol is priced at $0.30 per pound.[17] Shift conversion catalyst is priced at $53 per cu ft.[18] The $220,000 annual cost for the shift catalyst is based on a three-year catalyst life.

The average cost of the ninety-five percent hydrogen gas from the 200 MM SCFD TRW coal char to hydrogen plant was calculated using both utility financing and twelve percent discounted cash flow methods. The cost ranged from $3.00 to $3.51 per million Btu depending on the financing method (utility and DCF, respectively) utilized. The methodology for each of the financing methods is presented below:

TABLE 7-6. OPERATING COST

(90 Percent Plant Service Factor)

	MM$
Raw Material - Char (196 ton/hr, $15.00/ton)	23.18
Catalyst and Chemicals	
Hollister Dolomite (62 ton/hr, $11.50/ton)	5.64
Catalyst (Na_2CO_3) (8.6 ton/hr, $84.50/ton)	5.73
Potassium Carbonate (2 lb/hr, $9.75/100 lbs)	.01
Triethylene Glycol (9 lb/hr, $.30/lb)	.02
Shift Conversion Catalyst (at $53/$ft^3$, 3 year life)	.22
Power (14095 KWH, $.05/KWH)	5.56
Purchased Water (1100 M Gal/D x $.30/M Gal)	.11
Labor	
Process Operating Labor (10 men/shift, $7.50/man-hr)	.66
Maintenance Labor (.6 x 4.5 percent total plant investment)	2.67
Supervision (20 percent of Operating and Maintenance Labor)	.67
Administration and General Overhead (60 percent of total labor)	2.40
Supplies	
Operating (30 percent Process Labor)	.20
Maintenance (1.5 percent total Plant Investment)	1.48
Local Taxes and Insurance (2.7 percent total Plant Investment)	2.67
Ash Disposal (9 ton/hr, $1/ton)	.77
Total Net Operating Cost Per Year	51.99
Average Gas Cost for Utility Financing*	3.00/MM Btu
Average Gas Cost for DCF**	3.51/MM Btu

* The utility financing method utilized in determining this gas price is shown on page 28.

** The private investor financing method utilized in determining this gas price is shown on page 29.

Gas Cost Determination With Utility Financing (8)

Basis

20-year project life

90 percent service factor

5 percent per year straight line depreciation on total capital requirement excluding working capital

48 percent federal income tax rate

Definition of Terms

C = Total capital requirement, million dollars

W = Working capital, million dollars

N = Total net operating cost in first year, million dollar/year

G = Annual gas production, trillion Btu/year

d = Fraction debt (.75)

i = Interest on debt, 9 percent per year

r = Return on equity, 15 percent per year

p = Return on rate base, 10.5 percent per year

Equation for Return on Rate Base

$$p = (d)i + (1-d)r$$

General Gas Cost Equation

Gas cost on average* rate base, $/MM Btu =

$$\frac{N + 0.05\ (C-W) + 0.005\ \left[p + \frac{48}{52}\ (1-d)r\right]\ (C + W)}{G}$$

---

* Average rate base is one half of initial investment.

(8)

Gas Cost Determination With Private Investor Financing

Basis

20-year project life

16-year sum of the years digits depreciation on total plant investment

100 percent equity capital

12 percent DCF return rate

48 percent federal income tax rate

Definition of Terms

I = Total plant investment, initial charge of catalyst and chemicals, paid-up royalties, million dollars

S = Start-up costs, million dollars

W = Working capital, million dollars

N = Total net operating cost in first year, million dollars/year

A = Annual gas production, trillion Btu/year

Constant Gas Cost Equation at 12 Percent DCF Return

Constant gas cost a 12 percent DCF return, dollars/MM Btu =

$$\frac{N + 0.247I + 0.1337S + 0.2305W}{A}$$

7.8 PROCESS ECONOMIC ANALYSIS AND COMPARISONS

To evaluate the effects of variation in major process costs on the cost of hydrogen production, a parametric study of process economics was conducted. The prices of char, Na_2CO_3 catalyst and total plant capital investment were varied, one at a time, plus and minus fifty percent of the estimated base case values listed in Tables 7-5 and 7-6. The results are shown both in Figure 3 and in Table 7-7. It can be seen that gas costs are equally sensitive to changes in char prices and capital investment costs but not as sensitive to changes in Na_2CO_3 catalyst costs. At char prices between 7.50 to 22.50 $/ton, the price of hydrogen ranged by more than $1/MM Btu, from $2.49 to $3.55/MM Btu. When total plant investment was varied from $49,500,000 to $148,500,000 dollars, the price of hydrogen changed by about the same ratio, $2.49 to $3.54/MM Btu. Changes in Na_2CO_3 catalyst prices from $127 to $42/ton effected the price of hydrogen by only $.27/MM Btu, from $2.88 to $3.15/MM Btu.

The effects of variations in catalyst activity, attrition and poisoning rates were also considered. In order to place numerical values on such variations, a new process design would have been required for specific values of each parameter. The effects of variations in these parameters can however, be stated qualitatively. An increase in catalyst activity would result in a decrease in the cost of hydrogen production because of a decrease in the Na_2CO_3 catalyst makeup rate, a decrease in the solids circulating rate, a lower coal char requirement in the regeneration reaction, a reduced combustion air requirement and a reduced regenerator size requirement. An increase in catalyst attrition rate would tend to increase the amount of catalyst makeup required and result in a higher hydrogen production cost. The effects of variations in catalyst poisoning rates are similar to those related to catalyst activity.

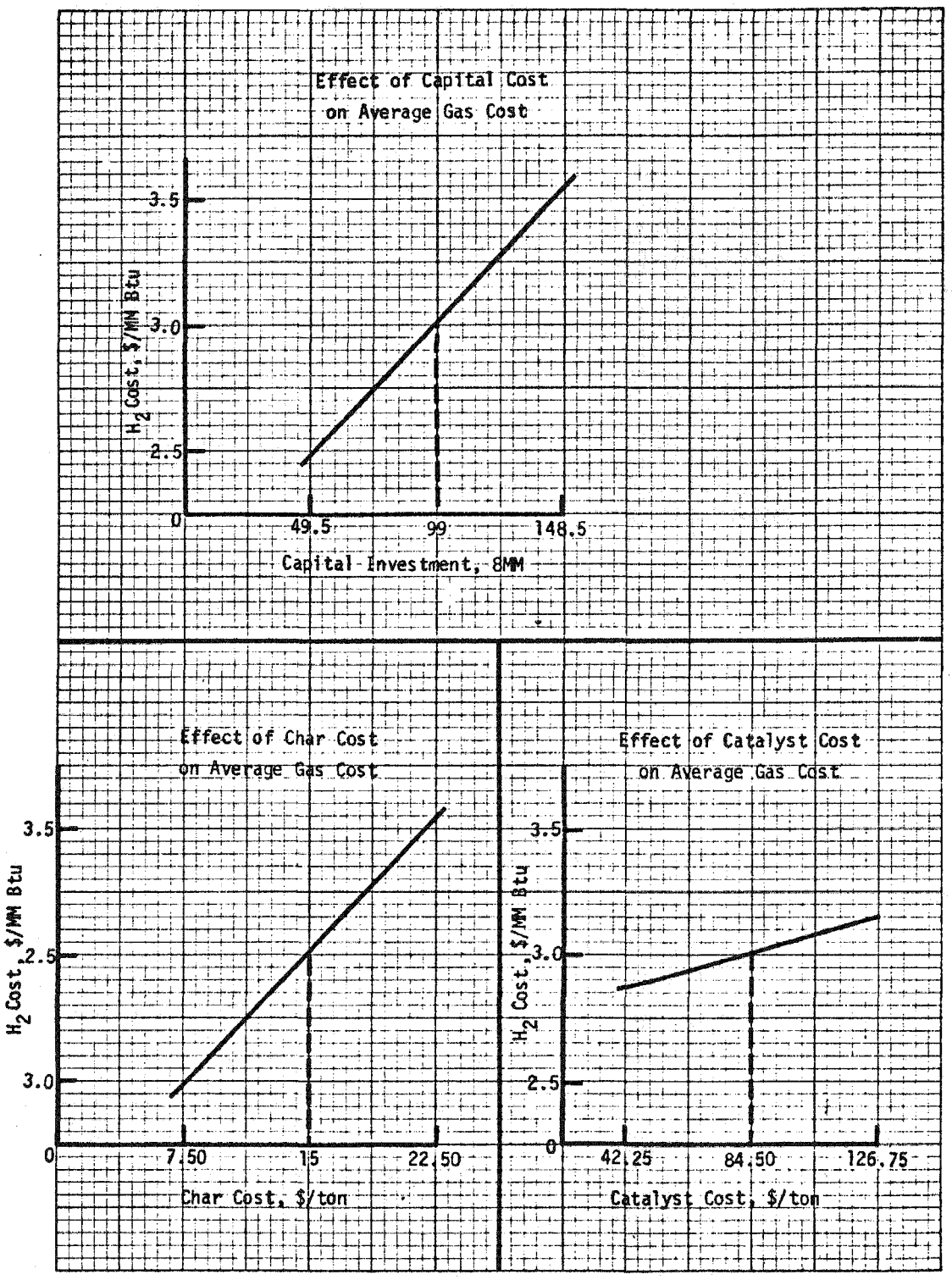

Figure 7-3. Cost Sensitivity Analysis

TABLE 7-7. SIGNIFICANCE OF COST VARIATIONS ON PROCESSING COST*

	Base Case	Char +50%	Char -50%	Na_2CO_3 catalyst +50%	Na_2CO_3 catalyst -50%	Cap. Inv. +50%	Cap. Inv. -50%
Capital Requirement - $MM							
Total plant investment	99	99	99	99	99	148.5	49.5
Initial charge of catalyst	0.7	0.7	0.7	0.7	0.7	0.7	0.7
Construction funds allowance	17	17	17	17	17	25.0	8.3
Start-up costs	10	12.7	8.0	10.9	9.8	11.3	9.4
Working capital	3	3.8	2.8	3	3	3.7	2.8
Total capital requirement	129.7	133.2	127.5	130.6	129.5	189.2	70.7
Operating Cost - $MM/YR							
Raw materials - char	23.18	34.77	11.59	23.18	23.18	23.18	23.18
Catalyst & Chemicals	11.62	11.62	11.62	14.49	8.76	11.62	11.62
Power	5.56	5.56	5.56	5.56	5.56	5.56	5.56
Purchased water	0.11	0.11	0.11	0.11	0.11	0.11	0.11
Labor							
Operating	0.66	0.66	0.66	0.66	0.66	0.66	0.66
Maintenance	2.67	2.67	2.67	2.67	2.67	4.01	1.34
Supervision	0.67	0.67	0.67	0.67	0.67	0.93	0.40
Admin. & Gen. overhead	2.40	2.40	2.40	2.40	2.40	3.36	1.44
Supplies							
Operating	0.20	0.20	0.20	0.20	0.20	0.20	0.20
Maintenance	1.48	1.48	1.48	1.48	1.48	2.23	0.74
Local taxes and insurance	2.67	2.67	2.67	2.67	2.67	4.01	1.34
Ash disposal	0.77	0.77	0.77	0.77	0.77	0.77	0.77
Total operating cost - $MM/YR	51.99	63.58	40.40	54.86	49.13	56.64	47.36
Average gas cost - $/MM Btu							
Utility financing	3.00	3.55	2.49	3.15	2.88	3.54	2.49
Discounted cash flow	3.51	4.05	2.98	3.64	3.38	4.27	2.75

* Costs for char, catalyst, and capital investment are varied ±50% of base case.

Shown in Tables 7-8 and 7-9 is a comparison of the economic elements of the TRW conceptual process and those of a liquefaction process (H-Coal),[1] a pipeline gas process (Synthane),[2] a commercial Lurgi pipeline gas process,[3] a Kopper-Totzek Synthesis Gas Process,[4] and an IGT Steam-Iron HYGAS Process.[5] In each process the estimated plant investment cost was adjusted using appropriate cost escallation indexes to reflect cost as of January 1977. Other elements of the total capital requirement were calculated using procedures identical to those utilized for the TRW conceptual plant estimate. A ninety percent service factor was used to estimate annual cost requirements. Uniform cost of coal, $18 per ton, and process operating labor, $7.50 per hour, were assumed. Catalyst and chemical cost were taken from the referenced documents.

As may be seen in Table 7-8, Process Economic Comparisons, the average costs per million Btu of product were calculated for the other five processes using both utility financing and discounted cash flow financing methods. The average cost of hydrogen from the TRW conceptual coal char process is about $0.06/MM Btu above the average of the six processes using utility financing and $0.19/MM Btu below the average of the six processes using private financing methods.

The six processes compared in Table 7-8 differ greatly in plant capacity from 68 to 408 billion Btu/day. In order to made a comparison between the elements of both the total plant investment and the net annual operating costs, the cost per million Btu of product per year was calculated. These values appear in Table 7-9, Process Cost Comparisons. When these costs are compared, the TRW process for hydrogen is the least capital intensive of the gas producing processes, although it is one of the more expensive processes to operate. This high operating cost is directly related to the comparatively high cost for catalyst and chemicals. Because of the lack of specific information on what constituted catalyst and chemical costs in some of the other processes, those costs were not adjusted to 1977 prices. It is therefore conceivable that the TRW catalyst and chemical cost is not as high, relative to the comparative processes,

TABLE 7-8. PROCESS ECONOMIC COMPARISONS
(MM$ per year basis)

Process	TRW Conceptual Catalytic Conversion of Coal Char to H_2	H-Coal[1] Coal Liquefaction Process	SYNTHANE[2] Pipeline Gas Process	LURGI[3] Commercial Pipeline Gas Process	KOPPER-TOTZEK[4] Synthesis Gas Process	IGT[5] Steam-Iron HYGAS Process
Plant Size, MM Btu/D	68,200	408,000	231,900	275,600	250,000	250,000
CAPITAL REQUIREMENT, MM$						
Battery Limits	83	385.6	283.3	249.9		
Offsites	16	143.3	131.8	115.2		
Total Plant Investment	99	528.9	415.1	465.1	452.0	1280
Initial Charge of Catalyst and Chemicals	1	3.2	1.5	5.2		7.3
Allowance for Funds Used During Construction	17	89.0	69.9	78.3	76.1	201.6
Startup Cost	10	40.7	42.3	39.7	39.9	42.3
Working Capital	3	16.3	10.9	14.7	13.8	29.0
Total Capital Requirement	130	678.1	539.7	603.0	581.8	1560.2
OPERATING COST, MM$						
Raw Materials	23.18	131.7	84.8	137.6	148.0	56.45
Catalysts and Chemicals	11.62	14.1	1.8	4.6	1.5	5.00
Power	5.56					
Purchased Water	.11	1.6	1.7	1.4	0.9	.65
Labor						
Process Operating Labor	.66	2.9	3.0	4.1	3.1	2.78
Maintenance Labor	2.67	14.3	9.4	12.6	12.2	34.56
Supervision	.67	3.4	2.5	3.3	3.1	6.07

TABLE 7-8. (Continued)

Process	TRW Conceptual Catalytic Conversion of Coal Char to H_2	H-Coal[1] Coal Liquefaction Process	SYNTHANE[2] Pipeline Gas Process	LURGI[3] Commercial Pipeline Gas Process	KOPPER-TOTZEK[4] Synthesis Gas Process	IGT[5] Steam-Iron HYGAS Process
Administration and General Overhead	2.40	12.4	8.9	12.0	11.0	21.86
Supplies						
Operating	.20	0.9	0.9	1.2	0.9	0.83
Maintenance	1.48	7.9	6.2	7.0	6.8	19.20
Local Taxes and Insturance	2.67	14.3	11.2	12.6	12.2	34.56
Ash Disposal	.77					
Total Gross Operating Cost Per Year	51.99	203.5	130.4	198.3	199.7	181.96
By-Product Credits	0	8.5	9.0	21.9	0.9	24.86
Total Net Operating Cost Per Year	51.82	195.0	121.4	176.4	198.8	157.10
Average Gas Cost, $/MM Btu						
Utility Financing	3.00	2.06	2.44	2.75	3.27	4.14
Discounted Cash Flow, 12%	3.51	2.50	3.05	3.33	3.88	5.91

TABLE 7-9. PROCESS COST COMPARISONS
($/MM Btu Basis)

Process	TRW Conceptual Catalytic Conversion of Coal Char to H_2	H-Coal[1] Coal Liquefaction Process	SYNTHANE[2] Pipeline Gas Process	LURGI[3] Commercial Pipeline Gas Process	KOPPER-TOTZEK[4] Synthesis Gas Process	IGT[5] Steam-Iron HYGAS Process
Plant Size, MM Btu/D						
CAPITAL REQUIREMENT, $/MM Btu/YR						
Battery Limits	3.70	2.88	3.72	3.87		
Offsites	.71	1.07	1.73	1.27		
Total Plant Investment	4.41	3.95	5.45	5.14	5.50	15.58
Initial Charge of Catalyst and Chemicals	.03	.02	.02	.06		.09
Allowance for Funds Used During Construction	.76	.66	.92	.86	.93	2.45
Startup Cost	.45	.30	.56	.44	.49	.51
Working Capital	.13	.12	.14	.16	.17	.35
Total Capital Requirement	5.79	5.05	7.09	6.66	7.09	18.98
OPERATING COST, $/MM Btu						
Raw Materials	1.03	.98	1.11	1.52	1.80	.69
Catalyst and Chemical	.52	.11	.02	.05	.02	.06
Power	.25					
Purchased Water	.004	.01	.02	.02	.01	.008
Labor						
Process Operating Labor	.03	.02	.04	.05	.04	.03
Maintenance	.12	.11	.12	.14	.15	.42
Supervision	.03	.03	.03	.04	.04	.07

TABLE 7-9. (Continued)

Process	TRW Conceptual Catalytic Conversion of Coal Char to H_2	H-Coal[1] Coal Liquefaction Process	SYNTHANE[2] Pipeline Gas Process	LURGI[3] Commercial Pipeline Gas Process	KOPPER-TOTZEK[4] Synthesis Gas Process	IGT[5] Steam-Iron HYGAS Process
Administrative and General Overhead	.11	.09	.12	.13	.13	.27
Supplies						
Operating	.01	.01	.01	.01	.01	.01
Maintenance	.07	.06	.08	.08	.08	.23
Local Taxes and Insurance	.12	.11	.15	.14	.15	.42
Ash Disposal	.03	--		.02		
Total Gross Operating Cost Per Year	2.32	1.53	1.70	2.20	2.43	2.21
By-Product Credits	0	.06	.12	.24	.01	.30
Total Net Operating Cost Per Year	2.32	1.47	1.58	1.96	2.42	1.91

as the values in Table 7-9 would indicate. The results of the economic analysis indicate that hydrogen produced by the TRW catalytic coal to hydrogen process is economically competitive on a dollar per million Btu basis with synthetic natural gas and liquid hydrocarbons produced from coal.

The final economic analysis of this process involves evaluating the results of a change in the basic design criteria used to develop the conceptual process design presented in this document. It is included as a result of recent developments in the TRW laboratory program. These recent results indicate that the gas composition assumed to be the product of the hydrogen generation reactions at 1200°F and 150 psia is probably too low in terms of hydrogen content (see Design Basis, Section 3, #6). Gases containing ninety-five percent hydrogen on a dry basis have been produced at 1200°F and 100 psia in TRW laboratory apparatus. A detailed conceptual process design would be required to accurately evaluate the effect of utilizing this new information. However, a rough estimate of the effect of utilizing the ninety-five percent hydrogen production in the hydrogen generator can be achieved by eliminating the cost of the following elements: the shift conversion reactors, the shift conversion catalyst, the gas sweetening section, the potassium carbonate solution, ninety-six percent of the equipment required for the production of 200 psia steam, and the total requirement for purchased power. These manipulations result in a capital investment savings of approximately 20 million dollars and a net annual operating cost savings of approximately 6 million dollars. The overall effect would tend to reduce the hydrogen product cost, calculated by the utility financing method previously described, by approximately 30 cents per million Btu. The resulting gas price is then approximately $2.70/ MM Btu.

8. CONCLUSIONS

Laboratory experimentation and engineering analysis conducted under this program have been successful in establishing the preliminary technical and economic feasibility of catalytically deriving hydrogen from coal char-steam reactions. The laboratory effort which has been centered around testing alkali catalyst performance and acceptor absorption characteristics, was able to successfully demonstrate several key performance properties upon which an eventual catalytic coal conversion process will depend. Engineering analysis of a conceptual hydrogen production process whose design is based in part on catalyst performance properties obtained from these studies and in part on engineering judgement, indicates that the economics of a catalytic process will be competitive with alternate processes which are currently being considered for deriving synthetic fuels from coal.

Specifically demonstrated in the experimental effort was the ability of abundantly available and relatively inexpensive materials such as sodium and potassium carbonate to effectively catalyze char gasification reactions to such an extent that rapid reaction rates are obtained for the conversion reaction in the 650°C to 700°C temperature range. Hydrogen is the principal fuel product produced from alkali catalyzed char gasification reactions, and at elevated reaction pressures in the presence of a carbon dioxide acceptor, 95% pure hydrogen is obtained. H_2S evolved during steam gasification of char is retained as CaS to a significant extent. Sodium and potassium carbonate are also effective catalysts for the char-oxygen-steam reaction. The high activities of both these catalysts can be achieved under either stationary-bed or fluidized-bed reaction conditions with as little as 5 to 10 weight percent of the dry powder admixed with char and the carbon dioxide acceptor. High catalyst activity with dry admixed catalysts is significant. From a process viewpoint, the result indicates that wet catalyst impregnation or dispersal on the reactant char surface is unnecessary. Catalyst recycle in a process can likely be accomplished more easily and in a cost effective manner than resorting to aqueous extraction and recovery from impregnated char waste residues.

In addition to the high catalyst activities demonstrated for sodium and potassium carbonate, both materials remain active through many combination char gasification-acceptor regeneration reaction cycles. Depending on the particular experimental conditions employed, the dry admixed catalysts can be used to catalytically gasify between 10 to 40 times their weight of coal char. In recycle performance, sodium carbonate is substantially better than the potassium salt. Recyclability performance as well as depending on catalyst type, depends also on char type, acceptor regeneration treatment temperature, and the presence of lime and stabilizing additives such as fluorspar and phosphate salts. Volatilization and conversion of alkali catalyst to less active forms are probable mechanisms for catalyst deactivation.

Preliminary engineering analysis indicates that a conceptual process based on alkali catalyzed char-acceptor-steam gasification reactions for high purity hydrogen production is less capital intensive than other advanced fossil fuel conversion processes being developed. The catalytic hydrogen process is competitive economically with other advanced processes when compared on a product cost per unit energy basis and represents a reasonably attractive alternative conversion process.

9. REFERENCES

(1). Process Evaluation Group . . . MMRD, Morganton, West Virginia, U.S. Dept. of the Interior, BOM, 50,000-Barrels-per-day-Liquid Fuels Plant, H-Coal Process-Illinois Coal, An Economic Analysis, Report No. 76-1, July 1975.

(2). Ibid., 250 Million-SCFD High-Btu Gas Plant, Synthane-Pittsburg Seam Coal, An Economic Analysis, Report No. 75-2b (Revision of report No. 75-2a).

(3). Vyas, K.C. SNG From Coal, IGT, July 1974.

(4). Franzen, Johannes E. PhD, and Eberhard K. Goeke, SNG Production Based on Koppers-Tozek Coal Gasification, Heinrich Koppers TMBH, ESSEN, FED. REP. Germany, Presented at Sixth Synthetic Pipeline Gas Symposium, O'Hare Inn, Chicago, Illinois, October 28-30, 1974.

(5). Ditman, Rodger, Factored Estimates for Western Coal Commercial Concepts Interim Report, C. F. Braun & Co., Alhambra, Calif. 91802. Evaluation Contract for Joint ERDA-A.G.A. Coal Gasification Program, October 1976.

(6). Prevailing calcium carbonate prices are $19 per ton. These prices include a $7 to $8 per ton delivery cost that would not be accured on locally available dolomite. Telephone information from FMC Corporation quoted Hollister dolomite at $11.50 per ton plus delivery, June 1977.

(7). Telephone information, Sales and Marketing, FMC Corporation, June 1977.

(8). Skaneser, Robert, Coal Gasification Commercial Concepts Gas Cost Guidelines, C.F. Braun & Co., Alhambra, Ca. 91802, Prepared for ERDA and AGA Contract No. E(49-18)-1235, January 1976.

(9). Vyas, F.C. and W.W. Bodle, "Cost of Synthetic Fuels from Coal and Oil Shale" prepared by IGT as input to Project Independance Blue print, August 1974.

(10). Crawford, C.L., L. Manson, D.S. Hopp, Fluid Bed Char Gasifier Process Design, prepared for ERDA, Contract No. E(49-18)-2213 and EX-76-C-01-2213, Task Order 21, November 2, 1976.

(11). Starkovich, J, et al. "Catalytic Conversion of Coal Energy to Hydrogen", TRW, prepared for ERDA, Contract No. E(49-18)-2206-7, January 1977.

(12). Curran, E.P., C.E. Fink, E. Corin, "CO_2 Acceptor Gasification Process", Research Division, Consolidation Coal Co., Library, Pa.

(13). Lowenheim, F.A., and M.K. Moran, Industrial Chemicals, Fourth Edition, John Wiley and Sons, 1975.

(14). Hougen, O.A., K.M. Watson, and R.A. Ragatz, Chemical Process Principles, Second Edition, John Wiley and Sons, New York, 1964.

(15). Guthrie, K.M. Process Plant Estimating Evaluation and Control, Craftsman Book Company of America, 1974.

(16). Peters, M.S. and K.D. Timmerhaus, Plant Design and Economics for Chemical Engineers, McGraw-Hill Book Company, N.Y., N.Y. 1968.

(17). Chemical Marketing Reporter, February 1977.

(18). Telephone information, Catalyst Information Dept., Catalyst and Chemicals Inc., June 1977.

(19). Starkovich, J., et. al, "Catalytic Conversion of Coal Energy to Hydrogen" Quarterly Technical Progress Report, January-March 1977, ERDA Contract No. E(49-18)-2206-10, April 1977.

(20). Taylor, H.S., H.A. Neville, Catalysis in the Interaction of Carbon with Steam and with Carbon Dioxide, Journal of the American Chemical Society 43,2055(1921).

(21). Kayembe, N., A.H. Pulsifer, Kinetics and Catalysis of the Reaction of Coal Char and Steam, Fuel 55,211(1976).

(22). Hendel, Y., Replacement of Platinum Vessels with a Pressure Device for Acid Dissolution in the Rapid Analysis of Glass by Atomic-Absorption Spectroscopy, Analyst 98,450(1973)

APPENDIX

Table A-1. Proximate, Ultimate and Sulfur Analysis Data for Coal Char Samples

Analysis	Coal Char							
	Colstrip		Synthane		FMC COED		Norit "A"	
	As Rec'd	Dry	As Rec'd	Dry	As Rec'd	Dry	As Rec'd	Dry
Proximate								
% Moisture	0.38	-	1.56	-	2.94	-	8.20	-
% Ash	15.78	15.84	27.87	28.31	14.90	15.35	7.90	8.61
% Volatile	4.47	4.49	5.95	6.04	20.58	21.20		
% Fixed Carbon	79.37	79.67	64.62	65.65	61.58	63.45		
Btu	12220	12267	10234	10396	11739	12095		
% Sulfur	0.87	0.87	0.16	0.16	2.83	2.92		
Ultimate								
Moisture	0.38	-	1.56	-	2.94	-	8.20	-
Carbon	82.47	82.78	67.76	68.83	74.73	76.99	83.90▲	91.39
Hydrogen	0.63	0.63	1.12	1.14	1.59	1.64		
Nitrogen	0.82	0.82	0.45	0.46	1.51	1.56		
Chlorine	0.01	0.01	0.02	0.02	0.01	0.01		
Sulfur	0.87	0.87	0.16	0.16	2.83	2.92		
Ash	15.78	15.84	27.87	28.31	14.90	15.35	7.90	8.61
Oxygen	-0.96	-0.95	1.06	1.08	1.49	1.53		
Sulfur Forms								
Pyritic Sulfur	0.08	0.08	0.03	0.03	0.00	0.00		
Sulfate Sulfur	0.00	0.00	0.01	0.01	0.07	0.07		
Organic Sulfur	0.79	0.79	0.12	0.12	2.76	2.85		
Total Sulfur	0.87	0.87	0.16	0.16	2.83	2.92		

▲Calculated as 100-(% moisture + % ash) = % carbon

APPENDIX

Table A-2. Emission Spectrographic Analysis of Ash Residues

Element	Char Ash			
	FMC COED	Synthane	Colstrip	Norit "A"
Si	18.0%	18.0%	22.0%	25.0%
Fe	24.0	5.0	2.5	2.9
Al	11.0	14.0	12.0	7.0
Ca	1.3	9.8	11.0	5.1
K	0.72	0.31	-	<0.10
Na	0.52	0.36	0.33	2.7
Mg	0.72	6.1	4.7	9.4
Ti	0.66	1.0	1.2	0.22
Mn	0.047	1.4	0.18	0.070
Ba	<0.10	0.32	0.14	<0.05
Be	0.00094	<0.0003	-	-
B	0.036	0.041	0.10	0.023
Pb	0.019	0.017	0.017	0.010
Ga	0.010	0.0084	0.0090	Trace
Cr	0.014	0.016	0.28	0.082
Ni	0.022	0.0051	0.0033	0.0035
Mo	0.0094	<0.002	-	<0.002
V	0.041	0.014	0.017	<0.004
Cu	0.014	0.0061	0.017	0.023
Zr	0.017	0.019	0.022	-
Co	0.0079	0.0025	-	-
Sr	0.027	0.084	0.12	0.042
Au	-	-	0.012	-
Ag	-	-	0.0035	0.00043
P	-	-	-	6.2
Zn	-	-	-	0.017

APPENDIX

Table A-3. Composition of Natural Acceptor Materials

Compound	Material		
	Hollister Dolomite	Minnekahta Limestone	Tymochtee Dolomite
$CaCO_3$	56.93[a]	96.37	42.75
$MgCO_3$	42.88	0.74	53.44
CaO	(31.9)[b]	(54.0)	(24.0)
MgO	(20.5)	(0.35)	(25.5)
SiO_2	0.57	1.49	1.76
Al_2O_3	0.24	0.25	
Fe_2O_3	0.13	0.29	0.54
Na_2O		0.51	
K_2O		0.33	
Acid Insolubles	0.70		
Ignition Loss	46.8		45.86

[a]All values reported as weight percent.

[b]Calculated on basis of carbonate present in sample.

Table A-4. Summary of FBR Catalyst Screening Results

System	Steam Reaction/Acceptor Regeneration Condition			Product Evolution Rate[e]											
				Reaction Cycle											
	Steam Flow (Moles Min-1)	Reaction Temperature (°C)	Acceptor Regeneration Temperature (°C)	1	2	3	4	5	6	7	8	9	10	11	12
FMC COED, CaO, Na_2CO_3 (19%:76%:5%)	0.33	650	500	2.75	3.20	3.22	3.11	3.28	3.18	3.01	2.51	0.77	0.44	0.99[d]	0.44
FMC COED, CaO, $Na_2B_4O_7$ (19%:76%:5%)	0.33	650	500	1.89	2.31	-[c]	0.46	0.46	2.09[a]	0.23	0.23	0.35[a]	0.11	0.23[d]	
FMC COED, MgO, K_2CO_3 (19%:76%:5%)	0.33	650	500	3.18	3.24	2.62	0.57	0.35	0.23[a]	0.44					
FMC COED, CaO, K_2CO_3 (19%:76%:5%)	0.33	650	500	2.87	3.00	3.13	2.47	1.47	0.44	0.33	0.45[a]	0.22	0.12	0.35[d]	
FMC COED, CaO, K_2CO_3 (19%:76%:5%)	0.33	650	950	3.16	2.44	0.50	0.54								
FMC COED, CaO, K_2CO_3 (19%:76%:5%)	0.33	650	900	2.91	2.89	1.35	0.77	2.12							
FMC COED, CaO, K_2CO_3, CaF_2 (18%:72%:5%:5%)	0.33	650	950	2.77	3.01	0.40	0.43								
FMC COED, CaO, NaF (19%:76%:5%)	0.33	650	950	2.54	2.61	3.29	2.47	2.12[b]	0.76						
FMC COED, CaO, $Na_2B_4O_7$ (19%:76%:5%)	0.33	650	950	2.63	2.83	0.70	1.24	0.50							
FMC COED, K_2CO_3 (95%:5%)	0.33	750	750-850	1.42	0.40										
FMC COED, K_2CO_3, CaF_2 (90%:5%:5%)	0.33	750	750	2.47	0.52										
FMC COED, CaO, Na_2CO_3 (19%:76%:5%)	0.33	650	950	2.86	3.18	3.11[b]	2.86	3.38	1.60	1.86	0.91				
FMC COED, CaO, $Na_2B_4O_7$, CaF_2 (18%:72%:5%:5%)	0.33	650	950	2.44	2.64	2.09	0.44								
FMC COED, K_2CO_3 (80%:20%)	0.33	650	500	3.13	3.49	0.53	0.23								
FMC COED, CaO, $Na_2B_4O_7$, CaF_2 (18%:72%:5%:5%)	0.33	650	500	1.63	2.11	2.16	2.47	1.60	0.48	0.24					
NORIT "A", CaO, K_2CO_3 (19%:76%:5%)	0.067	650	900	2.02	2.29	2.70	2.86	2.76	2.77	2.60					
NORIT "A", CaO, K_2CO_3 (19%:76%:5%)	0.33	650	900	1.58	2.10	2.13	3.12	3.23	3.03						
NORIT "A", CaO, K_2CO_3 (19%:76%:5%)	0.33	650	1000	1.71 2.44	1.91 2.58	0.32 0.12	0.35 0.00	0.24[a] 0.16[d]	0.36						
NORIT "A", CaO, K_2CO_3, CaF_2 (18%:72%:5%:5%)	0.33	650	1000	1.73	1.90	0.52									
NORIT "A", CaO, K_2CO_3, CaF_2 (18%:72%:5%:5%)	0.067	650	900	1.24	2.16										
NORIT "A", Hollister Dolomite, K_2CO_3, CaF_2 (12%:78%:5%:5%)	0.0067	650	900	1.10	1.35	1.04									
NORIT "A", Hollister Dolomite, K_2CO_3 (13%:82%:5%)	0.0067	650	900	1.14	1.51	1.53	1.04	0.68							
Synthane, Hollister Dolomite, K_2CO_3 (16%:79%:5%)	0.0067	650	900	1.41	0.18[c]	0.80	0.93								
Synthane, K_2CO_3 (95%:5%)	0.33	650	1000	0.59	0.10										
Synthane, K_2CO_3,CaF_2 (90%:5%:5%)	0.33	650	1000	0.46	0.26										
Synthane, Hollister Dolomite, K_2CO_3, CaF_2 (15%:75%:5%:5%)	0.0067	650	900	1.21	1.43	1.59	1.06								
Colstrip, Hollister Dolomite, K_2CO_3 (12%:83%:5%)	0.0067	650	900	1.84	1.20	1.37	0.59	0.89	0.78	0.57	0.67				
Colstrip, Hollister Dolomite, K_2CO_3, CaF_2 (12%:78%:5%:5%)	0.0067	650	900	1.55	1.12	1.48	1.13	0.22[c]	0.78						
Colstrip, Hollister Dolomite, K_2CO_3, CaF_2 (12%:78%:5%:5%)	0.0067	650	800	1.55	1.49	-[c]	1.44	1.03	0.81	1.02					
Colstrip, Hollister Dolomite, K_2CO_3 (12%:83%:5%)	0.0067	650	800	1.47	1.57	1.28	1.68	1.47	1.44	0.55	0.65				

[a] Spiked with 5% CaF_2

[b] Regenerated at 900°C rather than 950°C for this cycle

[c] Gas leak detected

[d] Regenerated at 900°C

[e] Moles product gas evolved per hour per mole initial carbon

Table A-5. Summary of Catalyst Recycle Experimental Results

SYSTEM				PRODUCT EVOLUTION RATE[a]												Usage[b] Ratio	C/S[h] Ratio
				Cycles													
Char	Acceptor	Catalyst	Stabilizer	1	2	3	4	5	6	7	8	9	10	11	12	13	14		
19% COED	76% CaO	5% K_2CO_3	—	2.87	3.00	3.13	2.47	1.47	0.44	0.33								19	0.399
18% COED	72% CaO	5% K_2CO_3	5% CaF_2	2.46	2.89	2.78	2.92	3.14	3.03	3.03	3.21	3.37	2.90	1.06	0.47			40	0.191
19% COED	76% CaO	5% Na_2CO_3	—	2.75	3.20	3.22	3.11	3.28	3.18	3.01	2.51	0.77	0.44					30	0.325
18% COED	72% CaO	5% Na_2CO_3	5% CaF_2	2.57	3.15	2.90	2.89	2.78	3.08	3.03	3.27	3.26	3.45	3.49	2.90	1.03	0.46	47	0.211
19% COED	76% CaO	5% $Na_2B_4O_7$	—	1.89	2.31	—[c]	0.46	0.46										11[d]	0.457
18% COED	72% CaO	5% $Na_2B_4O_7$	5% CaF_2	1.63	2.11	2.16	2.47	1.60	0.48	0.24								18	0.289
19% COED	76% CaO	5% NaF	—	2.64	3.01	2.87	2.78	3.11	3.09	3.13	3.15	3.09	3.13	3.05	1.33	0.44		46	0.547
19% COED	76% CaO	—	5% $Ca_3(PO_4)_2$	0.21														—	-
18% COED	72% CaO	5% K_2CO_3	5% $Ca_3(PO_4)_2$	3.01	2.94	3.04	3.42	3.09	2.25	0.92	0.81							22	0.351
17% COED	68% CaO	5% K_2CO_3	10% $Ca_3(PO_4)_2$	3.27	2.87	3.24	3.43	3.06	2.56[e]	1.19	0.76	0.66						22	0.318
17% COED	68% CaO	5% K_2CO_3	10% NaH_2PO_4	3.21	3.31	2.89	2.91	2.63	2.87	2.85	3.00	2.97	3.07	1.56	0.46			37	0.203
18% COED	72% CaO	10% NaH_2PO_4	—	0.10	0.31	0.53	1.05[g]											—	—
19% COED	76% CaO	5% K_2CO_3[f]	—	2.87	2.97	2.63	2.68	1.77	1.87	1.63								>26	<0.29
19% COED	76% CaO	5% Na_2CO_3[f]	—	3.09	2.97	3.15	3.00	2.91	2.83	2.55								>26	<0.37

a. Moles product gas produced per mole carbon per hour

b. Weight char catalytically gasified per unit weight of alkali catalyst employed

c. Leak in gas collection system noted

d. Usage ratio may be as low as 8

e. Estimate value due to system power failure during reaction

f. Catalyst dispersed by solution impregnation

g. Ash residue from 3rd cycle exposed to gas mixture of CO_2 in steam (0.2 mole fraction) at 650°C for 90 minutes.

h. Ratio of number of moles of catalyst used to mole SiO_2 in deactivated reaction mixture.

Table A-6. Summary of Catalyst Screening Results Obtained for Char-Steam Reaction.

Reaction System			Product Gas Evolution Rate[a]		Apparent Activation Energy
Catalyst	Sulfur Acceptor	Char	650°C	750°C	Kcal/Mole
5% NaF	—	95% COED	0.67	3.09	29
5% NaF	5% $CaCO_3$	90% COED	0.48	—	
5% $Na_2B_4O_7$	—	95% COED	0.14	0.93	36
5% $Na_2B_4O_7$	15% $CaCO_3$	80% COED	0.16	—	
5% $Na_2B_4O_7$, 5% CaF_2	—	90% COED	0.21	1.20	33
5% Na_3AlF_6	—	95% COED	0.26	1.06	26
5% K_2SO_4	—	95% COED	—	0.92	
5% K_2SO_4, 5% CaF_2	—	90% COED	0.14	—	
5% CaF_2	—	95% COED	0.20	1.10	32
—	5% CaO	95% COED	0.07	0.46	35
—	20% CaO	80% COED	0.09	—	
—	80% CaO	20% COED	0.18	1.13	35
—	—	100% COED	0.06	0.22	24

[a] Values expressed as moles product gas evolved per hour per mole carbon in starting mixture.

Table A-6. Summary of Catalyst Screening Results Obtained for Char-Steam Reaction (Cont'd)

Reaction System			Product Gas Evolution Rate[a]		Apparent Activation Energy
Catalyst	Sulfur Acceptor	Char	650°C	750°C	Kcal/Mole
5% K_2CO_3	—	95% COED	0.20	1.42	37
5% K_2CO_3	5% $CaCO_3$	90% COED	0.56	3.12	32
5% K_2CO_3	15% $CaCO_3$	80% COED	0.40	—	
5% K_2CO_3	75% $CaCO_3$	20% COED	3.60	—	
5% K_2CO_3, 5% CaF_2	10% $CaCO_3$	80% COED	0.62	—	
5% K_2CO_3, 5% CaF_2	—	90% COED	0.50	2.47	30
5% K_2CO_3	5% CaO	90% COED	0.48	3.37	37
5% K_2CO_3	5% MgO	90% COED	0.76	3.17	27
5% K_2CO_3	15% MgO	80% COED	0.47	—	
5% K_2CO_3, 5% Na_2CO_3	—	90% COED	1.89	—	
5% Na_2CO_3	—	95% COED	0.53	2.91	32
10% Na_2CO_3	—	90% COED	1.87	—	
5% Na_2CO_3	5% $CaCO_3$	90% COED	0.48	—	
5% Na_2CO_3	15% $CaCO_3$	80% COED	0.47	—	
5% Na_2CO_3, 5% NaF	—	90% COED	0.46	—	

Table A-7. Steam Mass Flowrate Required to Achieve 0.5 Foot Per Second Fluidization Velocity for Various Pressures

Pressure psig	Steam Flow Rate grams/sec.	Initial Specific Steam Rate, Hr
Atmospheric	0.020	11.5
40	0.033	19.0
80	0.050	28.8
100	0.070	40.3

☆U.S. GOVERNMENT PRINTING OFFICE: 1978-740-306/ 9414 REGION NO. 4